DEVELOPMENT AND CHARACTERIZATION OF A HYDROGEN PEROXIDE SENSOR USING CATALASE IMMOBILIZED ON A PYROELECTRIC POLY(VINYLIDENE FLUORIDE) FILM

by

Lawrence Hinkle Arney, Jr.

Dissertation submitted to the Faculty of the
Virginia Polytechnic Institute and State University
in partial fulfillment of the requirement for the degree of

DOCTOR OF PHILOSOPHY

in

Chemistry

APPROVED:

R. E. Dessy, Chairman

J. F. Wolf

J. G. Mason

G. L. Long

J. O. Glanville

April, 1989

Blacksburg, Virginia

DEVELOPMENT AND CHARACTERIZATION OF A HYDROGEN PEROXIDE SENSOR USING CATALASE IMMOBILIZED ON A PYROELECTRIC POLY(VINYLIDENE FLUORIDE) FILM

by

Lawrence Hinkle Arney, Jr.

Raymond E. Dessy

Department of Chemistry

(ABSTRACT)

This dissertation describes the design, development and results of a simple, inexpensive, rugged, pyroelectric heat-of-reaction detector that can be made in many configurations. The measured heat of reaction results from the reaction of a substrate on an enzyme. The enzyme is immobilized in a flow channel with a pyroelectric polymer film, poly(vinylidene fluoride) or PVDF. The sample is introduced into the flow channel using flow injection analysis technology. The heat from the reaction causes the pyroelectric material to produce an electrical potential proportional to the change in temperature which, in turn, is proportional to the substrate concentration. This potential is amplified and recorded.

A differential instrument amplifier produces a difference signal from a sample and reference PVDF film. This removes noise caused by stray electromagnetic radiation and piezoelectric pressure responses.

A conventional Flow Injection Analysis unit was employed. The FIA flow rate was four ml/min and the time from injection to peak maximum was less than three seconds, with a return to baseline of less than

thirty seconds. This gives a quick analysis time and a reasonable number of analyses per unit time. Data interpretation is straight forward, peak height is proportional to the concentration.

A 70 µl sample gives a good response. Larger samples do not improve the signal. The system showed minimum detectable number of moles that is comparable to other methods, 7×10^{-8} moles.

The detector showed good response for more than two orders of magnitude. The results show excellent correlation to the modeled system of heat transfer through the PVDF sensor.

To:

my inspiration and my wife

ACKNOWLEDGEMENTS

I would like to thank the following people for helping me with experimental details. The cell housings were made with the assistance of and the Virginia Tech Physics Shop. The aluminum blocks were anodized with the help of . suggested and provided the polyimid siloxane copolymer. of Solvay, Inc. donated a sample of Solef Piezo Film, poly(vinylidene fluoride), and provided some information about pyroelectrics and PVDF. Samples of AD515's and AD625's were donated by Analog Devices. I heartily suggest giving Analog Devices a call for any problems or to discuss your electronics problems. They seemed to be very knowledgeable about their products and were very willing to send samples of their products. The solenoid power supply was a Heath variable AC supply on loan from the Electronics Shop. I would also like to thank the Electronics Shop and Dr. Tanko for the use of their plotters to plot the figures presented here. , , , and provided valuable electronics suggestions. The PC board for the first stage amplifier was fabricated in the Electronics Shop. helped with the gold sputtered PVDF films.

I would like to thank Dr. R. E. Dessy for bringing together a good group of people with varied backgrounds. The Forth plotting package by and predecessors was very helpful. The Forth Y-term data transfer package by was very nice for transferring data to the IBM-PC. Forth programming assistance from , and other members of the Laboratory Automation and Instrument

Design group is also greatly appreciated, as well as the general discussions about life, lab and the pursuit of happiness.

I would like to thank for introducing me to chemistry in high school and for nurturing this interest in college.

I would like to thank my family for not asking too often how much longer, and for their support through graduate school.

And I would like to thank my wife, , for reading and correcting this dissertation and for keeping me on track and encouraging me through the rough times. She is my inspiration.

TABLE OF CONTENTS

LIST OF FIGURES

LIST OF TABLES

I. INTRODUCTION

Enzyme analyses are becoming more common because of the high degree of selectivity that enzymes have for a compound or a series of similar compounds. Enzymes have mainly been used either to convert the substrate of interest to a compound that is easier to detect spectroscopically, or to a material for which an ion specific electrode is available. These methods, however, have limitations. Solutions must be suitable for spectroscopic analysis and not be turbid or contain other competing highly-colored species. The electrochemical approach requires that there be a selective membrane for the product of interest.

An improvement over the above methods would be to measure another product of the reaction, namely the heat of reaction. Microcalorimeters have been used to monitor an enzyme-substrate heat of reaction, but the cost of a microcalorimeter has limited its widespread use. Thermistors have been placed at the end of columns packed with immobilized enzymes and measure the temperature change of a solution as a substrate reacts with the enzyme. Using a thermistor to measure the concentration of an enzyme-active substrate works well, but a simpler, more flexible approach is needed.

This dissertation describes the design, development and use of an inexpensive pyroelectric heat-of-reaction detector. The heat of reaction measured is from the decomposition of hydrogen peroxide by an enzyme, catalase. This enzyme is immobilized in a flow channel with a pyroelectric polymer film, poly(vinylidene fluoride). The hydrogen

peroxide sample is introduced into the flow channel using flow injection analysis technology. The heat from the decomposition of the hydrogen peroxide causes the pyroelectric material to produce an electrical potential proportional to the change in temperature which, in turn, is proportional to the hydrogen peroxide concentration. This potential is amplified and recorded. This design involves the novel use of a pyroelectric material measuring the heat of reaction of a substrate on an enzyme.

The next chapter is a brief introduction to heat-of-reaction detectors. Chapter III gives an introduction to the theory behind the design of this instrument. Chapter IV describes the materials used and the experiments performed to characterize the instrument. Chapter V is an overview of the thought process that led to the final instrument with a summary of components in the final system. The results and their comparison to a mathematical model of the system are presented in chapter VI.

II. HISTORICAL

A. Methods for Measuring Thermal Change

1. Thermocouple

There are several temperature sensors that are small enough to be used as an effective thermal detector for a flowing system. One, the thermocouple, is a temperature-to-voltage converter. It is created by welding or soldering two different metals wires together. A voltage develops at three places in the thermocouple circuit. A voltage develops in both wires when the ends are at different temperatures. This voltage is a function of the metal and is proportional to the temperature difference. A voltage also develops at the junction of the dissimilar metals. This voltage is a function of the metals and the temperature at the junction. When electrical contacts are made from a microvoltmeter to the thermocouple, two more thermocouple junctions are made. For normal operation, connections between the voltmeter leads and the thermocouple are kept at a constant temperature, usually by placing them in ice water. This is the reference temperature for the circuit. The response is approximately linear and for copper-constantan, a common thermocouple, is 40 μV per degree. This thermocouple can be used down to -183 C. One tungsten alloy thermocouple can be used up to 2800 C.[1]

2. Platinum Resistance Thermometer

Another metallic property that can be used to measure temperature is electrical resistivity. A metal's resistance increases almost

linearly with temperature. At absolute zero, the resistance of a metal falls to zero. As the temperature approaches room temperature, the resistance changes by about 0.4% per degree. Therefore, this method for determining temperature is not as sensitive as others. But this method is the world standard for measuring temperature for the range from -270 to 660 C. Approximately 100 ohms of high-purity platinum wire is wrapped on a ceramic core with care taken to put no stress on the wire. This creates a relatively large sensor compared to a thermocouple or thermistor.[1]

3. Thermistor

Another resistance temperature sensing device is a thermistor. A thermistor is made from a semiconducting material. It takes advantage of the decreasing resistance of a semiconductor with an increase in temperature, as shown by equation II-1,

$$R = R_0 \, e^{E/kT} \qquad \text{II-1}$$

where R is the thermistor resistance and R_0 and E are constants dependant on the individual thermistor unit. T is absolute temperature and k is Boltzmann's constant. The non-linear response may seem troublesome but its the exponential nature can cause the rate of resistance change to be rapid over a small temperature range. At room temperature, thermistor resistances can change up to 5% per degree change. If care is not taken, a thermistor can take its own temperature through resistive heating.[1]

B. Calorimetry

1. Titration Calorimetry

Titration calorimetry measures the heat produced when a titrant and titrate react. There are two types of titration calorimeters, incremental and continuous. There are also two methods for determining the amount of heat produced, isoperibol and isothermal. The isoperibol detector measures the amount of heat produced and corrects for system losses. The isothermal detector attempts to maintain the system at one temperature and measures the energy required to do so. To simplify data interpretation, these systems need to have thermal time constants significantly longer than the reaction being studied. The isoperibol incremental calorimeter adds a known amount of titrant to the reaction vessel and then waits for the system to come to equilibrium. Then another addition of titrant is made. This is continued until no further heat change is noticed. This system is good for slow reactions. The isoperibol continuous calorimeter adds the titrant at a specific rate and provides a continuous readout of heat produced with time or titrant added. For an accurate titration, the reactions for this system must proceed faster than for the titration method. This calorimeter must have a quick response to the heat produced and be corrected for thermal lag. Isothermal titration calorimeters are better for slow, long term, low heat reactions such as that produced by bacterial activity.

Reaction vessels as small as 1.5 ml have been developed. For isoperibol calorimeters, the problem with these small reaction vessels is that the heat leak modulus is inversely proportional to the size of the vessel. Small vessels require larger correction factors for both size

and time, creating larger uncertainties in the measurements. Isothermal calorimeters do not require this correction because there is negligible heat loss to the surroundings. A typical isothermal response time is one or two minutes.

2. Flow Calorimetry

Flow calorimetry adds known volumes of two reactants in a mixing vessel. Again, the heat can be measured by one of two methods. Measuring the heat-of-reaction or heat produced by physical interaction is called a heat conduction flow calorimeter. An isothermal flow calorimeter maintains the temperature of the reaction coil and measures the energy required to do so. Response times for flow calorimetry experiments can range from 2 seconds to 30 minutes. Isothermal flow calorimetry has the best overall characteristics for continuous flow techniques. It has good sensitivity with low sample consumption and the least amount of data manipulation because of the isothermal nature of the system. Minimum heat changes of 0.2 mJ have been reported.[2]

C. Enzyme Probes

1. Potentiometric Enzyme Probes

Several methods have been employed to probe enzyme reactions. These methods have centered on both thermal probes and reaction product specific probes. A potentiometric enzyme electrode is a potentiometric, species-specific electrode with an enzyme layer on the surface. The reaction of a substrate on the enzyme produces a substance that will cause a change at the electrode if the product diffuses to the

electrode. pH electrodes have been used to make glucose, urea and penicillin electrodes.[3,4] A problem with these electrodes are that they are not linear over large pH range and cannot be used with high ionic strength solutions such as body fluids. Ion specific electrodes have also been used to make enzyme probes. A solid state, cyanide sensitive electrode was used to determine amygdalin concentrations in solution. It was made by immobilizing ß-glucoside on the electrode.[5] Ion specific electrodes are not extremely specific. Other ions prevent low concentration determinations.

Gas sensitive electrodes are somewhat immune to the problems from above. Several enzyme/substrate reactions produce gas as one product. Immobilizing an enzyme on the correct gas sensitive electrode will produce an enzyme electrode. CO_2, O_2 and NH_3 selective electrodes have been used to create substrate specific electrodes. The major problem of this type of electrode is fouling of the membrane.[6]

2. Amperometric Enzyme Probes

Current sensing electrodes coated with enzymes have been used to determine substrate concentration in solution. While they are similar to the potentiometric electrodes, described above, having a diffusion controlled response, amperometric electrodes remove species from the solution. This creates a concentration gradient around the electrode. Most applications involve immobilizing enzymes on O_2 and H_2O_2 electrodes.[7,8] The instrumentation needed to perform sensitive current measurements is expensive.[6]

3. Thermal Enzyme Probes

a. Thermistor Heat-of-Reaction Detector

A thermistor based detector has been developed using a short chromatographic column with an enzyme immobilized on the packing material. The thermistor was placed at the outlet of the column and was able to measure 1 mM of a trypsin substrate, and down to 10^{-5} M glucose with an immobilized glucose oxidase. This system could handle up to 20 samples per hour.[9] A differential arrangement was examined using two columns, one containing active enzyme, the other containing inactive enzyme, with a thermistor at the end of each. This reduced the baseline drift but did not increase sensitivity significantly. Glucose was measured at 0.05 mM.[10] Another differential thermistor technique measured the temperature difference between the inlet and outlet of 25 mm long column. The response from this system compared favorably with current clinical methods for the determination of urea and could analyze 40 samples per hour.[11]

In 1977 a general enzyme thermistor was developed. One of the applications developed was a hydrogen peroxide sensor. Catalase was immobilized in a short column and a thermistor was placed at the outlet. The detector had good sensitivity, but the response time was long. A linear response was measured from 5×10^{-5} to 10^{-2} M. After the peroxide sample injection, a one minute response time was reported.[12]

One of the main problems with the systems described above is configuration. It is difficult to get the thermistor in close proximity to the enzyme column. Systems have been described where the thermistor has been incorporated into the column, and these provide greater

sensitivity than systems where the thermistor was placed directly at the end of the column. However, these involve an even greater design problem. Workers continually search for a method that will allow rapid change of columns, an operation that is difficult with an embedded thermistor.

Thermal enzyme probes using enzymes immobilized on thermistors have also been developed. One such detector used two thermistors, one coated with an enzyme, the other serves as a reference, to determine the concentration of glucose solution down to 3 mM and urea down to 5 mM with a response time of less than 10 seconds. A hydrogen peroxide sensor using immobilized catalase was also developed. It had a response time of about 10 seconds and a linear range from 0.01 to 0.5 mM with an error of less than 3% at concentrations above 0.01 mM.[13] The thermistors were placed in a well stirred solution of the enzyme substrate. The reaction is kept at a steady-state through stirring. The temperature difference between the thermistors is proportional to the concentration of the substrate.

These thermal probes suffer from several problems. The response time requires relatively large amounts of sample. The thermistor must be well matched and have a thermal common mode rejection of at least 10^{3}. Noise from stirring is also a problem. The solution has some thermal gradients which limit the detection range.

In an effort to remove some of these problems, a flow cell was constructed containing an enzyme-coated thermistor. Laminar flow by the thermistor should reduce noise due to mixing. A urea sensor was developed, but showed only a fifth of the sensitivity of non-flow

sensors with a limit of detection at 1 x 10^{-4} M and a linear range from 1 x 10^{-3} to 1.5 x 10^{-2} M urea. A response time of 3 minutes was reported with another 3 minutes for return to baseline. The thermistors were sensitive to mechanical pump noise. The formation and trapping of bubbles on the thermistor creates a vastly different heat flow environment for a small sensor. This puts an upper concentration limit on many enzyme/substrate systems which produce gas. These authors also found that the thermal noise increases with the flow rate, but higher flow rates are more desireable because of the faster response times.[14]

b. Fiber Optic Heat-of-Reaction Detector

In 1984, a fiber optic heat-of-reaction detector was developed that used the decomposition of substrate on an enzyme immobilized on an optical fiber to produce a thermal stress in that fiber.[15] This stress caused a change in the light propagation properties of this fiber. Laser light was launched into this fiber and a second reference fiber. The output of these fibers was deployed on to a diode array where the coherent light produced an interference pattern. This fringe pattern would shift with stresses induced in the fiber. Therefore, the temperature change from the substrate decomposition could be monitored by the shifting fringe pattern on the diode array.

A minimum detectible quantity for the decomposition of urea on urease is reported at 5 mM. The minimum detected quantity for hydrogen peroxide decomposing on catalase is 1.95 mM. A reasonably large amount of sample was also required. The response for this system was slow and not reproducible. A positive deviation from a linear response was

noticed for the catalase/peroxide system. No explanation was given for this. One possible explanation for this observation is that the bubbles that formed on the enzyme insulated the fiber. This would change the thermal propagation properties and the heat produced from the reaction would be effectively trapped by this air layer. This would result in a stronger than expected response at higher concentrations.

III. THEORY AND LITERATURE REVIEW

A. Enzymes

1. Introduction

The word enzyme was coined by Friedrich Wilhelm Kühne in 1878 for catalytically active substances that had previously been called ferments. It is derived from the Greek words en, in, and zyme, leaven.[16] Enzymes reduce the activation energy for a specific reaction by providing an active site which provides an alternate path conducive to the reaction being catalyzed. The reduced activation energy usually increases reaction rates by many orders of magnitude.

2. Immobilization

Enzymes, for the most part, are difficult to isolate and purify. Often reactions involving enzymes prohibit the recovery of active enzyme. To conserve enzyme, therefore, immobilization is used. There are two types of immobilization: entrapment in a matrix or in a microcapsule, and chemical bonding, either covalently or by adsorption.[17] One of the preferred immobilization agents is glutaraldehyde.

Glutaraldehyde, pentanedial, will react with two amines to produce a diimine as shown below.

$$2\ R\text{-}NH_2 + O{=}CH\text{-}(CH_2)_3\text{-}CH{=}O \longrightarrow R\text{-}N{=}CH\text{-}(CH_2)_3\text{-}CH{=}N\text{-}R + 2\ H_2O \qquad \text{III-1}$$

Glutaraldehyde's reaction mechanism with protein is not well understood, likewise, the structure of glutaraldehyde in solution has not been established. Amino acid assays of crosslinked enzymes indicate

glutaraldehyde preferentially reacts with lysine units, although not exclusively.

Lysine $^{+}H_3N(CH_2)_4CH(NH_2)COO^{-}$

Lysine is one of the few amino acids with a primary amine available for reaction with an aldehyde. After immobilization of catalase with glutaraldehyde, one study showed the catalase activity decreased about 20% over two weeks but then showed no further decrease.[18]

3. Catalase

Catalase (H_2O_2:H_2O_2 oxidoreductase; EC 1.11.1.6), MW 249,000, is a stable enzyme made up of four 60,000 dalton polypeptide chains which contain an iron atom.[17] Mild crosslinking partially unfolds the polypeptide chains but does not significantly decrease the enzyme activity. The decomposition of peroxide by catalase is proposed to be a two step process as pictured in Figure 1. In the first step, a peroxide molecule replaces a water molecule as one ligand on the iron atom. In the second step, a second peroxide molecule associates with the iron, displacing a water molecule. This intermediate eliminates an oxygen molecule, and returns the enzyme to the original form.[20] This reaction is the fastest known enzyme reaction. One catalase molecule can decompose up to 10^7 hydrogen peroxide molecules per second.

The catalase decomposition of hydrogen peroxide is an exothermic reaction. The ΔH for the decomposition of aqueous hydrogen peroxide is -94.7 kJ/mole.[18] In this study, the heat produced by this reaction causes a pyroelectric film to produce an electric potential.

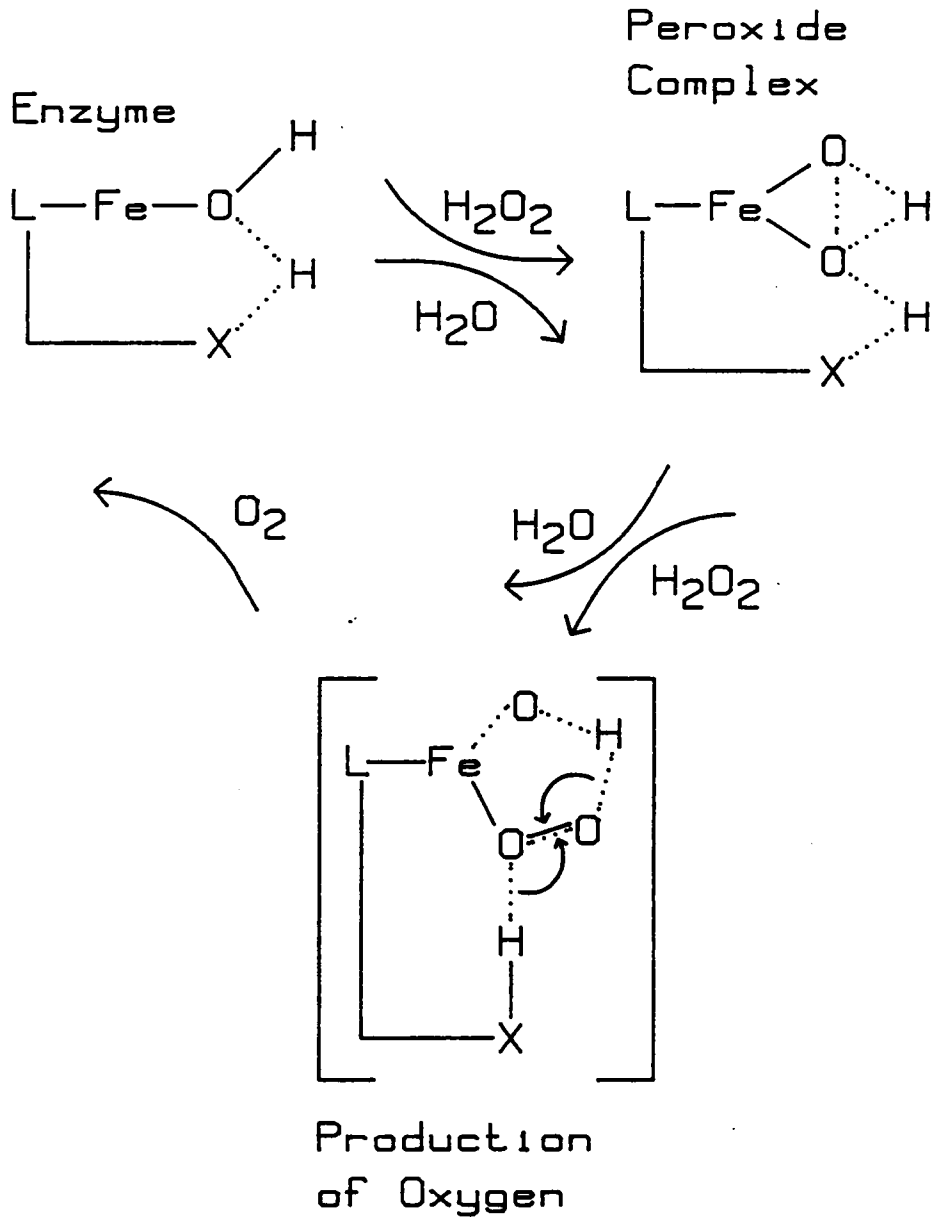

Figure 1. A proposed mechanism for the decomposition of enzyme. In the first step, a peroxide molecule replaces a water molecule as one ligand on the iron atom. In the second step, a second peroxide molecule associates with the iron, displacing a water molecule. This intermediate eliminates an oxygen molecule, and returns the enzyme to the original form.

B. Pyroelectricity

1. Introduction

A piezoelectric material is a dielectric material with an oriented crystal structure in which ions are displaced and the dimensions of the material are changed when an electric field is placed across the material thus inducing a dipole. The induced strain is proportional to the electrical field. Likewise, when this dielectric is stressed, the dimensions are changed and an electric field is induced across the material. The electrical field is proportional to the stress.

A pyroelectric material is a piezoelectric material that also changes polarization with changes in temperature. Physically, temperature causes a change of positive and negative polarization charges on certain portions of noncentrosymmetrical crystals. Thermal expansion and contraction change the dipole moment of the crystal. The change in polarization is proportional to the temperature change. All pyroelectric materials are piezoelectric.[21,22,23] Appendix D defines terms and equations dealing with pyroelectricity.

If a change in temperature changes the dipole moment, an electric field will be produced. Although the dipole moment cannot be directly measured, the temperature coefficient of the dipole moment can be determined by measuring the change in electric field with temperature. This temperature coefficient is the pyroelectric coefficient.[24,25]

2. Theory

These phenomena can be understood by looking at the crystal structures of piezo and pyroelectrics. Twenty-one of the thirty-two crystal

structures are noncentrosymmetrical. These twenty-one point groups define the crystal structures that show piezoelectric properties. Ten of these structures can exhibit spontaneous electrical polarization. An external electric field generated by this polarization cannot be measured if the material is too conductive. This conductivity allows the developed charges to migrate, neutralizing the internal moment. If the material is an insulator, however, charges will be attracted to, and trapped on, the surface. This charge distribution on the surface of the insulator is relatively stable.

Pyroelectricity may be divided into two types, primary and secondary. Primary pyroelectricity is the pyroelectric effect due only to "the change with temperature of positive and negative polarization charges on certain portions of crystals belonging to certain classes." [23] Secondary pyroelectricity is caused by deformations in the pyroelectric material due to a change in temperature; it is the piezoelectric effect due to temperature change. A pyroelectric which is clamped so that it cannot change size with temperature will only exhibit primary pyroelectricity. Both primary and secondary pyroelectricity will contribute to the signal from an unclamped film. Secondary pyroelectricity is further divided into uniform heating and non-uniform heating. Non-uniform heating is a special case of heating. Uniform heating heats the entire material evenly, while non-uniform heating involves a temperature gradient through the material. Many piezoelectrics which are not usually classed as pyroelectric, such as quartz, will show a small pyroelectric effect with non-uniform heating due to strains caused in the material from the uneven heating.

Pyroelectricity was first observed in natural crystals such as tourmaline and Rochelle salt. In the 1940's, pyroelectricity was discovered in polycrystalline ceramics, such as barium titanate. One of the strongest pyroelectrics discovered is triglycine sulfate. TGS, used as a detector for FTIR spectroscopy, has a pyroelectric coefficient of 2×10^{-8} C/cm^2 K.

3. PVDF

Poly(vinylidine fluoride), or PVDF as it shall be called in this paper, was discovered to have piezoelectric properties in 1969 by Kawai.[24] He theorized that if some crystals, modified ceramics and natural organic materials showed piezoelectric properties, synthetic materials with the proper dipole, orientation and insulative properties should also be piezoelectric.

PVDF, as its name suggests, is synthesized by polymerizing 1,1-difluoro ethene, $CH_2=CF_2$, so that there is a head to tail polymerization, $-CH_2-CF_2-CH_2-CF_2-$ resulting in the α phase, or phase II, of the polymer as shown in Figure 2.A. The chain coils in a helix of about 60° every four repeating units. This phase is the most thermodynamically stable.

To make PVDF into a piezo and pyroelectric, a film is heated to above its T_g and below its melting point, usually around 120°C, and stretched. Solvay stretches their biaxial film by 400%. A monoaxial film is stretched in one direction. A biaxial film is stretched in two perpendicular directions. Stretching in one direction makes the polymer chains line up in the stretch direction, making it stronger in the

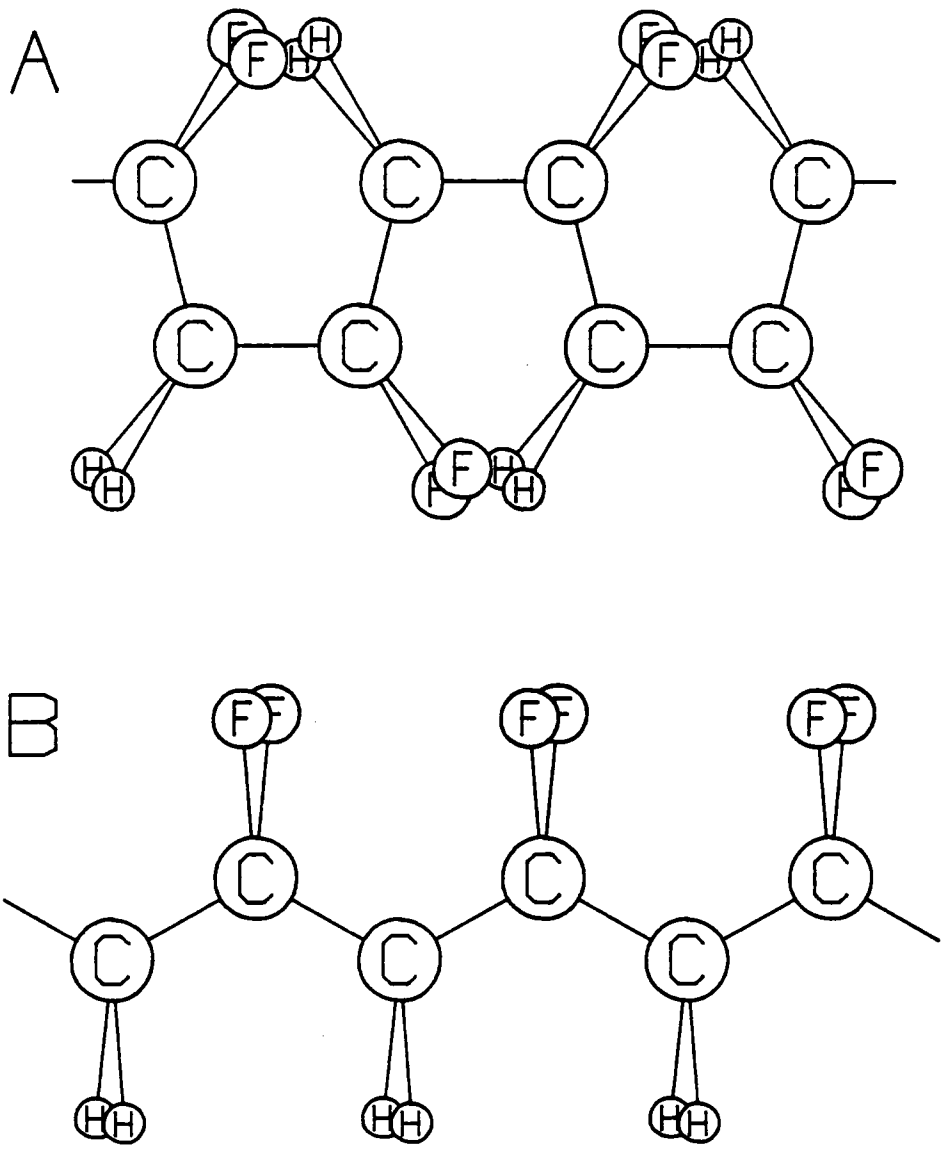

Figure 2. The α- and β-phase of PVDF. A. A representation of a PVDF chain segment of the more thermodynamically stable α-phase or phase II which is not piezo or pyroelectrically active. B. A representation of the pyroelectric β- phase or phase I of PVDF.

stretch direction but weaker in the transverse direction than a biaxial film. A monoaxial film also has different piezoelectric properties in the stretch and transverse directions. A biaxial film has uniform piezoelectric properties.[27]

This stressed and heated film is placed in a strong electric field which causes the electronegative fluorines to align toward the positive pole and the hydrogens to align toward the negative pole as shown in Figure 2.8. The film is then cooled in the electric field, yielding the β phase, or phase I, film of PVDF. This PVDF is approximately half crystalline.[28]

Bergman and coworkers were the first to measure a large pyroelectric coefficient for PVDF.[29] There is some argument in the literature about the source of the pyroelectric signal. Furukawa claims that secondary, dimensional pyroelectricity is minor and primary pyroelectricity is dominant. He then appears to contradict himself by saying that the pyroelectric response of PVDF is difficult to separate into the primary and secondary components because of the compressibility of the material. He asserts that the amorphous regions will deform from pressures resulting from expansion and contraction of the crystalline regions making measurement of the primary and secondary components difficult.[30] Kepler and Anderson have reported that less than 15% of the pyroelectric signal is due to primary pyroelectricity.[31] Furthermore, they claim that about 50% of the pyroelectric signal is due to secondary pyroelectricity.[32] They theorize that, at room temperature, up to a third of the pyroelectric signal could be caused by reversible changes in crystallinity, an effect which has been observed in polyeth-

ylene.[33] A similar effect has been shown to occur in PVDF employing x-ray crystallography.[34,35] The percentage of rigid crystalline regions in a sample of ß-form PVDF fell from 50% to 43% over a 20 - 60 C temperature interval.[36] Another factor that is thought to be involved is the highly oriented nature of the amorphous phase. This has been demonstrated by NMR studies.[37] Sussner and Dransfeld believe that piezo polarization occurs at the positive metal electrode by injection of charges from the electrode and alignment of CF_2 dipoles at the metal boundary. This involves a metal-polymer interfacial phenomena. These workers claim the polarization of PVDF is strongest at the interface between the polymer and the positive electrode and is not at all homogeneous through the volume of the sample.[38] Wada and Hayakawa believe that the inhomogeneity of the elastic and thermal expansion properties of the film are the major source of the piezo- and pyroelectricity in PVDF.[39]

PVDF was chosen for this study because it is relatively inert to normal environment, stable with time and available at a reasonable price. Most other pyroelectric materials are hygroscopic, fragile, not stable (the pyroelectric coefficient degrades with time) or expensive.

C. FIA

1. Introduction

Flow injection analysis, FIA, is an analytical technique that can be adapted to almost any wet chemical analysis. FIA was developed simultaneously by Ruzicka[40] and Stewart.[41] Ruzicka and Hansen from Denmark developed their techniques using segmented flow techniques and

a modular, add-what-you-need system. At FDA, Stewart, Beecher and Hare developed an FIA system using chromatographic techniques. FIA works on the theory of laminar flow and merging zones and that every sample is treated exactly the same. (Appendix E defines some FIA terms.) The simplest FIA system consists of a sample loop, a detector, a reaction coil, and a pump. The sample loop injects a segment of sample, called the bolus, into the flowing stream. The reaction coil is the segment of tubing between the sample loop and the detector. The length and diameter of the reaction coil and the sample size determine the amount of dispersion of the carrier stream into the sample bolus. The carrier stream can push the sample from the sample valve to the detector or the carrier stream can react with the analyte of interest in the sample to provide a product that is easier to detect. A sample bolus in a stream flowing under constant pump speed will reach the detector in the same amount of time as any other sample with the same amount of mixing with the carrier stream. This property allows kinetic studies or examination of unstable species. Reactants in the carrier stream will disperse farther into the sample bolus as a function of the distance the bolus has traveled down the tubing. Thus reactions can be at different stages at different places in the bolus as it reaches the detector. With the proper tailoring, any stage of a reaction can be monitored.

2. Dispersion

The amount of mixing between a sample bolus and the carrier stream at the detector is called the dispersion. The dispersion coefficient is the ratio of the initial concentration of a sample bolus to the

maximum concentration passing the detector. Dispersion coefficients of less than three are considered limited dispersions. Dispersions of greater than ten are large dispersion coefficients. A dispersion coefficient of one means the maximum concentration of the analyte at the detector is the same as the initial concentration in the sample loop and the reaction coil was not long enough for the carrier stream to disperse into the sample bolus. This dispersion is the type used in this study.

PVDF needs a temperature change to produce a signal. For this sensor, a minimum dispersion of the sample bolus in the flowing stream is desired to bring a sharp concentration gradient and the maximum substrate concentration to the detector. A gradual increase in substrate concentration will give a gradual increase in temperature which is harder to detect. A dispersion of one is desireable. A short "reaction coil" will give sharp leading and trailing edges. (The words, reaction coil, are placed in quotes because the carrier stream does not react with the peroxide sample, the stream pushes the sample to the detector.)

In FIA, the concentration profile is ideally a Gaussian distribution, where a longer reaction coil will produce a concentration profile with a larger standard deviation around the maximum. A "mixing tank", an area in the flow stream that has a larger cross-sectional area than the rest of the stream, will cause the trailing edge to tail badly. This stretching out of the peak causes an asymmetric Gaussian peak shape. The flow channel containing the detector in this study acts as a mixing tank.

3. Filtering Data

Data containing random noise can often be smoothed with a digital filter. In 1962, Savitzky and Golay[42] presented an elegant method by which data was filtered simply by fitting a third or fourth-order, least-squares curve to a small segment of the data, and using the center point from this curve as a point in a new data set. The number of points in the small segment of the data fitted with the curve is called the width of the filter. Calculating the least squares curve for a cubic or fourth order equation at each point would be very time consuming for a large data set, but Savitzky and Golay derived a simple equation and a table of weighting factors that, with simple math, will calculate a point at the center of the curve. The corrected table for the third order filter is presented in Appendix A. To calculate the point m in the filtered data set for a Savitzky-Golay filter of width 2n+1, point m and the set of n points from either side of point m in the unfiltered array, 2n+1 points, are multiplied by the corresponding weighting factors, summed and divided by a normalizing factor. The point m+1 is then treated in the same way. This filtering technique does not allow the first and last n points in the data array to be filtered correctly. Savitzky and Golay present tables for data smoothing with filter widths from 5 to 25 points which fit cubic to quintic curves to the data, as well as tables that will take first through fifth derivatives of the data. To be most effective, the filter width should be the same width as the smallest peak of interest. This technique was applied to all data sets described in this work.

This chapter has presented the tools used to develop the PVDF based instrument. The next chapter describes the materials used and the experiments performed to characterize the instrument.

IV. EXPERIMENTAL

A. Components

1. PVDF

The piezoelectric/pyroelectric films were obtained from Pennwalt and Solvay Corporations. Pennwalt supplied a monoaxial film coated with a layer of nickel covered by a layer of aluminum. Solvay supplied a biaxial film coated with aluminum. Pennwalt marked the stretch and poling directions on the film. Since Solvay makes a biaxial film, they do not need to mark a stretch direction, but they do not mark the poling direction either. The poly(vinylidene fluoride) polymer, coated on both sides with metal electrodes, will be referred to as the PVDF film. The means for conducting the potential produced by the film from the aluminum electrodes will be called the electrical connection.

The PVDF film was best cut with a sharp blade, such as a new blade in an Exacto knife. A metal ruler was needed for cutting straight lines to the proper length. Scissors and dull blades left the edges stretched and wrinkled causing them to fold and make electrical contact across the two electrodes.

The pyroelectric coefficient, p, for PVDF is -2.5×10^{-5} Coul/m^2 K.[22,43] A one degree change will produce approximately a 10^{-7} Coulombs potential per square centimeter. PVDF has a specific resistance of $10^{13}\Omega$-m which gives 3 square centimeters of a 40 μm film a resistance of approximately $4 \times 10^{11}\Omega$. The quantity of heat necessary to produce unit temperature change in a unit mass is called the thermal capacity.[44] For PVDF, the thermal capacity, C_T, is 1.3 J/g K.

2. Catalase Immobilization Procedure

The general procedure for immobilizing the enzyme, as discussed in chapter III, used the following reaction to link amines on the catalase to amines on the bovine serum albumin, BSA, via a dialdehyde, glutaraldehyde.

$$BSA\text{-}NH_2 + O{=}CH\text{-}(CH_2)_3\text{-}CH{=}O + H_2N\text{-}Catalase \longrightarrow$$

$$BSA\text{-}N{=}CH\text{-}(CH_2)_3\text{-}CH{=}N\text{-}Catalase + 2\ H_2O \qquad \text{IV-1}$$

Both catalase and BSA are large proteins and, therefore, can crosslink at more than one place. This crosslinking process can decrease the number of active sites by distorting the catalase, but crosslinking can also keep the enzyme from denaturing as easily as the free enzyme by not allowing the protein as much mobility.

Although the immobilization procedure changed as the detector evolved, the general method did not change significantly. A typical immobilization was as follows. Thirty milligrams of BSA and five milligrams of catalase were added to one hundred microliters of water in a small testtube, mixed well and chilled to around ten degrees C. Then, ten microliters of chilled glutaraldehyde were added with a micropipet, stirred, and applied immediately to the area of immobilization. This solution was allowed to crosslink until firm; around five minutes. The enzyme was rinsed with a 10% glycine solution to cap free aldehyde units on the glutaraldehyde and then rinsed with water.[15]

3. Flow System

The portion of the flow cell where the solution flows by the PVDF and enzyme will be called the flow channel. The block in which the

flow channel was milled will be referred to as the cell. The cells were constructed in the Virginia Tech Student Physics Shop. The sides of cells were roughly flattened with an end mill and smoothed with fine sandpaper on a flat surface. The flow channels and electrical connection channels were milled with end mills. The holes for inlets, outlets, and electrical connections were drilled on a drill press. Tapped holes were made with a standard English tap set and the Cheminert connections were finished with a bottom tap.

The pumps used were a VirPump one speed peristaltic pump, a reciprocating piston pump from a Hewlett/Packard liquid chromatograph, and a Gilson continuously-variable speed, four-channel, peristaltic pump.

The tubing used was 0.3 mm inner diameter (i.d.) Nylon 6 tubing. This tubing allowed easy fabrication of flow connections using Cheminert connectors.

The sample injection valve was a Rheodyne six-port, two-way valve. A Rheodyne pneumatic actuator was purchased to automate the injection.

Two 110 AC volt solenoids controlled the air supply to the pneumatic actuator.

4. Computers

The data was acquired on a LSI-11 with 20k of memory using the language Forth. The data was stored through a data transfer program on another LSI-11 with 8 inch Pertec AED drives. An Analog Devices model 1030 programable ADAC, an analog-to-digital and digital-to-analog converter, was used for taking data. The analog-to-digital conversion

was triggered by sending a bit pattern to bits 3 and 4 of the control status register. An octal 30 gave a conversion in the +/-10 volt range, and 20 chose the +/-5 volt range, a 10 selected the +/-2 volt range and a 0 gave a conversion in the +/-1 volt range. Although the Forth program was written to switch between these ranges depending upon the output of the electronics, most of the data was taken in the +/-10 volt range because the signal was strong enough to be amplified within this range.

Two Forth program packages were modified to suit the needs of the research. A graphics package was modified to automatically scale and plot data using the parameters stored with the data. A data transfer package written to accommodate the Y-term protocol was modified to transfer data to an IBM PC for data manipulation.

An AT&T 6300, using the software package Lotus, was also used to manipulate and plot data, and, using Turbo BASIC, to model the heat flow through the PVDF film. Generic Cadd was used to plot the data presented in this dissertation.

5. Power Supplies

Two Lambda power supplies were used, one for the computer and one for the control on the reed relay to the solenoids. A Heath variable AC power supply was used to power the solenoids. A small, +/- fifteen volt power supply ran the amplifier electronics.

6. Electronics

The thermostatting system consisted of a commercial set point controller and a thermistor which controlled a modified 300, 600, 1200 watt hair dryer.[45]

Two reed relays were actuated by five volts and controlled the power to solenoids controlling and injection loop.

The amplifiers used to amplify the signal from the pyroelectric material, PVDF, were the RCA CA3140 and the Analog Devices AD515 and AD625.

The evolution of the support electronics began by wire wrapping the components of the circuit being tested. Wire wrapping allowed for rapid construction of new designs with more reliability than socket breadboarding and less time than etching a PC board for the new circuits. The circuits were designed for maximum flexibility. Good quality fourteen and sixteen pin sockets were used for the amplifiers, resistors and capacitors, to allow easy testing and modification. Variable resistors were wire wrapped and soldered in place because the pin placement precluded using sockets. High quality, low noise, tantalum or polystyrene capacitors were used for decoupling capacitors and components in the circuits. Precision resistors were used when matched sets of resistors were necessary. Ground loops in the circuits were avoided and, when possible, grounds were arranged in a star pattern, where all component grounds radiate from a single point which was connected to ground. This grounding procedure helped avoid problems with different ground potentials. Decoupling capacitors were added to the +/-15 amplifier power supply to decrease the amount of

ripple noise transmitted to the amplifiers. The ripple in the voltage from the power supply was about 4 mV. Inductor/capacitor couples were added to later amplifiers to further condition the power supply.

B. Chemicals

Chemicals used for the immobilization were glutaraldehyde and glycine from Fisher and bovine serum albumin (BSA) and catalase from Sigma. Two types of catalase from bovine liver were used, first, Sigma catalog number C-40, a purified, thymol-free powder with 10,000 to 25,000 units of activity per milligram of protein. Later, Sigma catalog number C-30, a crystalline suspension in water containing 0.1% thymol as a preservative was used. For catalase, one unit of activity will decompose one μmole H_2O_2 per minute at pH 7 and 25°C at concentrations near 10 mM.[46] The commercial suspension had 10,000 to 30,000 units of activity per milligram, and there was 100 mg "suspended" in five milliliters. The suspension settled to the bottom and had to be mixed again before each use to get approximately the same catalase concentration. The carrier stream was distilled, deionized water. Triton X-100, octyl phenoxy polyethoxyethanol, a non-ionic surfactant from Sigma, was used to minimize the bubble size. Ten percent hydrogen peroxide was used to make test solutions. The chemicals used for the standardization of hydrogen peroxide solutions were ammonium molybdate, soluble starch, sulfuric acid, potassium iodate, potassium iodide, sodium thiosulfate and sodium carbonate.

C. Solutions

1. Carrier Stream

The carrier stream was prepared by boiling two liters of distilled, deionized water, adding 2 or 3 drops of Triton X-100 and allowing this solution to cool overnight. Deionized water was used because certain ions can act as interferants in enzyme reactions. The water was boiled to reduce the amount of dissolved gases in the carrier stream. Thus, boiling the carrier stream helped dissolve bubbles that were a product of the H_2O_2/catalase reaction that stuck to the film between injections. Triton X-100 was added after large oxygen bubbles were observed sticking to the immobilized enzyme. The Triton X-100 caused the bubbles to be released from the film at a much smaller diameter, which allowed more peroxide solution to reach the enzyme. The smaller bubbles also produced less pressure noise as they flowed out of the cell and through the waste tube. Data from before and after adding Triton X-100 are shown in Figure 3.

2. Standardization Solutions

The starch indicator solution was made from soluble starch.[44]

The 1 N and 4 N H_2SO_4 were made by diluting concentrated H_2SO_4. These solutions were used to acidify the reaction media.

A 3% $(NH_4)_2MoO_4$ solution was prepared by dissolving 1.5 mg in 50 ml H_2O. This solution initiates the peroxide and iodide conversion to water and iodine.

An approximately 0.1 N thiosulfate solution was made by dissolving 25 g (0.1 M) $Na_2S_2O_3 \cdot 5H_2O$ and 0.1 g Na_2CO_3 in 1 l of freshly boiled and

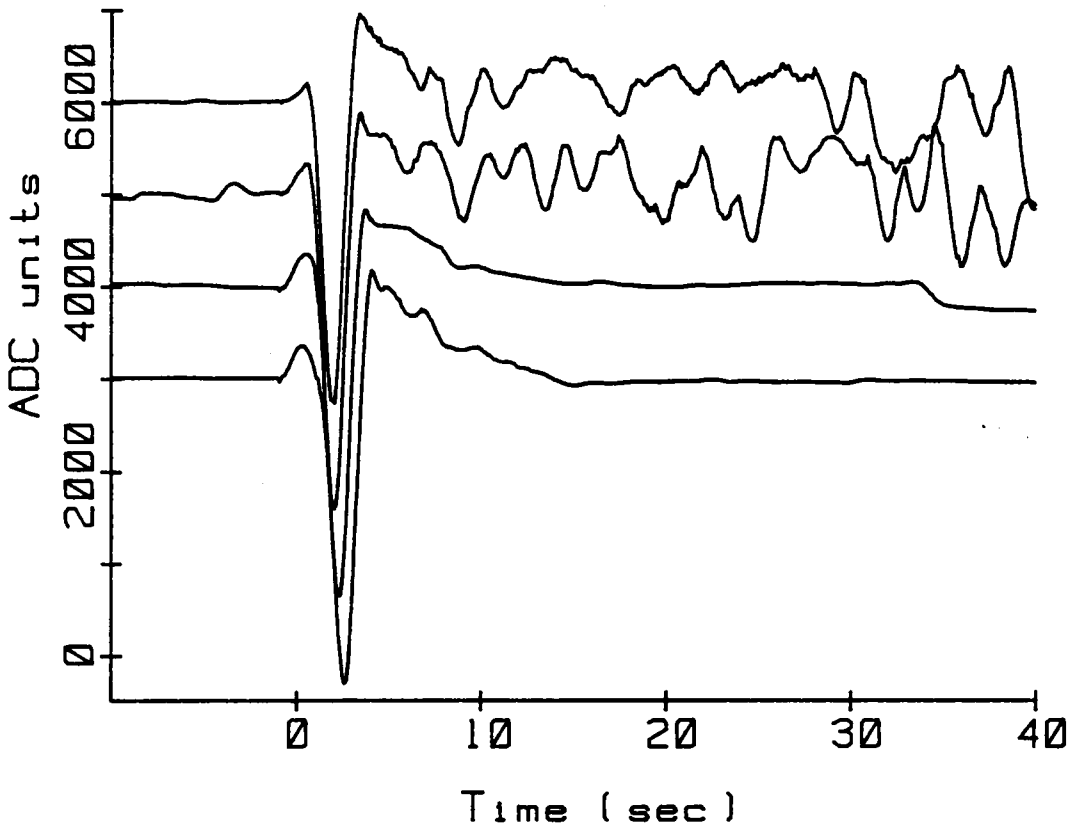

Figure 3. Representative data showing response of system before (top two data sets) and after adding Triton X-100.

cooled distilled water; this solution was allowed to stand one day before it was used.

D. Standardization Procedure for H_2O_2

A secondary method for determining the concentration of hydrogen peroxide was used.[47] A thiosulfate solution was standardized by titrating an acidified iodide solution containing a known quantity of KIO_3. The iodate was quantitatively converted to iodine as follows:

$$IO_3^- + 5I^- + 6H^+ \longrightarrow 3I_2 + 3H_2O \qquad \text{IV-2}$$

This solution reacts with the thiosulfate solution as follows:

$$2\ S_2O_3^{2-} + I_2 \longrightarrow S_4O_6^{2-} + 2\ I^- \qquad \text{IV-3}$$

A starch indicator was used to determine the endpoint. The titration had to proceed slowly or the thiosulfate would decompose in the acid solution to produce a colloidal sulfur dispersion.[48]

To determine the concentration of the peroxide solutions, a known quantity of dilute solution was pipetted into an acidified iodide solution. The peroxide converts the iodide to iodine as follows.

$$H_2O_2 + 2I^- + 2H^+ \longrightarrow I_2 + H_2O \qquad \text{IV-4}$$

The iodine in this solution was then titrated slowly with the standardized thiosulfate solution.

E. System Flow Characterization with Photomultiplier and Dye

The characteristics of the flow channel were determined photometrically. To determine what a sample bolus looked like flowing into and out of the sample flow channel, a photometer and a dye, bromothymol blue, were used to monitor the dispersion of the solution. The photo-

meter had a cell with a red diode on one side and a photomultiplier on the other. The photometer cell has been constructed so that it would accept Cheminert connectors with tube plugs. This made the connector about 3 mm longer than a normal Cheminert connector. Therefore, an extra length of tubing, 10 cm of 0.1 mm i.d., had to be added to keep the cell from leaking. The back pressure generated by the smaller size tubing did not create any flow difference, the volume per unit time was approximately the same with and without the added tubing.

1. Flow Dynamics Before and After Cell

This experiment was divided into parts; the bolus profile on entering the flow channel, and the profile at the exit.

Experiments were run with a 70 µl and a 150 µl sample loop. 70 µl was the smallest sample loop volume the Rheodyne sample valve could deliver. This sample loop consisted of the two sides of the sample valve connected together without any other tubing in the loop. The 150 µl sample loop was made by connecting a tube between the two sides of the valve. The small tubing to the photometer was connected to the output of the sample loop. A 10 ml Erlenmeyer flask was filled with the bromothymol solution. With a syringe, the solution was drawn through the sample loop until the blue color reached the syringe. The Forth data acquisition program took 10 points per second for 100 seconds beginning 10 seconds before sample injection.

2. Flow Dynamics Through Flow Channel

The experiment above was repeated with the small tubing to the photometer connected to the output of the flow channel and the output of the sample loop connected to the input.

V. INSTRUMENT DESIGN

A. Introduction

The goal of the research was to demonstrate the feasibility of building a simple heat-of-reaction detector using a pyroelectric film. With the growing interest in biosensors, it was decided that the decomposition of a substrate on an enzyme would provide the necessary heat-of-reaction.

The first requirement for this sensor was a method to immobilize the enzyme, catalase, so that the enzyme activity was not significantly altered, and the enzyme lifetime increased.

The next consideration was where it should be placed. The enzyme should be immobilized so the rate of temperature change experienced by the pyroelectric film will be the greatest.

Next, the size, placement and configuration of the pyroelectric film had to be delineated. Both the exposed area and the thickness of the PVDF film could be varied. The configuration for measuring a signal from the PVDF film could be either a direct measurement from a single film or a sample/reference arrangement using multiple films. If a reference film was necessary, the position in relation to the sample film also needed to be considered.

Finally, a whole host of design problems came under consideration as the sensor began to show promise. These included:

1. Thermal transfer properties of the PVDF film to the cell
2. The flow channel area and volume.

3. Volume and concentration limits of the analyte necessary to produce a measurable signal at the PVDF film.

4. The flow rate, as well as the composition of the stream carrying the analyte.

5. Production of bubbles by a reaction and the effect of the bubbles on the rest of the system.

6. Variables important in choosing a pump for the carrier stream.

7. Designing a flow system for a pressure sensitive detector.

8. An adequate amplification system for the nanoamp signal produced by the PVDF film so that the current or the voltage could be measured.

9. The hardware and electronics to support an automated sample injection.

10. A program to acquire data from the amplifier output that had the ability to allow change in data rate and gain of the programable analog-to-digital converter.

This chapter will describe the evolution of the instrument design from its conception to the final working version.

B. Instrument Evolution

1. Enzyme Immobilization Procedure

The first goal was to immobilize the catalase on the pyroelectric film in a manner that would not greatly decrease the activity of the enzyme. To immobilize the catalase, 35 mg BSA and 5 mg catalase were added to 100 µl water, mixed well and chilled. Then, 10 µl glutaraldehyde were added with a micropipet, and this solution was stirred

and spread on the PVDF film with a glass rod. This solution was allowed to crosslink until firm. The enzyme was rinsed with glycine solution to cap free aldehyde units and then rinsed with water. This method provided a thick film that adhered well to the PVDF film.

2. Detection of Signal

The next step was to assemble the electronics to measure the signal from a temperature change across the PVDF film and to see if the heat of decomposition of peroxide on the immobilized enzyme gave a detectable signal. The first attempt at measuring a signal from the pyroelectric material consisted of a square of PVDF film with its edges epoxied to a glass slide and wire electrical connections silver epoxied to each side. These wires were connected to the input of a Corning analog pH meter, used in the millivolt mode. A deflection of the meter's needle was observed when hot or cold water was added to a beaker of water containing the PVDF film sensor. A broader signal that developed at a later time was also seen when concentrated peroxide was added to the beaker with enzyme immobilized on the exposed side of the film.

3. Amplification of Signal

The next challenge was to amplify the signal seen on the pH meter sufficiently for the computer's analog-to-digital converter. Using the glass slide described above, the wires were connected to the plus and minus inputs of a CA3140 amplifier with a feedback resistor from the output to the inverting input. The output of this CA3140 was connected to the inverting input of another CA3140. This amplifier was designed

as a standard invertor amplifier with a variable amplification and a variable reference voltage at the non-inverting input. The output from the second amplifier was connected to the analog-to-digital converter, ADC, of an LSI-11. The data was collected by a simple program that used an external clock to determine the speed at which the data was taken. The signal was very noisy and showed some response to hot and cold water and to peroxide; but, the data was also extremely variable and thus not acceptable.

Using the same set up described above, an electrical connection was made from the backside of the PVDF film to the center tap of a potentiometer. The end taps of the potentiometer connected to plus and minus fifteen volts. This allowed variable voltages to be applied to the film. The wire from the exposed side of the PVDF film was connected to the non-inverting input of a CA3140 amplifier. This amplifier was configured as a current follower. The second stage invertor amplifier remained the same. This configuration gave more stable results. When hot water and peroxide were added, the resulting peak shapes were different. The peak generated by the addition of the peroxide took longer to develop than the peak generated by the addition of hot water, indicating the signal was indeed from the decomposition of the peroxide by the enzyme.

4. Data Acquisition Program

After a signal was recorded from the amplifier above using a crude acquisition program, the program was revised to better control the data acquisition. The ADC initiated a conversion under the command of a

start pulse from a real time clock.[47] The speed of the real time clock was programable from 0.1 Hz to 10 kHz. Bit 7 of its control status register was used to start the clock and bits 0, 1 and 2 controlled the speed. An octal 101 ran the clock at 10 kHz and a 106 set the clock speed to 0.1 Hz. Except when looking at noise components at high frequency, or at long term noise, the clock was usually set to 10 Hz.

The program was installed as a "task" in Forth, which when activated by the definition AQR acquired the number of points left on the top of the parameter stack. For example, 1000 AQR stored the next 1000 analog-to-digital conversions in the array DAT, at the speed indicated in the variable SPEED, and the voltage scale indicated in the variable SCALE. After the data was acquired and stored in the array DAT, the data was stored to disk with the definition DATA_SAVE. This would store only 500 data points per disk block. In the first six data addresses in the block, DATA_SAVE also saved information about the conditions under which the data was taken. DATA_SAVE stored the largest and smallest numbers in the array and the number of data points in the data set, which allowed the calculation of the number of consecutive disk blocks of data in the scan. Also stored were the numbers in the variables SCALE and SPEED. A zero was stored in address six of the disk block for use as a scaling factor in one of the data manipulating routines. These numbers were used in setting up the scales for plotting. Appendix C has a complete listing of the final Forth control and data manipulation programs.

5. Cell Design I

A simple flow-injection-analysis system was used to carry the peroxide sample to the catalase. This required a cell to be built that would hold the PVDF film and the enzyme and provide a flow channel. Theoretically, the ideal shape of the flow channel would be oval and as thin as possible with inlet and outlet holes as close to the ends of the oval as possible. This shape has the best flow characteristics resulting in minimum dispersion of the bolus. The shape of the flow channels used in this study were not quite oval; they had parallel edges and were semicircular on the ends because of the milling process by which they were made. Trade off's in volume of the flow channel and active area of the film had to be made. The volume of the flow channel should be as small as possible, reducing dead volume; but, the area of PVDF film must be large enough to produce a measurable potential and good signal-to-noise ratio.

The first cell housing was made from two Plexiglas blocks. Clear Plexiglas was used so that the flow channel could be observed and problems such as wrinkles or folds in the PVDF film or dissolving aluminum electrode on the PVDF film. The flow channel was fabricated by milling a channel 3.18 cm (1.25 inches) long with a 0.318 cm (0.125 inch) end mill 0.254 cm (0.1 inch) deep in a flattened, smooth block of Plexiglas. A 0.159 cm (0.0625 inch) hole was drilled at each end of the flow channel for entrance and exit from the flow channel. On the opposite side from the flow channel two 0.635 cm (0.25 inch) deep holes were drilled and tapped with #28 threads for Cheminert connectors.

Another area at the end of the cell was milled for electrical connections to the PVDF film.

6. Electrical Connections - Copper Tape

The first method for making electrical connections to the PVDF film electrodes in the cell was by copper adhesive tape. Electrical connections were made by cutting approximately 5 mm of the adhesive tape and soldering leads from the amplifier to the copper side of the adhesive strips. Then, the paper protecting the adhesive was removed and pressed on the uncoated corners of enzyme coated PVDF film. Soldering had to be done quickly or the adhesive charred and did not stick.

After a few uses, the adhesive failed. To relieve strain on the adhesive joint, a hole in the cell block was milled to hold the adhesive squares and electrical leads stationary. The soldering thickness and the placement on the PVDF film had to be exact so that the cell would clamp without leaking. Even then, the leads had to be replaced every few runs because the adhesive would debond from the PVDF film.

7. Flow Delivery System

The first flow delivery system to the Plexiglas cell was a two liter reservoir suspended from a ring stand. The problem with this method of delivering the carrier stream was variable flow. When the solenoid switched the sample stream in line the flow rate would drop. Also, when oxygen bubbles formed from the peroxide decomposition, the flow rate would fluctuate. This fluctuation could be seen in the flow meter.

The first sample valve, in line just before the Plexiglas cell, was a small bore, six connector, manual sample valve by Rheodyne. The valve connections, as seen in Figure 4, were numbered and connected as follows: 1 was the input from the flow stream, 2 the output to the flow channel, 3 the sample loop entrance, 4 the sample reservoir, 5 a syringe for drawing the sample in to the sample loop, 6 the sample loop exit. In the configuration shown in the figure, the sample loop is in the inject mode where 2 is connected to 3, 4 connected to 5, and 6 is connected to 1. When the valve is rotated by 60 degrees, the sample loop can be filled by drawing the sample from the Erlenmeyer flask through the loop into the syringe. The sample valve was bolted to the metal box holding the cell so that the valve could be operated from outside of the box.

The sample loop was made by connecting sample valve connector 3 to connector 6. Connecting 3 directly to 6 gave a sample loop volume of about 70 µl. Most of the experiments were run in this manner. Adding a length of tubing between these connectors gave a larger volume. Volumes of up to 1 ml were tested. The larger sample loops did not give any improvement in signal. This is explained in section VI.C.3.

8. Sealing the Flow Channel

Clamping the cell blocks together did not provide a good enough seal to keep the flow channel from leaking. Another method was tried.[39] Four strips of Teflon were placed around the edge of the flow channel between the PVDF film and the block with the flow channel milled into it. Because of Teflon's ability to flow under pressure,

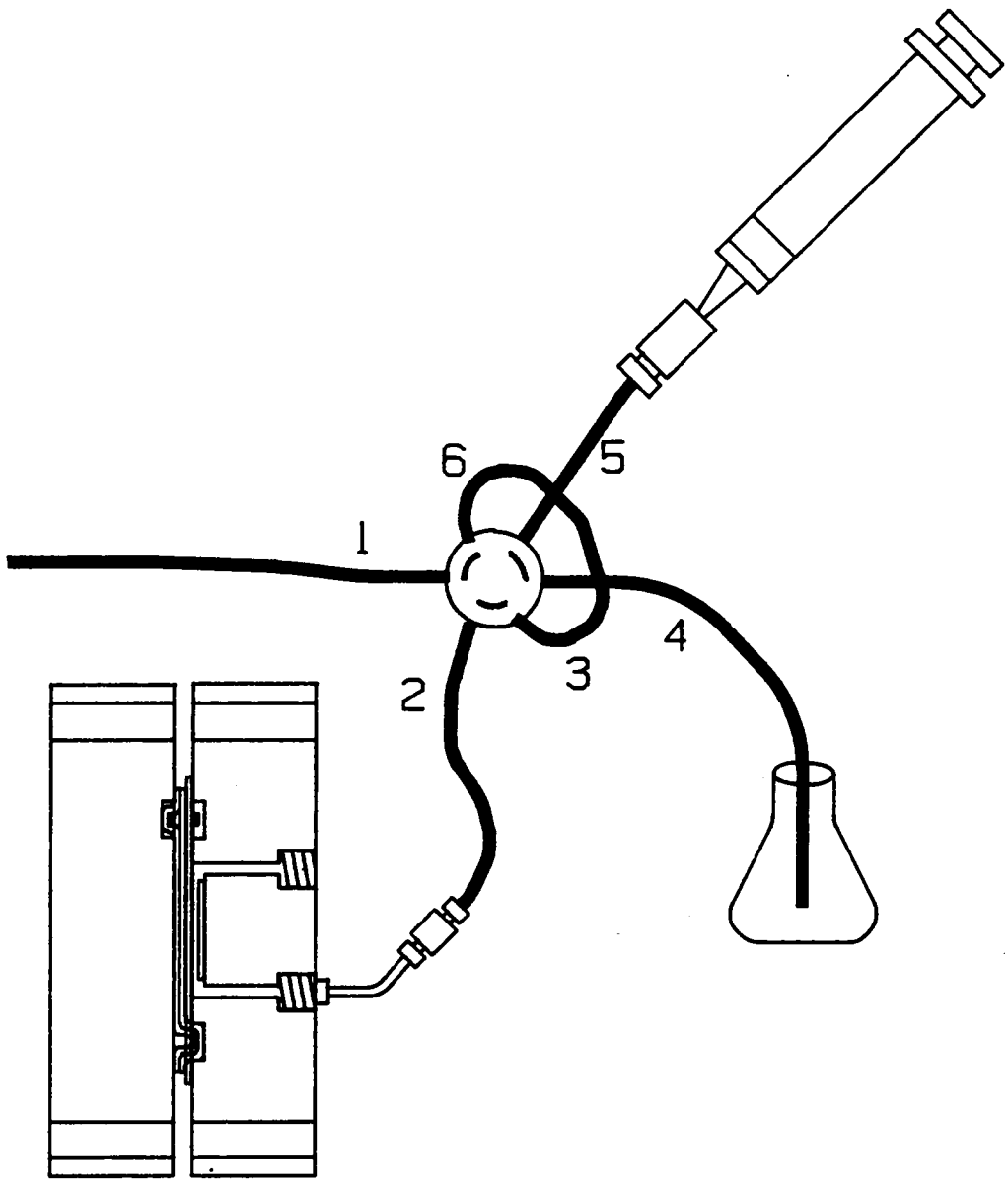

Figure 4. A standard chromatographic type injection valve.

this made an excellent seal. Problems with the Teflon seal are discussed in section 23 of this chapter.

9. Cell Design II

Using this first cell, a low frequency, drifting signal, as well as high back pressure, was observed in the flow system. A flow channel with a larger surface area would have a lower back pressure and was thus constructed.

The second cell was also milled from a smooth, flat Plexiglas block. A 1.91 cm (0.75 inch) long, 0.254 cm (0.1 inch) deep channel was made with a 0.953 cm (0.375 inch) end mill. Holes were drilled for Cheminert connectors and a place was milled for electrical connections.

10. Charge Amplifier

The signal observed from the above cell drifted, so the amplifier arrangement was changed. Because PVDF film is a dielectric, the film acts as a capacitor. The components in a charge amplifier, Figure 5, are also capacitors. The amplifier functions by following the charge on the input capacitor, the PVDF film, by charging the feedback capacitor. The problem with a charge amplifier is that if the input capacitor is not a perfect capacitor, the output of the circuit will drift over time. PVDF film is not a perfect capacitor and thus drift was observed.

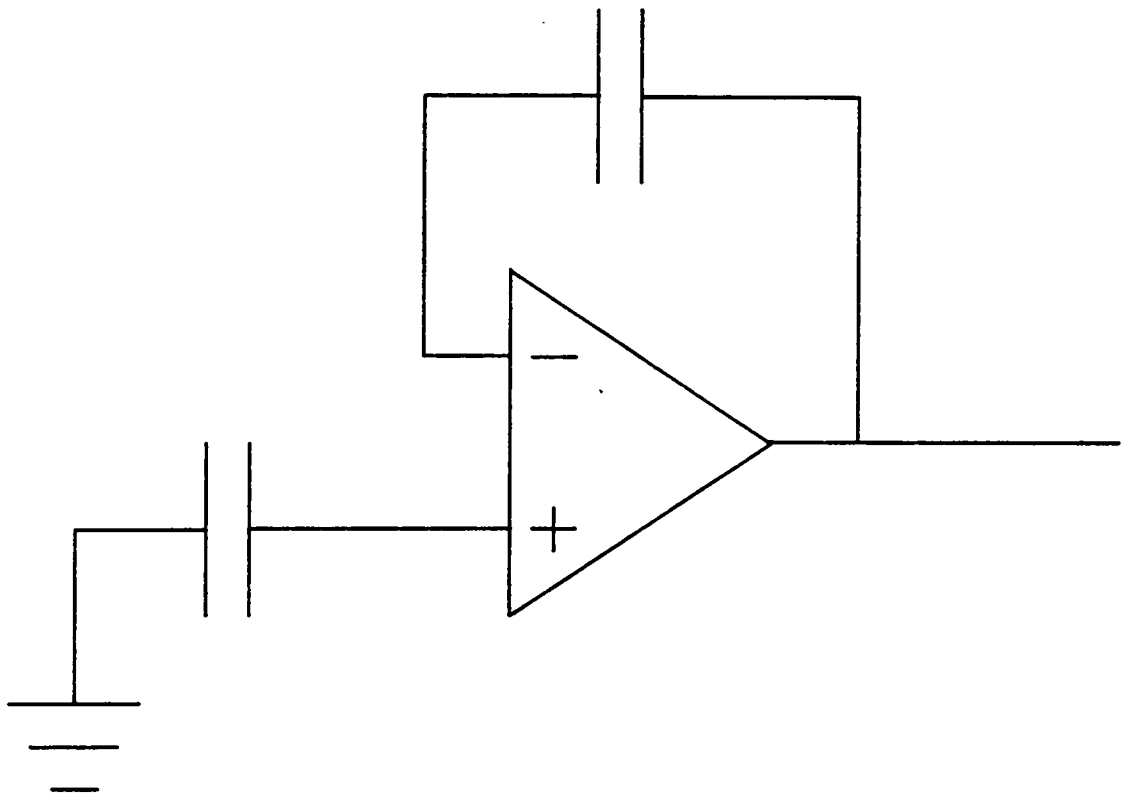

Figure 5. A standard charge amplifier.

11. Electromagnetic Shielding

It was observed that the signal fluctuated when someone walked near the cell. The aluminum electrodes of the PVDF film make excellent antennae. Therefore, the cell was placed in a metal box shielded with an aluminum foil covered cardboard box top. The shielding box and top were grounded directly to the building's electrical ground to help reduce stray electromagnetic radiation. The amplifiers were in their own grounded metal casing, also in the cell box, to keep the length of the leads from the cell as short as possible. The power supply for the amplifier was outside of the shielding box and had a shielded cable connecting it to the amplifier box. A thermally insulative material was used to cover the inside of the shielding box.

12. Electrical Connections - Alligator Clips

At this time, the Plexiglas cell was modified to accept another type of electrical connection, alligator clips. Two small alligator clips were modified by flattening the teeth. Then, electrical insulation in the form of shrink wrap was placed on the top half of one clip and on the bottom half of the other so that when clipped to the film, electrical connection was made only through one side of the clip. The leads from the amplifier were clamped and soldered to the clips. The leads were then clipped to the PVDF film through slots cut in Plexiglas so that they were making electrical connections to opposite sides. If the measured resistance was infinite, the experiment proceeded. If not, there was an electron path around or through the PVDF film. The bolts were then loosened, and enzyme film cleaned from around edges of

the PVDF film. The edges of the PVDF film were checked for folds or any electrical connection from one side to the other. Finally, the alligator clip electrical connections were checked to see if one had cut through the film.

The response from this system with the charge amplifiers was better; the standard deviation from baseline was lower. This was mostly due to the housing of the cell in the metal box. The baseline drift seen before was still present.

13. Comparitor Amplifier

The next amplifier studied was a comparitor. With the feedback capacitor removed from the previous charge amplifier, the electrical arrangement became a comparitor. The input from the PVDF film was compared to the other amplifier input and the output would swing to the positive or negative extremes of the amplifier. The second input was controlled by a digital-to-analog converter, DAC. The DAC could be incremented or decremented to keep the comparitor at the null point where small changes would make the output swing one way or the other. Under these circumstances, the voltage from the film was the same as the voltage coming from the DAC. The number controlling the DAC thus corresponded to the transducer output. This value was monitored at ten hertz. In this configuration the computer was used as the feedback component in the operational amplifier circuit. This system worked for slow and small signals, but could not keep up with the rapid changes that occurred at higher concentrations and higher frequency noise. The software could only do 300 cycles a second. Signals that used half of

the 12 bit, 4096 step, DAC range would take seven seconds for the computer to make a comparison, and by that time the peak would be over.

14. Heater / Thermostat

At this stage, a heater and thermostat were used to investigate raising the temperature of the cell and the box. The efficiency of the enzyme improves slightly as the temperature approaches body temperature. Although, the elevated temperature increased the signal, installation of the heater decreased the signal-to-noise ratio due to its noise characteristics. Electromagnetic noise from the heating coils and mechanical vibrations from the fan were sources of this noise.

To help the carrier stream come to equilibrium with the temperature in the cell box, 3 meters of 0.3 mm i.d. Nylon tubing was added. This tubing was wrapped around a plastic bottle of water in the box with the cell. Improvement in baseline stability was not noticed but this feature remained part of the apparatus.

15. Automated Injection Valve

The manual injection valve, used up to this point, had two problems: the peak position could not be accurately reproduced and the pressure pulse generated during the switching of the valve was variable. A pneumatic actuator was added in an attempt to achieve reproducible pressure pulses and to allow the computer to control the injection time so that the peak position information would be reproducible. Reproducible pressure pulses were never achieved.

A schematic of the sample loop actuator control is shown in Figure 6. The pneumatic actuator was controlled by the computer through the parallel port. Bits 1 and 2 of a parallel port were connected through buffers to two reed relays which were activated by a five volt supply. The relays were used to switch 110 volts AC to the two solenoids. There were three Forth definitions which controlled the solenoids, FIL, INJ and SET. FIL set bit 1 and cleared bit 2 which turned the valve to the fill position. INJ turned the valve to the inject position by setting bit 2 and clearing bit 1. SET set both bit 1 and 2 which turned off both reed relays controlling the solenoids. SET was necessary because the solenoids overheated if they were left on for long periods. The solenoid power supply was a Heath variable AC supply. The 5 volt supply to the reed relays was a Lambda supply, separate from the computer power supply. Switching the reed relays caused large fluctuations in the supply voltage level which caused the computer to stop if they shared a supply.

This actuator-controlled sample-delivery system did reduce the size of initial pressure pulse, thus improving the response of the sensor; however, there were problems with immobilizing the catalase.

16. More Enzyme Immobilization Procedures

Three methods for immobilizing the catalase were tried in the hopes of finding a more reproducible technique for keeping the catalase in place.

To slow down crosslinking reaction, the immobilization was done in a cold room at about 4°C. (The cold room at times got up to 15°C

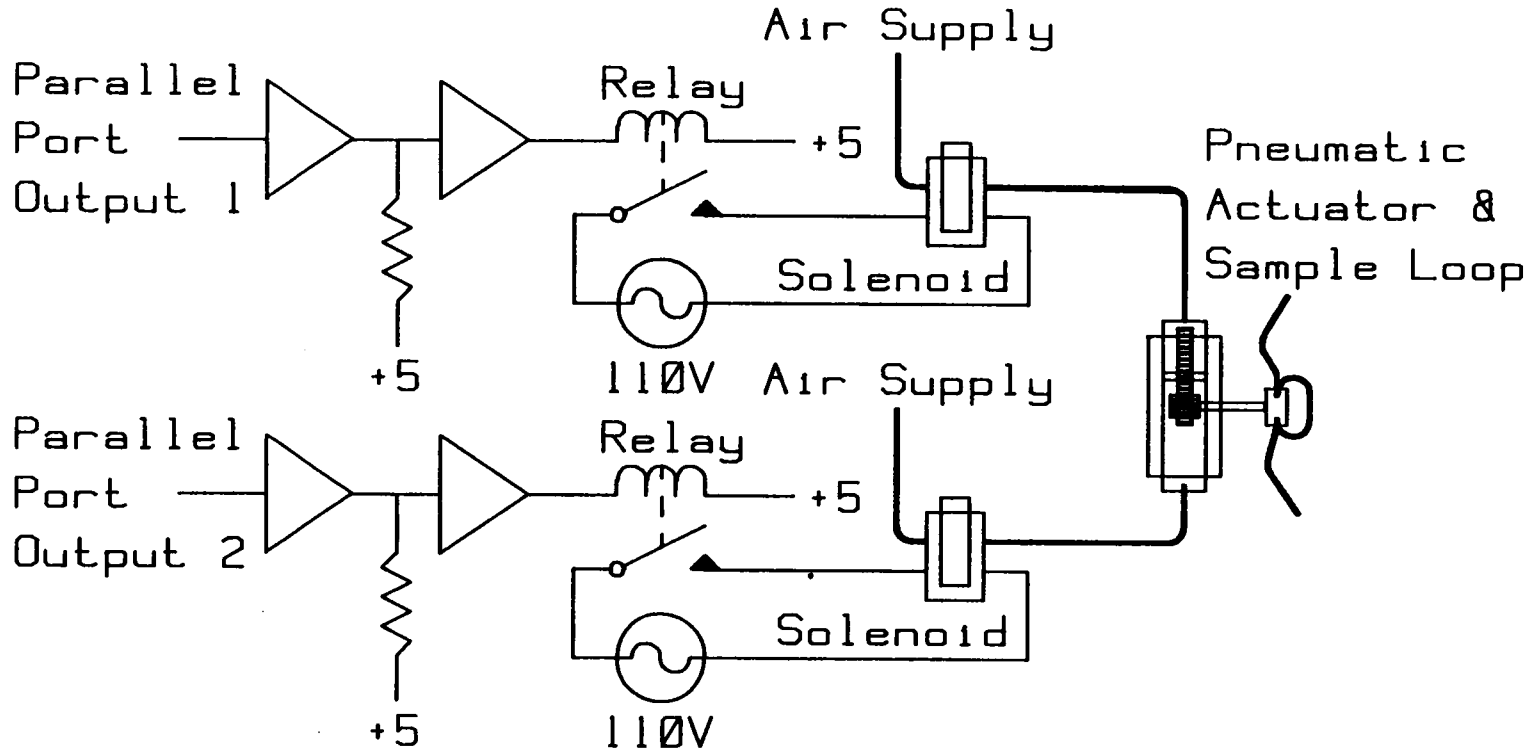

Figure 6. A schematic of the solenoid control electronics.

because of problems with the air conditioning unit.) Glutaraldehyde, glycine solution, water and PVDF film were chilled in the cold room. 35 mg BSA and 5 mg catalase were mixed well with 100 µl water in a small testtube and chilled. 10 µl glutaraldehyde was added, stirred and spread on the PVDF film. This mixture was allowed to crosslink for 10 minutes before rinsing with glycine solution to cap any free aldehyde units. Finally the film was rinsed and stored in water until the cell was ready to be assembled.

Problems existed, however, with the production of the enzyme film. It was difficult to obtain the same thickness and, at times, the immobilized enzyme occluded the flow channel. It was also difficult to cast the enzyme film the correct size for the flow channel, so that the cell would assemble without enzyme overflow at the sides. Flow of enzyme would often cause electrical connection problems. To correct this, the assembled cell had to be taken apart, cleaned and then reassembled.

Another method for applying the enzyme layer to the PVDF film was spin coating. This was attempted in order to obtain a thinner, more reproducible enzyme layer. The glutaraldehyde, glycine solution, water, PVDF film and the spin coater were chilled in the cold room. The BSA and catalase were mixed as above. The PVDF film was taped to the spin coater, with tape placed over where electrical connections would be made. The spin coater was turned on low speed and immediately after 10 µl glutaraldehyde was added to the solution. It was poured on the spinning PVDF film and let crosslink for a few minutes. The film

was then rinsed with glycine solution to cap any free aldehyde units, rinsed and stored in water until the cell was ready to be assembled.

The spin coat method did not work because the rate of crosslinking was too rapid which caused the enzyme films to come out patchy or lumpy.

A doctor's blade was also tried, however, the PVDF film was not rigid enough for easy application.

Catalase was also immobilized in Nylon 6 tubing instead of on the PVDF film. It was predicated on the thought the enzyme layer was acting as a thermal boundary between the reaction and pyroelectric film. The H_2O_2/catalase reaction took place in the tubing before reaching the PVDF film. Theoretically, the heat produced in the tubing would cause a signal when the heated liquid reached the pyroelectric film.

To pretreat the inner walls of the Nylon 6 tubing for immobilization, four to six molar HCl was injected quickly with a syringe. If the injection was done slowly the tube clogged with pieces of Nylon. The HCl treatment turns the tubing from translucent to opaque. The HCl roughens the sides of the Nylon tube making it a better surface for physical adhesion to occur between it and the crosslinked enzyme. After the HCl treatment, the tubing was rinsed with deionized water for several hours. The catalase was immobilized by first circulating a 30% glutaraldehyde solution for an hour with a peristaltic pump and then injecting 5 ml of a 5 mg/ml catalase solution. The solution was allowed to sit in the tubing overnight, occasionally mixing it with a syringe. Alternatively, the solution was circulated in the tubing by means of a peristaltic pump for two to three hours.

The data obtained from this Nylon tube-immobilized enzyme was not acceptable. A signal could be detected but it was broad and noisy. The temperature profile was too broad and the temperature change at the pyroelectric was not as large as when the enzyme was immobilized in the flow channel. The bubbles formed from the H_2O_2/catalase reaction caused too much pressure noise to obtain a usable signal.

17. Gold Coating of Aluminum Electrodes

An initially acceptable enzyme film made by the first cold room method described above degraded rapidly due to dissolution of the aluminum electrode next to the flowing stream. In an attempt to correct this, 200 μm of gold were sputtered onto a piece of PVDF film. The procedure followed for sputtering was to tape the film to a Plexiglas square that had been cut to fit in the sputter coater. Three pieces of film could be sputtered at one time. The edges of the film were taped to prevent gold being sputtered around the edges and making electrical connection between the two electrodes. Gold sputtering increased the working lifetime of the aluminum electrodes, but the gold did not adhere well to the aluminum.

18. Pumps

As noted above there were problems with the gravity feed flow system. A one speed peristaltic pump was examined as an alternative. The output from this pump was too pulsed to be useful, and the pressure regulator on the pump was too variable to get a reproducible flow rate.

A third flow system examined was a reciprocating piston pump typically used in liquid chromatography. A large pulse at the end of each stroke made this pump unacceptable.

The final pump was a Gilson variable-speed, four-channel, bi-directional, peristaltic pump. Some smaller pulses could still be detected by the PVDF film.

To help remove some of the effect of these pulses, a small reservoir was connected to the system tubing by a T. This reservoir was connected at its other end to a pressure gauge, Figure 7. The back pressure, approximately 10 psi, caused the reservoir to partially fill. This had the analogous effect of a low pass RC filter in an electrical circuit. The reservoir acted like a capacitor, with the back pressure from the rest of the flow system acting like a resistor. This addition reduced the pressure pulses considerably.

At flow rates lower than 4 ml/min, the signal to noise ratio was smaller since the temperature change felt by the PVDF film was more gradual. As the pump speed was increased the magnitude of the pressure pulses increased making it more difficult to measure small signals. These limits bracketed the speed of the system.

19. Data Manipulating Programs

Forth programs were then written to manipulate the data. Baseline correction was done by taking the average of the first fifty points and subtracting this number from all of the points in the array.

A twenty-one point Savitzky-Golay filter was used to remove higher frequency noise from the data.[12] The filter width caused an artificial

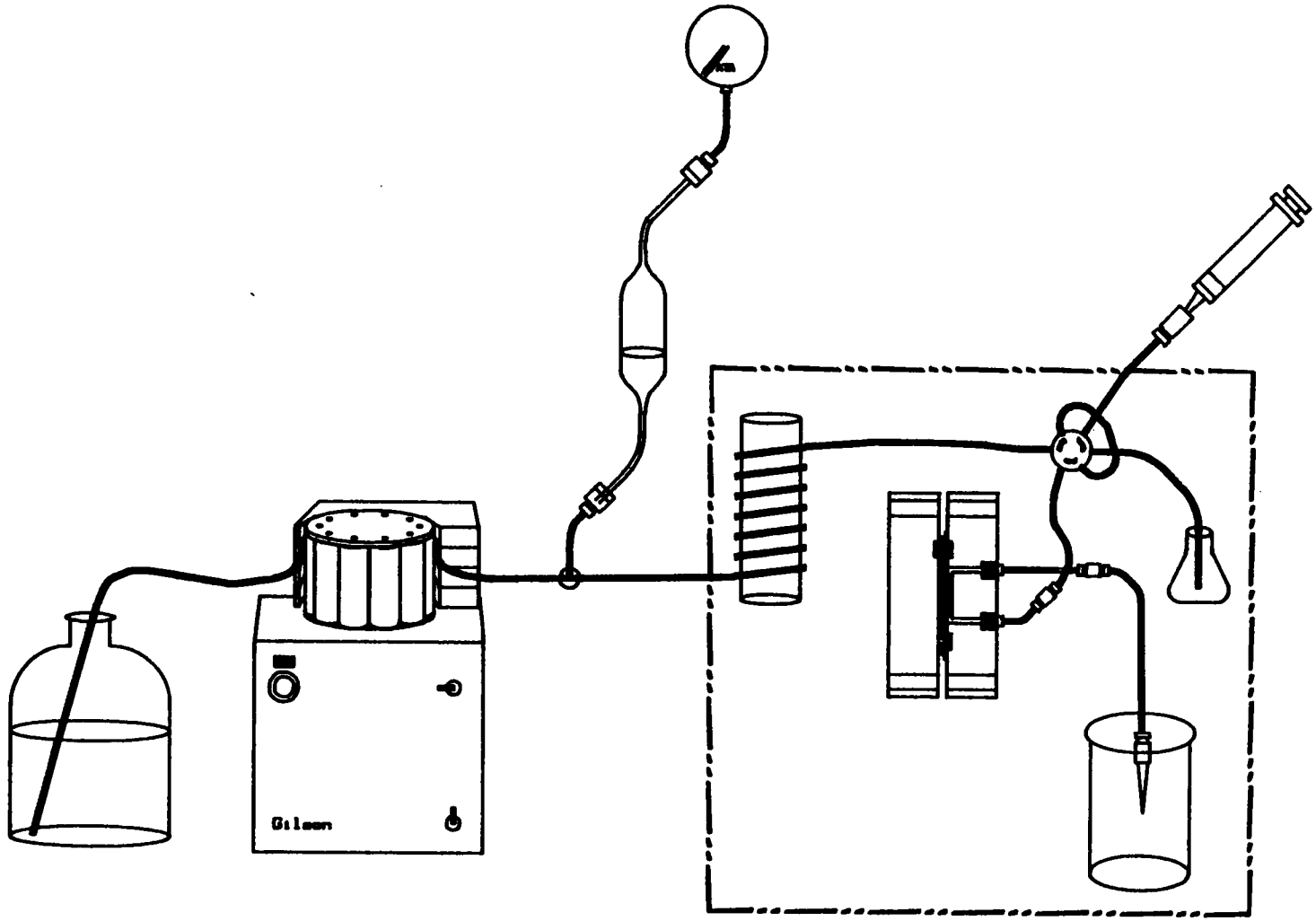

Figure 7. A pictorial representation of the flow system.

widening of the large pressure spike induced by the solenoid switching the sample valve as seen in Figure 8.

After the pressure peak, a three sigma change from baseline was used to determine the start of a peak. This information was used to determine the start of integration limits when peak areas were calculated and to test for reproducibility of the peak beginning. Three σ was picked as a reasonable, statistical difference from baseline, greater than 99% confidence limit. By observing the data, the best place to take the baseline was determined to be from 1.5 to 2.5 sec after the sample injection because the peak did not occur until at least five seconds after injection. Comparing the three σ differences both before and after applying the Savitzky-Golay filter, showed that the filtered data gave more reproducible results. Two methods of determining the start of the peak were tried. In the first approach, the average baseline and standard deviation were calculated for the first ten points. Subsequently, the first data point outside of the average plus or minus three standard deviations, three σ, was then found and the time of that point was stored. The other method kept a running average and standard deviation through the data set checking the next point to see if there was a three σ difference from the average.

Since the peak approaches baseline slowly, three variations were used to find the "return to baseline." The first variation searched for the return to within three σ of the original baseline after a peak maximum. This variation did not always work because of baseline drift. The three σ point would often occur too early if the baseline had

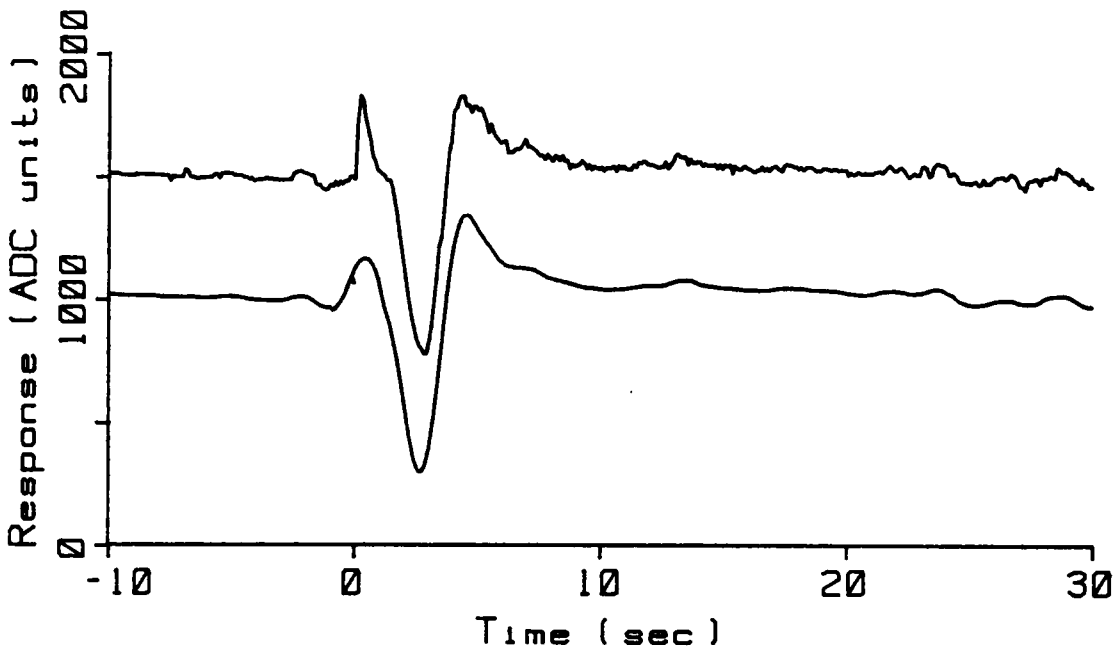

Figure 8. Representitive data showing response of system before (top) and after applying Savitzky-Golay filter.

drifted up, or if the baseline had drifted down sufficiently the three σ point would not be found. The second and third variations calculated an end average baseline and a standard deviation for the last one hundred points. The second variation then worked backward through the data and found the first point that deviated three σ from the end average baseline. The third variation started at the peak maximum and worked through the data until the program found the first data point within the three σ limit. None of these variations worked very well and reproducibility with consecutive injections was poor. Part of the problem with the second and third variations was there was increase in the amplitude of the noise at higher concentration caused by bubbles sticking to and releasing from the walls of the tubing. As the bubbles moved through the waste tube, they caused small, rapid pressure fluctuations to occur that were registered by the PVDF film.

The numbers obtained above were used as integration limits. Integration of the data would frequently over run the bounds of single precision integer mode, since integration was done by summing the data from the beginning of the peak until the end. When the integration approached the single precision limits of $+/-2^{15}$, the program would perform a divide-by-two on the integration array and the data array, update a counter, and then continue the integration. The counter was stored in the 6th disk block address with the integrated data so that the data, when plotted or used in calculations, would be correctly scaled. To scale the data to the correct magnitude, the integrated data was multiplied by 2 raised to the power of number in the counter.

The integrated data was very smooth but the resulting area determined from the integrated data was more variable than the peak height from the same data sets. This was because the baseline wandered and the "return to baseline" was not consistent. Thus, peak height was chosen as the method for measuring the signal.

20. Waste Tubing

During this study, bubbles were noticed sticking in the waste tubing. A larger diameter, shorter tube was connected to the exit from the flow channel. The waste container was also moved into the box. Baseline noise amplitude was noticeably smaller.

21. Electrical Connections - Aluminum Screw

The unused portion of the PVDF film may cause a decrease in sensitivity. The potential developed in the flow channel area would spread over a wider area. Since resistance is inversely proportional to area, the larger area would allow more electrons to leak through the film thus reducing the potential available for detection. To cut down the unused portion of the film sandwiched in the block, the cell was modified so that electrical connections to the PVDF film were made through aluminum screws as shown in Figure 9.

Electrical connections were made by drilling and tapping a hole in each block for electrical connection to each side of the film near the flow channel. #36 holes were drilled in each block close to, but outside of the flow channel. To keep from tapping the complete hole, #28 holes were drilled on top of the #36 holes leaving about 1 cm next

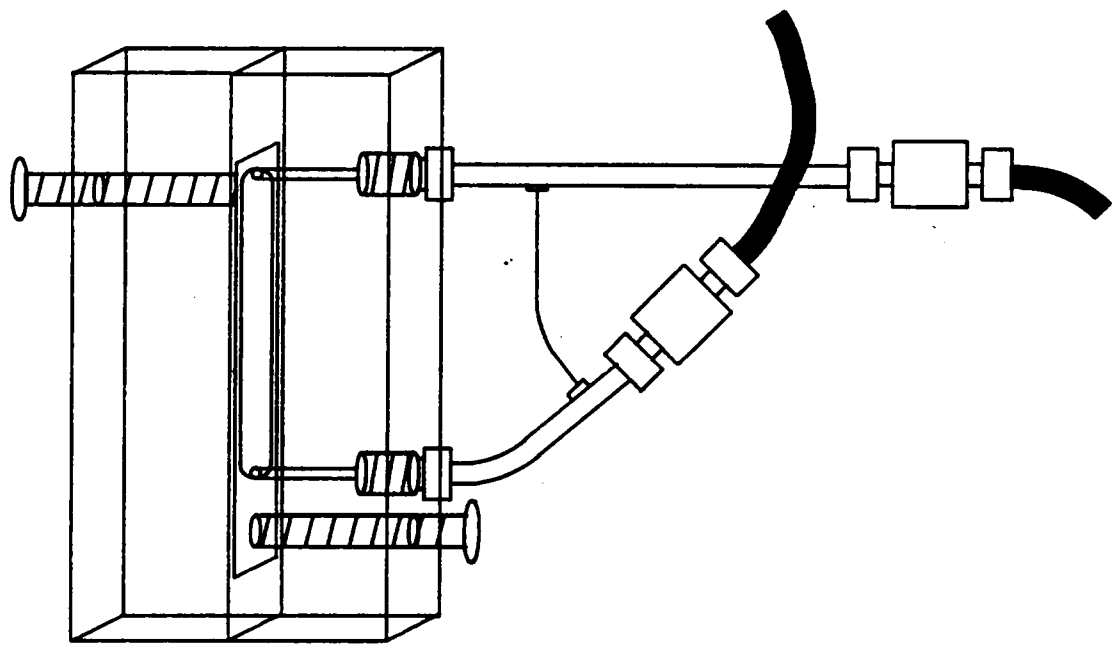

Figure 9. A representation of the cell using screws as electrical contacts.

to the flow channel to tap. The #36 portion of the hole was tapped with a #6 32 thread tap. A #6 32 thread aluminum screw with the end filed smooth and rounded was inserted. Aluminum screws were used because the PVDF film electrodes were aluminum and like metals will not react with each other. An alligator clip was used to make electrical connection from the aluminum screw to the amplifier. The aluminum screw was periodically removed to sand the tip to remove oxide buildup. This design worked as well as the previous design, but showed no noticeable improvement.

22. Cell Design III

The use of metal cells was explored to see if the thermal properties of the metal would cause a larger temperature difference across the PVDF film by providing a thermally conductive backing for the PVDF film instead of a thermally insulating material, such as the Plexiglas.

A 2.54 cm (1 inch) square piece of brass was cut into two 7.5 cm (3 inch) pieces. One side of each was flattened with fine sandpaper. A 2.54 cm (1 inch) long and 0.254 cm (0.1 inch) deep flow channel was milled with a 0.635 cm (0.25 inch) end mill. Holes were drilled for Cheminert connectors. Holes were drilled on either end of the blocks to accept bolts to hold the cell together. The PVDF electrodes were isolated from the brass by a Teflon film.

Electrical connections in the metal cells were made by the same screw method pictured in Figure 9. Electrical connections were made through wires that had been threaded through holes drilled through the axis of two 0.635 cm (0.25 inch) Nylon screws. These wires had small

disks of silver epoxy at the screw tips. The holes in the cell block for the Nylon screws were drilled so that the silver disks made electrical connection in the corners offset from one another. This offset prevented the film from being pushed into a hole opposite the connection.

A 200 mV electrical potential developed across the PVDF film in the brass cell. This potential was attributed to dissimilar metal contact. The next step was to make the cell from aluminum.

Two 2.5 by 5 by 7.5 cm (1 x 2 x 3 inch) blocks of aluminum were squared and one side of each was flattened with fine sandpaper. The milling for the flow channel was done as in the brass cell. Four holes were drilled at the corners of each block for bolting the cell together. Then the blocks were anodized to create an electrically nonconductive layer of aluminum oxide. However, the anodization did not provide a nonconductive layer; VOM probes laid on the surface at the corners showed very little resistance. The electrical connections were made through the Nylon screws. The PVDF film electrodes were isolated from the aluminum blocks by sheets of Teflon. Again, when the cell was assembled, a potential of up to 200 millivolts developed across the PVDF film. Trying to measure a weak signal superimposed on 200 mV noise was very difficult. Data from this cell also showed large baseline drift.

The next cell variation was a combination of the Plexiglas and metal cells. The half of the cell with the flow channel was made of Plexiglas. The backing for the PVDF film was an aluminum block. This half of the cell was grounded. The rational for this cell was that

only the thermal transfer through the PVDF film was of interest and that the metal exposed to the flow channel could some how be associated with the potential being developed. This cell was first tried with a Teflon seal around the flow channel. But, there was a still a large electrical potential developed in the cell and the signal drifted badly.

23. Polyimid Siloxane Copolymer Seal

One source of the noise seen in previous cells came from the Teflon seal. When Teflon and aluminum are in intimate contact, the aluminum fluorinates and becomes soluble in the flowing stream, causing the aluminum electrodes on the PVDF film to dissolve.[91] This electrochemical reaction occurring at the electrodes influenced the electrical signal being recorded, as a voltage of up to 200 millivolts was measured.

A polyimid siloxane copolymer was suggested as a pliable and inert sealing material to replace the Teflon.[92] To transform the polyimid siloxane powder into a cast film, the powder was first dissolved in THF in a wide, shallow beaker, 5 g per 100 ml. The solution was placed on a magnetic stirrer-hotplate at low heat, below the boiling point of THF, 67°C, for several hours until most of the material dissolved and the solvent evaporated, resulting in a viscous solution. The solution was poured, by decantation, on a flat, glass surface taking care to retain the particles that had settled in the bottom of the beaker. The solution was spread by rotating and tilting the glass. The solvent was allowed to evaporate from the film overnight, resulting in a rubbery, bubble-free film, free of THF. The film was approximately 1 mm thick.

To prepare the polyimid siloxane seal, a rectangle about 1 cm larger on all sides than the dimensions of the milled areas of the flow channel and the electrode connection areas (about 2.5 by 7 cm) was cut from the cast film. This rectangle was centered over the milled areas of the cell and the cell was sealed with four bolts and a C-clamp. After a few minutes, the cell was taken apart and the seal removed. The outlines of the milled areas were clearly stamped in the film. The film was cut exactly around the oval flow channel area. For the two electrical connection areas, a segment was cut out of the middle of the impressed area approximately as wide as the flow channel, 0.635 cm (0.25 inch), was cut. Cutting out only the center of the electrical connection areas allowed for some electrical isolation.

The seal would sometimes allow water to wick between the films resulting in problems with the electrical contacts. For the most part, however, this seal worked well. Now, pressure pulses were the limiting noise component. To remove this noise factor required a cell redesign-

.

24. Cell Design IV

The redesigned cell allowed two layers of PVDF film, a sample and a reference layer. Figure 10 shows an exploded view of the cell described below.

To construct this cell, two Plexiglas blocks, dimensions approximately 2.5 by 5 by 7.5 cm (1 x 2 x 3 inches), were squared and one side of each was flattened with a 7.5 cm (3 inch) end mill. This side was further flattened and smoothed with 600 grit sandpaper and water. A

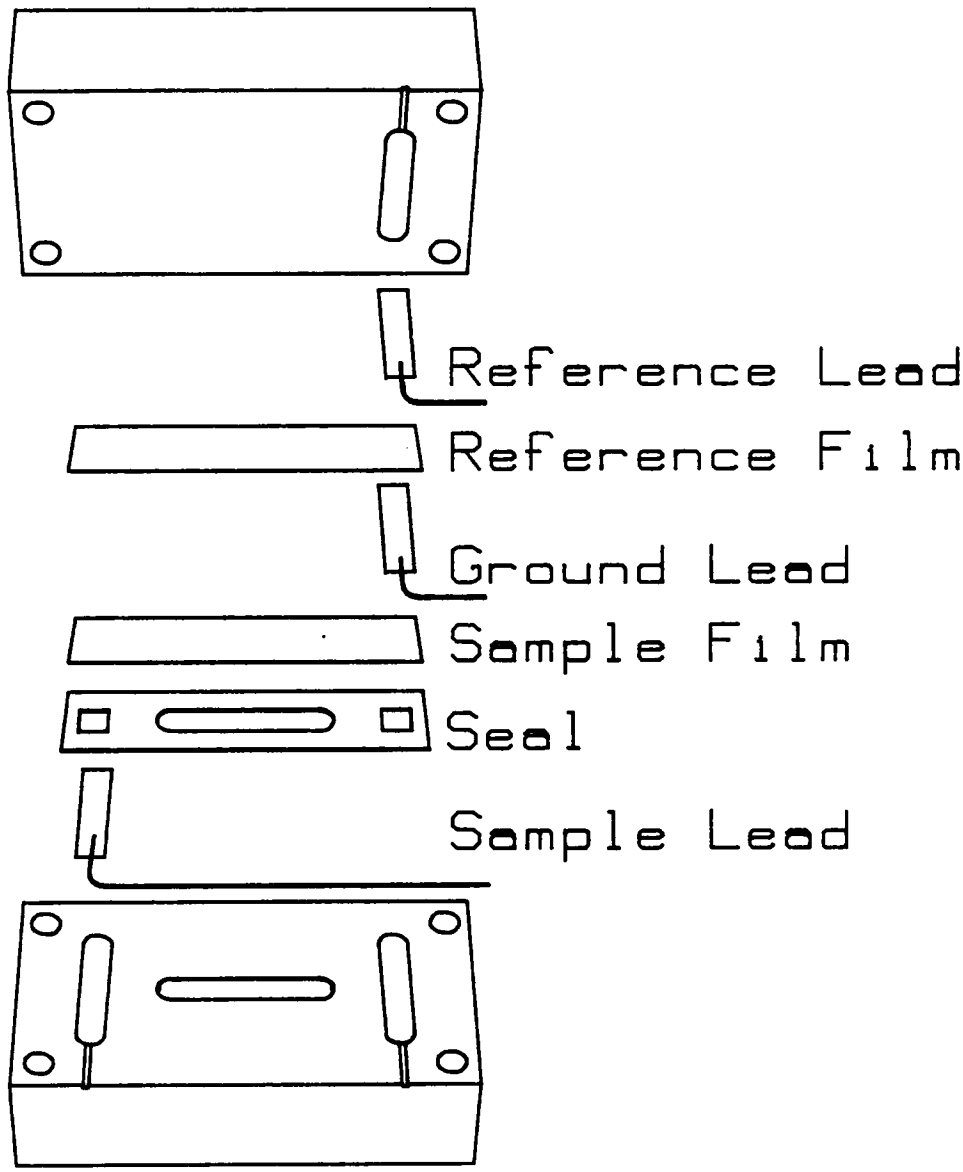

Figure 10. An exploded view of the double laminate cell.

flow channel was milled with a 0.635 cm (0.25 inch) end mill in the flattened side of one Plexiglas block measuring 0.577 cm (0.227 inch) wide by 2.786 cm (1.097 inch) long by 0.046 cm (0.018 inch) deep. Thus, the flow channel surface area was 1.54 cm^2 (0.238 square inch). The volume, without taking into account the volume lost from the immobilized enzyme or added volume from the seal thickness, was 0.070 ml (0.0043 cubic inch). From the flow channel side, a 0.159 cm (0.0625 inch) hole was drilled at each end of the length of the flow channel for inlet and outlets. From the opposite side of the flow channel, at the two 0.159 cm (0.0625 inch) holes, 0.635 cm (0.25 inch) deep holes were drilled and tapped with 28 thread holes for Cheminert connectors. Care had to be taken when these holes were made and tapped. The Cheminert connectors need a flat connecting surface to make a good seal. When the holes were threaded, the threading was started with a regular tap but was finished with a flat bottom tap. Caution also had to be taken not to insert the tap too far; if the tap was forced to the bottom of the hole, the Plexiglas would crack and chip giving a poor Cheminert seal.

0.635 by 2.54 by 0.254 cm (0.25 by 1 by 0.1 inch) slots were milled at each end of the flow channel, as well as in the flat side of the other Plexiglas block, for electrical connections to the PVDF film with silver-painted copper springs.

The two halves of the cell were held together by four large bolts, with washers, at the corners. A C-clamp was added for pressure in the middle, because the bolts did not provide enough pressure to seal the flow channel.

25. Electrical Connections - Double Laminate

The final pyroelectric film arrangement, as shown in Figure 10, used two layers of PVDF film, which is called a double laminate or a bimorph. This meant there were three electrical connections to the films. This double laminate was used to help cancel out pressure effects and stray electromagnetic radiation by taking the difference between the output of two films. The piezoelectric pressure noise was minimized by using a bimorph with poled sides of the same sign together and the middle grounded as a reference for both films. When the bimorph was exposed to a change in pressure, both films sensed the same pressure and so the outside plates developed the same potential. This is analogous to pressing on two springs stacked one on top of the other; they both feel the same pressure. In the bimorph, the differential potential due to pressure should be approximately zero. Since the temperature wave propagates through the top layer before reaching the bottom layer, a temperature difference can still be measured. The enzyme-coated first, "sample," layer of PVDF film developed a potential from temperature changes in the flow channel before the second, "reference," layer of the bimorph.

For this set of configurations, the outputs from the film were a ground to the electrodes between the two films, a sample output from the electrode in contact with the solution, and a reference output from the electrode furthest from the flow channel, next to the Plexiglas cell. The connections to the PVDF film were made through silver-coated, spring-loaded electrical contacts. The films were clamped in

the cell in opposite poling directions, like poled sides together, so the outside films gave electrical signals of the same sign for like piezoelectric conversions.

The parts of this cell were assembled on the Plexiglas block with the flow channel milled into it, Figure 10, After the enzyme was immobilized, the sample electrical connection was put in the end of the cell with the single milled slot and taped in place at the edge. The seal was positioned around the flow channel and over the electrical connection slots, and then the corners of the seal were taped in place. The sample layer of PVDF film was placed over the flow channel and the edges taped over the electrical connection to prevent the reference or ground electrodes on the PVDF film from touching the sample electrical connections. The electrical connection attached to the cable shield (ground) was put in the slot at the other end of flow channel. Then, the sample film was pushed into the slot under the ground and was taped in place. The reference layer of PVDF film was placed over the sample layer being sure that the film was in the opposite poled orientation as marked before cutting. The reference layer was taped in place on the edges of the film at the ground electrical connection so that the ground and reference electrical connections did not touch. The second electrical connection was bent into place so that the electrical connection fit into the milled slot in the other Plexiglas block. The other Plexiglas block was then put into place. The films were kept in position by tightening the four screws and the C-clamp.

To determine that electrical connections were proper, the resistance was measured with the VOM. If the resistance was measurable, the

cell was taken apart and checked for folds in the film or improperly taped edges.

26. Differential Amplifier

The next stage involved building an amplifier that would accept the signals from the sample and reference PVDF films, take the difference between them, and amplify the result.

The first differential amplifier, Figure 11, had the outsides of the film, the sample and reference outputs, connected to the non-inverting inputs of two RCA CA3140 amplifiers. The non-inverting inputs were used because they have a very high input impedance, 10^{13} ohms. Making this first stage of amplification a non-inverting voltage amplifier allowed measurements to be made with as little perturbation as possible to the small current coming from the film. Precision feedback resistors were used. A precision feedback resistor was connected to the inverting input, and a precision resistor of the same resistance was connected from the non-inverting input to ground. This arrangement was wire wrapped and gave usable results, but the baseline signal would not stay on scale even with offset nulling. Amplification at each step was probably too large.

Another amplification step was added, as seen in Figure 12. This stage involved a current-to-voltage converter for both the reference and sample outputs. An AD515 is an electrometer with a high impedance input, $10^{13}\Omega$, and a very small input bias current, 300 FA. The electrometer packaging was a TO-99 can with gold coated leads, an offset null capability and a guard pin, pin 8, connected to the case.

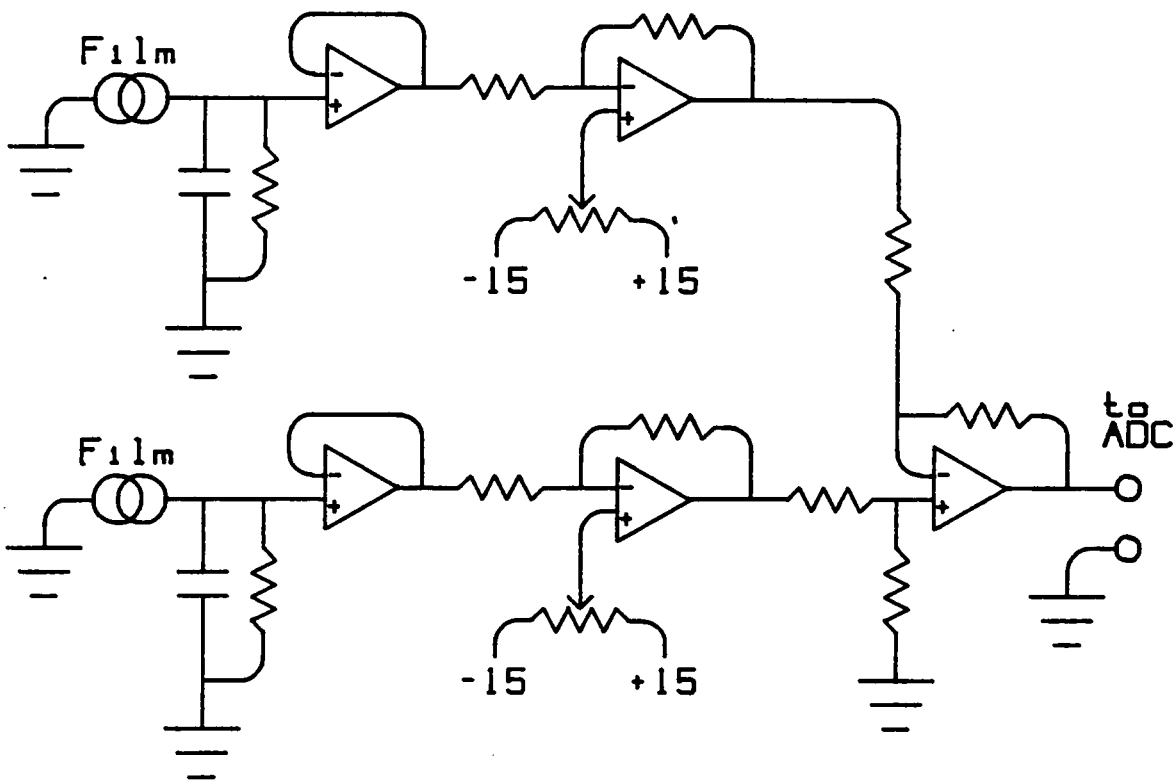

Figure 11. The schematic of the amplifying circuit using all CA3140 operational amplifiers.

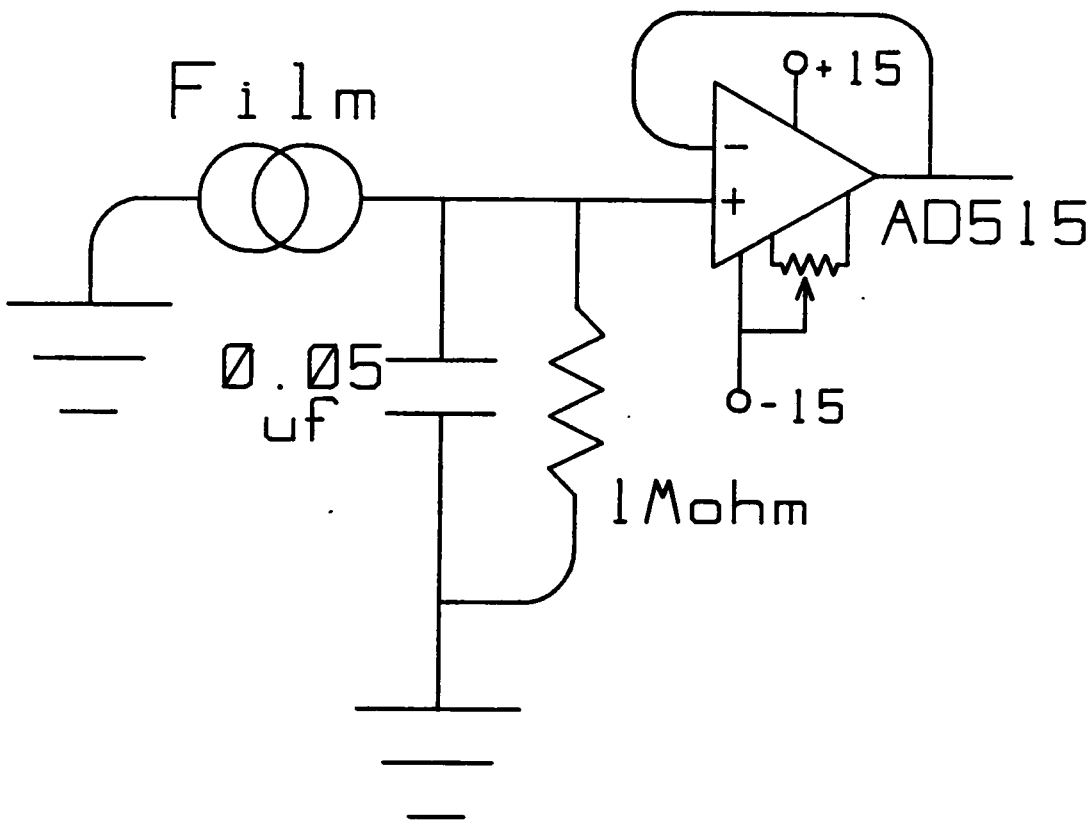

Figure 12. The schematic of the amplifying circuit using AD515 electrometers as the first stage of amplification in a current-to-voltage configuration.

Pin 8 allowed the case to be driven at the same potential as the inputs to minimize voltage leakage between the case and the input. The case also shielded the amplifier from stray electromagnetic radiation. A one megohm resistor and a 0.05 μf capacitor were also connected to these inputs and to ground. The capacitor was installed to remove high frequency noise. The second stage of amplification was a pair of inverting amplifiers. The outputs of the AD515s were connected to the inverting inputs of two CA3140s through a matched pair of precision resistors. A matched pair of precision feedback resistors were used. The gain was controlled by the ratio of the two resistors. The non-inverting inputs were connected to the center taps of 20 kΩ, 20 turn variable resistors whose ends were connected to plus and minus 15 volts. The variable resistors allowed selection of a reference voltage so that the outputs of the second stage could be adjusted to zero volts before the scan started. The results obtained from this amplifier were acceptable. A measurable, reproducible signal was detected, but there was still some high frequency noise. In an attempt to reduce noise picked up in the leads, a PC board was designed so that it could be mounted immediately adjacent to the side of the cell block, Figure 13. The board contained only the two AD515s and an inductor/capacitor network to condition the power to the board. Electrical connections to the AD515s were made through shielded coax cables. The PC board had a ground plane as well as the guard rings. The guard rings were driven to the same potential as the non-inverting input of the AD515s by the output of the AD515s. All components were soldered in place except the electrometers, which were socketed in gold coated, 8 pin, solder-tail

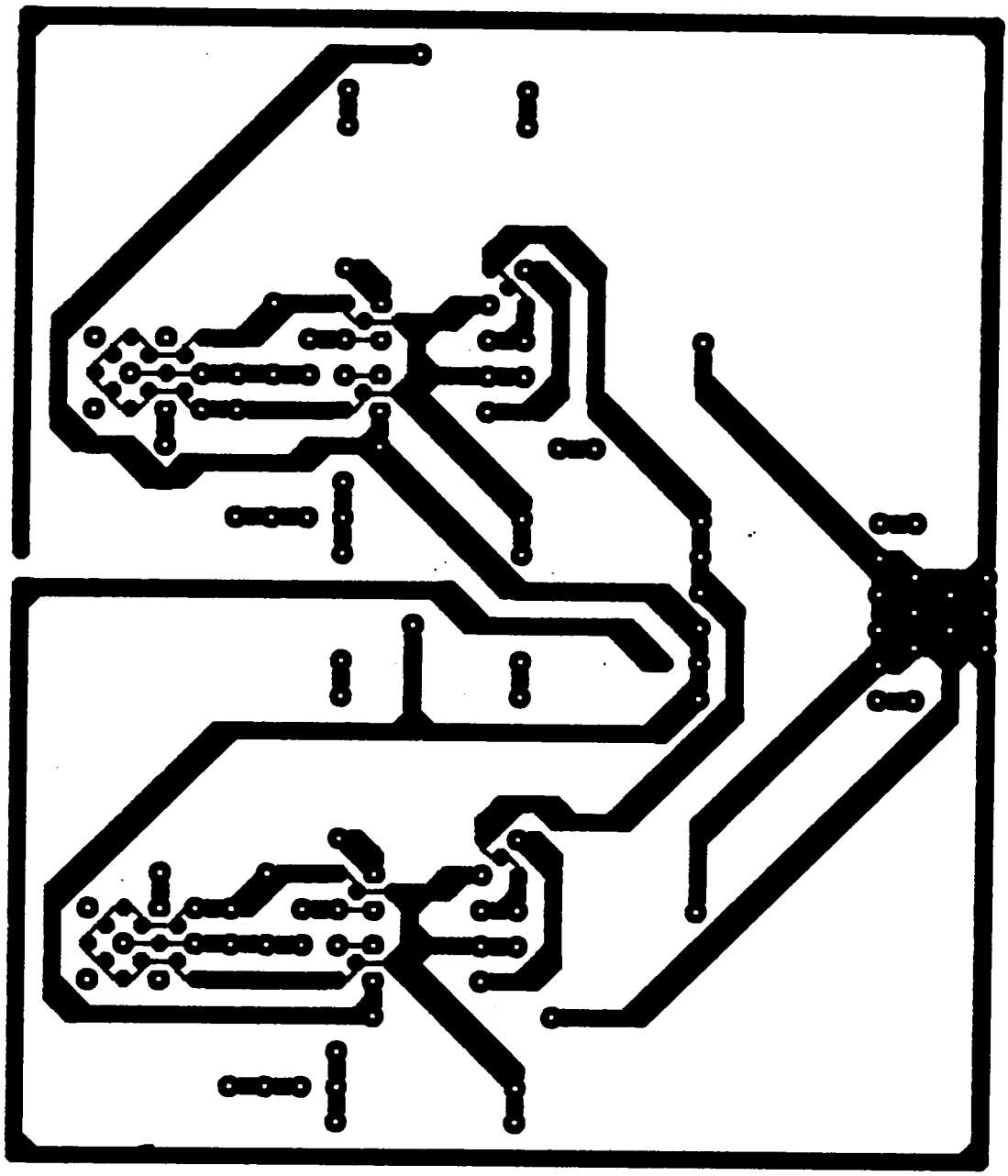

Figure 13. The artwork for the printed circuit board made to mount the AD515 electrometers.

sockets. The sockets allowed easy replacement of the amplifiers for checking the circuit, a necessity since the AD515 is fairly sensitive to static shocks and needed to be checked when problems arose. After the components were affixed to the board, it was washed with pure ethanol to remove finger prints and other oils that could provide conductive paths for parasitic leakage between input and supply traces on the PC board.

On examining the circuit in Figure 11, one observes that the second half of the amplifier system is an instrument amplifier. Therefore, an AD625 was used to replace the three CA3140s as shown in Figure 14. The AD625 is a low cost, resistor programable gain, precision instrument amplifier DIP that can have gains from 1 to 10,000. The gain is controlled by three resistors, two of the same resistance, R_F, and a third, R_G, which control the gain through the following equation.

$$G = (2R_F/R_G) + 1 \qquad V\text{-}1$$

Analog Devices recommends using 20kΩ resistors for R_F to minimize RTO noise, offset voltage and offset voltage drift.[33] Higher gains lowered the maximum frequency response, but these cutoff frequencies were at least three orders of magnitude higher than the frequency of the signal used in this system. Gains of 80 and 200 were used.

The final amplifier system, Figure 14, used the pair of AD515 electrometers in the double laminate design described above. These AD515s were connected to the films by 10 cm of small diameter shielded coax cable. The electrometer outputs were connected to the AD625 instrument amplifier which had been wire wrapped on a protoboard and

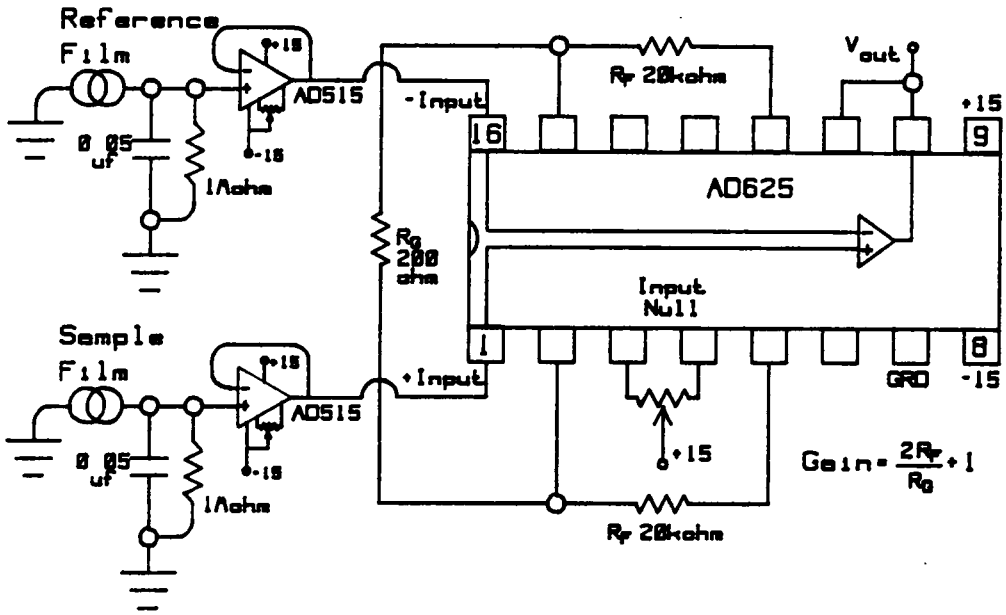

Figure 14. The schematic of the complete amplifying circuit using an AD625 instrument amplifier as the difference amplifier.

placed in a shielded box. The output of the AD625 was connected to the analog-to-digital converter.

27. Enzyme Immobilization Site

The final location for enzyme immobilization was in the flow channel, itself. In this configuration, the sample flowed between the enzyme and the pyroelectric film. Since the film measures only temperature differences, faster temperature changes are better. The peroxide decomposition heats the water passing by at 4 ml/min giving a sharp initial temperature change. The lateral mixing of the flow stream is faster than the thermal transfer would be through the enzyme layer if the enzyme was immobilized directly on the PVDF film. The final temperature change would be sharper than in previous designs because the carrier stream displaces the warmed solution, returning the flow channel to the original temperature.

5 to 10 mg bovine serum albumin, BSA, was mixed with 50 µl of catalase solution and cooled to 12 - 15°C. 5 µl of glutaraldehyde were quickly added and stirred. 30 µl of this solution were immediately spread over the surface of the flow channel. More than 30 µl caused a restriction in the flow channel. Care was taken to leave about 3 mm space at the ends of the flow channel for the inlet and the outlet of the flow channel. The crosslinking was allowed to progress for 2 to 5 minutes resulting in a firm gel. The cell had to be assembled immediately to prevent the enzyme layer from drying out. This method gave a calculated thickness of about 0.2 mm, but was thicker due to hydration. The total cell "flow" volume was approximately 0.1 ml.

28. Location of Cell

There was still high frequency noise in the baseline. PVDF film is also pressure sensitive and vibrations will cause an electrical signal. The cell was sitting on a wood desk that had several fans sitting on it, too. Moving the cell to an adjacent cabinet reduced the amount of high frequency noise in the data. Putting the metal box on rubber stoppers decreased the noise even further. Figure 15 shows an average baseline before and after moving the cell.

29. Thickness Study

Solvay makes 9 μm, 25 μm and 40 μm thick PVDF films. These were each tried in the above cell. The 9 μm film was very flimsy, difficult to handle, and gave a very weak signal. The 25 μm film was easier to use than the 9 μm, but the 40 μm film gave a stronger, more reproducible signal. One reason is the average temperature difference between the films will be greater for the thicker films, giving a stronger signal for the same temperature change. This is discussed further in the next chapter.

30. Film Modification Discovered through Modeling

After modeling the thermal flow, discussed in the following chapter, it became apparent that a thermal insulator between the sample and reference layers should increase the differential output signal seen between the layers. The modifications to the cell were simple, two extra layers of PVDF were placed between the sample and reference

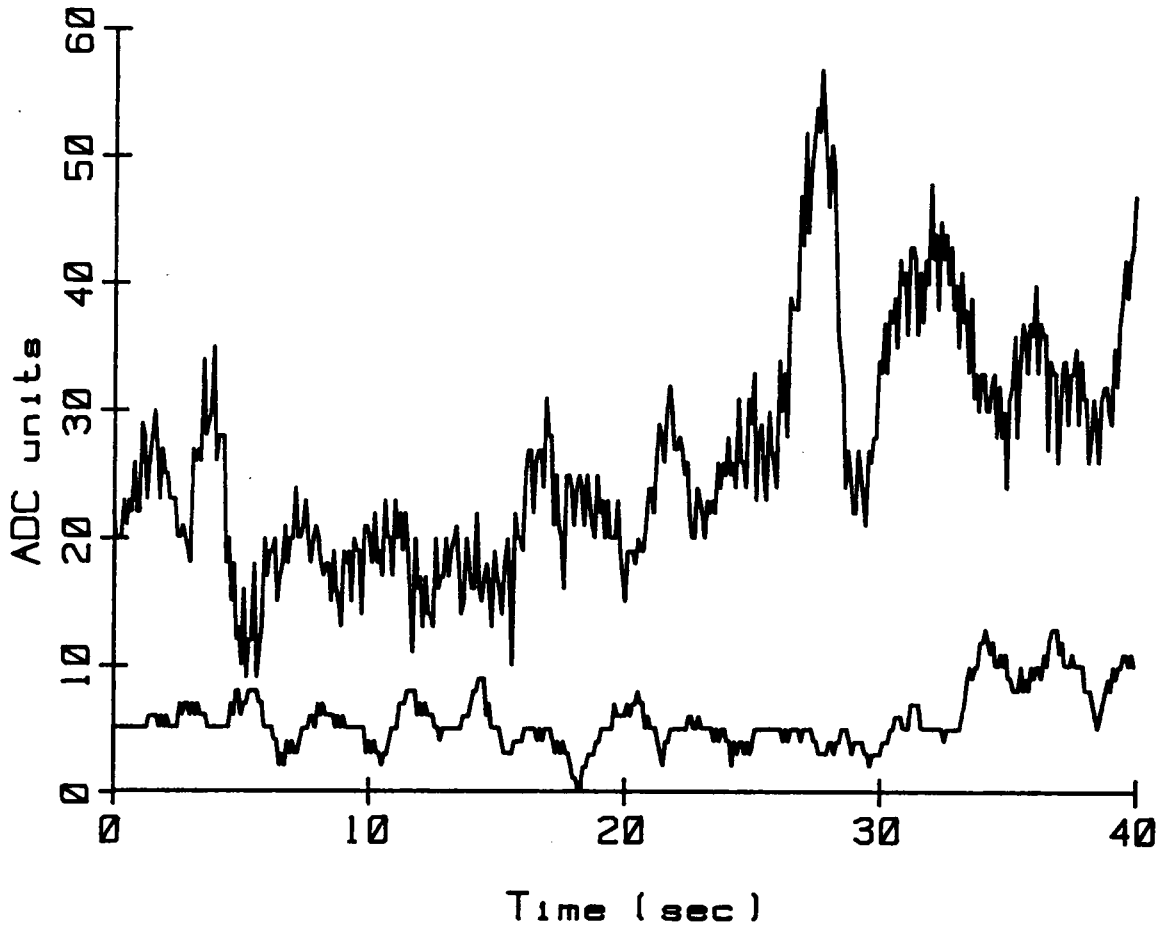

Figure 15. Data taken directly before (top) and after moving the sensor from a vibrating surface to a non-vibrating surface.

layers, giving the thermal wave 80 μm further to travel. All of the electrodes on the center two films were grounded so that no signals were obtained from these electrodes. The response for this configuration is shown in the next chapter.

C. Summary

The components of the working instrument are summarized below. 50 μl of catalase solution were immobilized by covalent crosslinking with 5 μl of glutaraldehyde to 10 mg bovine serum albumin, a large protein. 30 μl of this solution were placed in the flow stream. The catalase showed very little degradation after immobilization and was very active after crosslinking. The enzyme was immobilized across the flow channel from the PVDF film, allowing mixing of the flow stream to be the primary method of heat transfer. The final PVDF film configuration was a double laminate using two 40 μm thick films. The area of the film was as small as was conveniently possible without making electrical contact difficult. The cell was milled from Plexiglas; metal cells presented more problems and showed no improvement in the results. The flow channel was long and narrow, but not narrow enough to constrict flow. The volume of the cell was the same order of magnitude as the sample volume. The flow rate, at 4 ml/min, was fairly rapid for a FIA system. Even with the rapid flow, the signal took almost a minute to come back to baseline. A surfactant was added to the carrier stream to keep the bubbles formed small. A low-pulse peristaltic pump was used to pump the carrier stream and this was followed in the flow stream by a depulser. A two-stage amplifier was built with the first stage being

a current-to-voltage converter for both a sample and reference PVDF film and the second stage being a difference amplifier. Some of the major noise sources isolated were electromagnetic radiation and mechanical vibration. These were minimized by placing the cell and amplifier in a grounded shielding box on vibration suppressing mounts. Another major source of noise resulted from the chemical interaction between the Teflon seal and the aluminum electrodes. This problem was alleviated by changing the seal to polyimid siloxane. Programs were written and modified to control the sample injection, acquire, manipulate and plot the data.

The next chapter will describe the results obtained from the instrument described above.

VI. RESULTS AND DISCUSSION

A. Instrument output

The conditions used to conduct the experiments are as follows. A hydrogen peroxide stock solution, approximately one molar, was standardized by the method described in chapter IV. Hydrogen peroxide solutions were made by successive dilution by half starting at approximately one molar. Data was taken at concentrations of 1 M, 0.5 M, 0.25 M, etc., until the peak was not discernible from the baseline. All materials for rinsing and diluting were kept in the shielding box containing the cell to minimize the temperature difference between the solutions and flowing stream. Each set of data was taken at ten hertz, with ten seconds of baseline before injection of peroxide sample. After the data was taken, the baseline was corrected to zero ADC units and a twenty-one point Savitzky-Golay filter was applied to the data to remove the high frequency noise.

Figure 16 shows a representative set of data at different concentrations. There are three peaks that occur during each data set. The first peak is a pressure peak that occurs at time zero when the solenoid switches the sample loop in stream. This peak is sharp in the unfiltered data, but the Savitzky-Golay filter broadens it as discussed in chapter V.19. The negative peak is the response from the heat of reaction of the peroxide in the flowing stream with the immobilized enzyme. The positive, third peak results from cooling and is explained further in section 3 of this chapter. Each scan shown is the average of five scans at one concentration. The "maximum" was measured as the

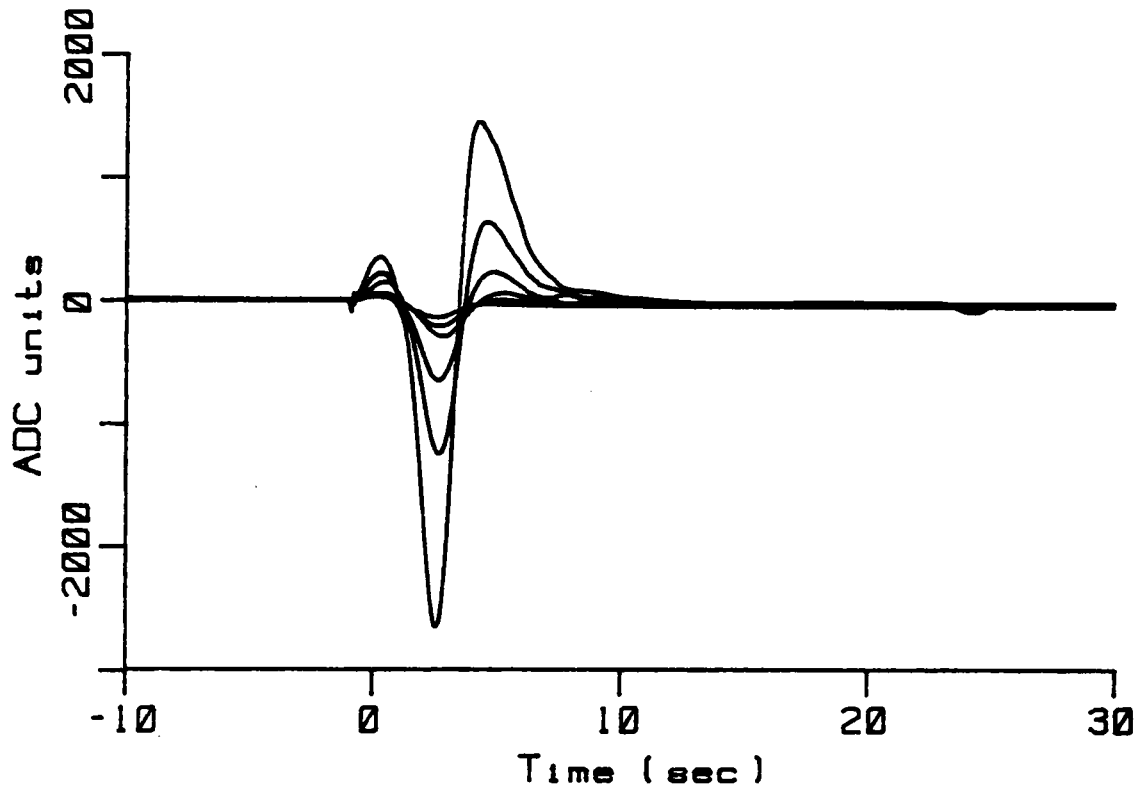

Figure 16. A representative set of data at different concentrations. The first peak is a pressure peak that occurs at time zero when the solenoid switches the sample loop in stream. The negative peak is the response from the heat-of-reaction of the peroxide in the flowing stream with the immobilized enzyme. The positive, third peak results from cooling.

absolute difference between the average baseline before injection and the maximum negative signal. The peak heights decrease by approximately half as the concentration of the peroxide is diluted by half for each line on the plot. Figure 17 is a calibration curve constructed by calculating the best line (linear regression) through the maximum peak heights for the five runs at each concentration shown in Figure 16. The following table gives the average peak height, standard deviation, and percent standard deviation for the data shown in Figures 16 and 17.

Table 1. Data from Figures 16 and 17 showing peak heights and standard deviations for five points at each concentration.

Concentration (molar)	Peak Height (ADC units)	St.D.	%St.D.
1.00	2664.6	47.4	1.79%
0.500	1247.7	53.5	4.31%
0.250	662.5	58.3	8.82%
0.125	300.3	23.0	7.73%
0.0625	214.2	15.6	7.33%
0.0312	141.2	21.9	15.5%

The correlation coefficient of the linear regression is 0.995. The points shown are the actual maximum peak heights and the vertical lines through the data points show plus and minus 2.776 standard deviations, 2.776 σ, from the average, or a 95% confidence limit for a data set with four degrees of freedom. Because of the rapidity of the rate of reaction, up to 10^7 molecules of peroxide per second per molecule of catalase, and peroxide concentrations used, the limiting step of the reaction is the hydrogen peroxide diffusion to the catalase. Therefore, in the concentration range presented here, the response should be linear.

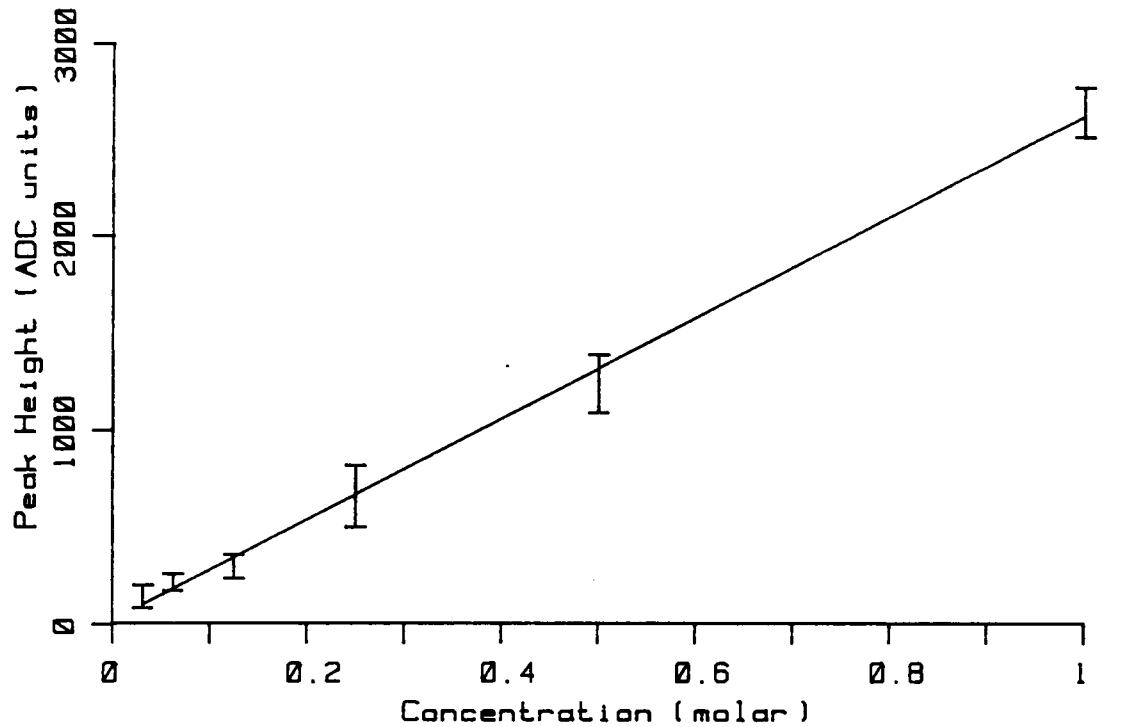

Figure 17. A calibration curve constructed by calculating the best line (linear regression) through the maximum peak heights for the five runs at each concentration shown in Figure 16.

The average peak heights and average standard deviations for fifteen sets of comparable concentration series are presented in the following table as well as the number of points contributing to each.

Table 2. Responses from 15 set of comparable data comparing peak heights and standard deviations.

Concentration	Peak Height	St.D.	%St.D.	# Pts.
1.00	2271.1	115.	5.41%	70
0.500	1095.9	97.3	8.25%	74
0.250	576.4	49.7	7.37%	70
0.125	318.5	33.9	12.3%	70
0.0625	201.9	25.2	21.3%	60
0.0312	145.5	26.2	24.9%	50
0.0156	105.0	22.4	15.5%	30
0.00781	66.4	19.5	35.0%	27
0.00391	49.1	17.7	45.5%	18

The linear regression correlation coefficient for the peak height data is 0.9988.

B. Calibration

1. Reproducibility Within One Set of Data

A plot of the average standard deviation of response versus concentration for all data used to characterize the final sensor design, Figure 18.A, shows the standard deviation increases with concentration. This was, in part, due to the noise caused by the production of oxygen bubbles; larger bubbles were produced at higher concentrations. However, a plot of the average percent standard deviation (standard deviation * 100 / average peak height) versus concentration shows, Figure 18.B, that it tends to increase with decreasing concentration. This means that a smaller peak height with the same absolute amount of

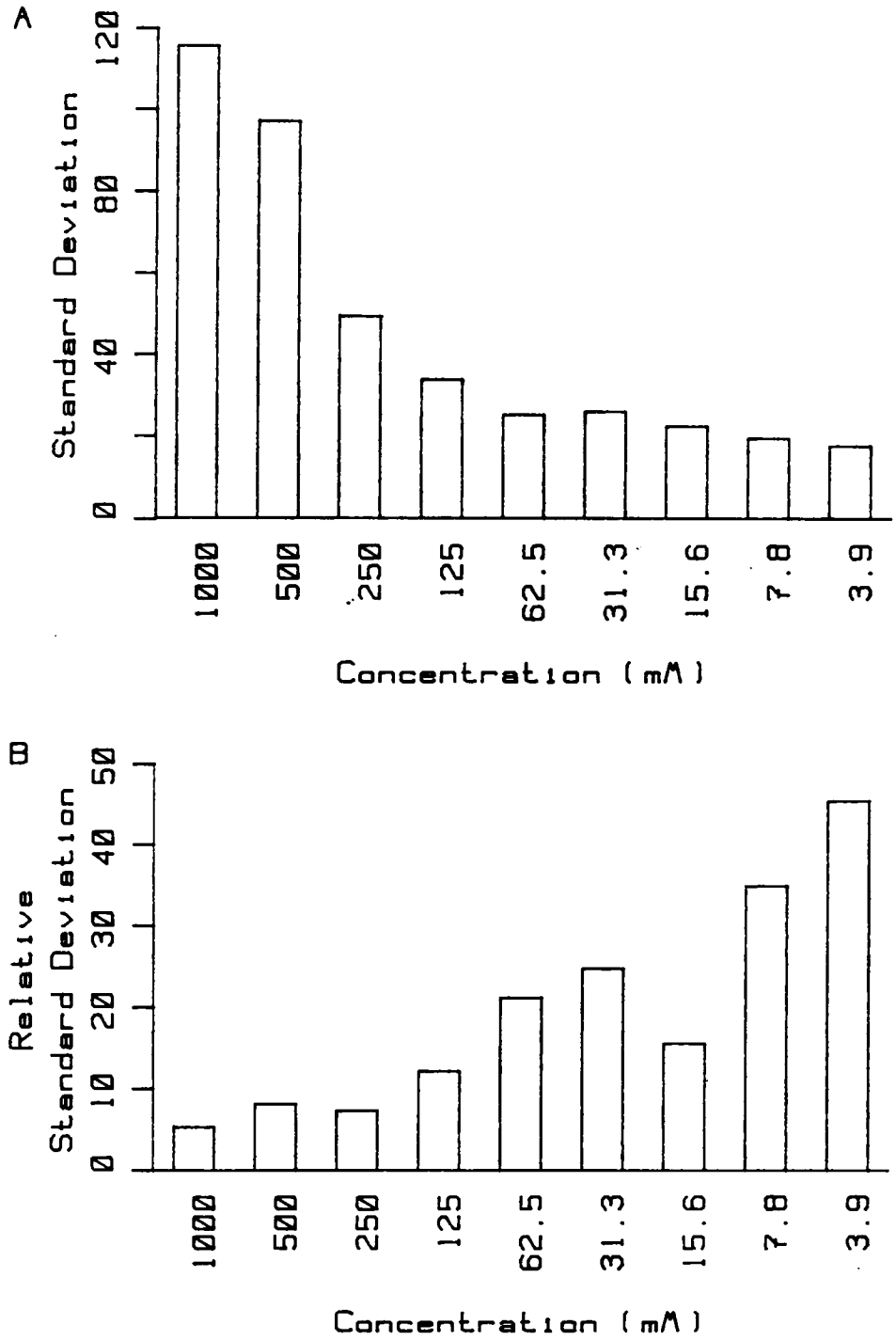

Figure 18.A. Standard deviation versus concentration. B. Percent standard deviation versus concentration.

noise will show more percent variance. The responses at lower concentrations will be less accurate, as expected.

At a few points, the graphs do not follow these trends. This is because of differences in the number of "good" runs that were made at any concentration. For different enzyme preparations, the minimum detectible quantity changed. Data was also taken as time would permit. No runs were stopped and continued later in the interest of keeping the variation due to time at a minimum. Occasionally, the maximum response at high concentrations would saturate the amplifiers and a flat line would occur. This would preclude using the first concentration but not the rest of the set of data.

2. Reproducibility Between Different Sets of Data with One Enzyme Preparation over Time

Figure 19 shows that the reproducibility for different runs within an enzyme-film preparation for two enzyme-film preparations. Plot 19 shows the response, as measured from the average peak height, decreases with decreasing concentration. Runs A through E show similar responses. However, the average response of the fifth data set, run E, is significantly smaller than the first four sets. The first four data sets were run within six days and the last was run two weeks later. After going out of the measurable range at the highest concentration (due to negative amplifier offset not a more intense signal) the response of this series of samples quickly dropped off. After one order of magnitude change in concentration the signal could not be measured. Other enzyme-film preparations have lasted for more than a

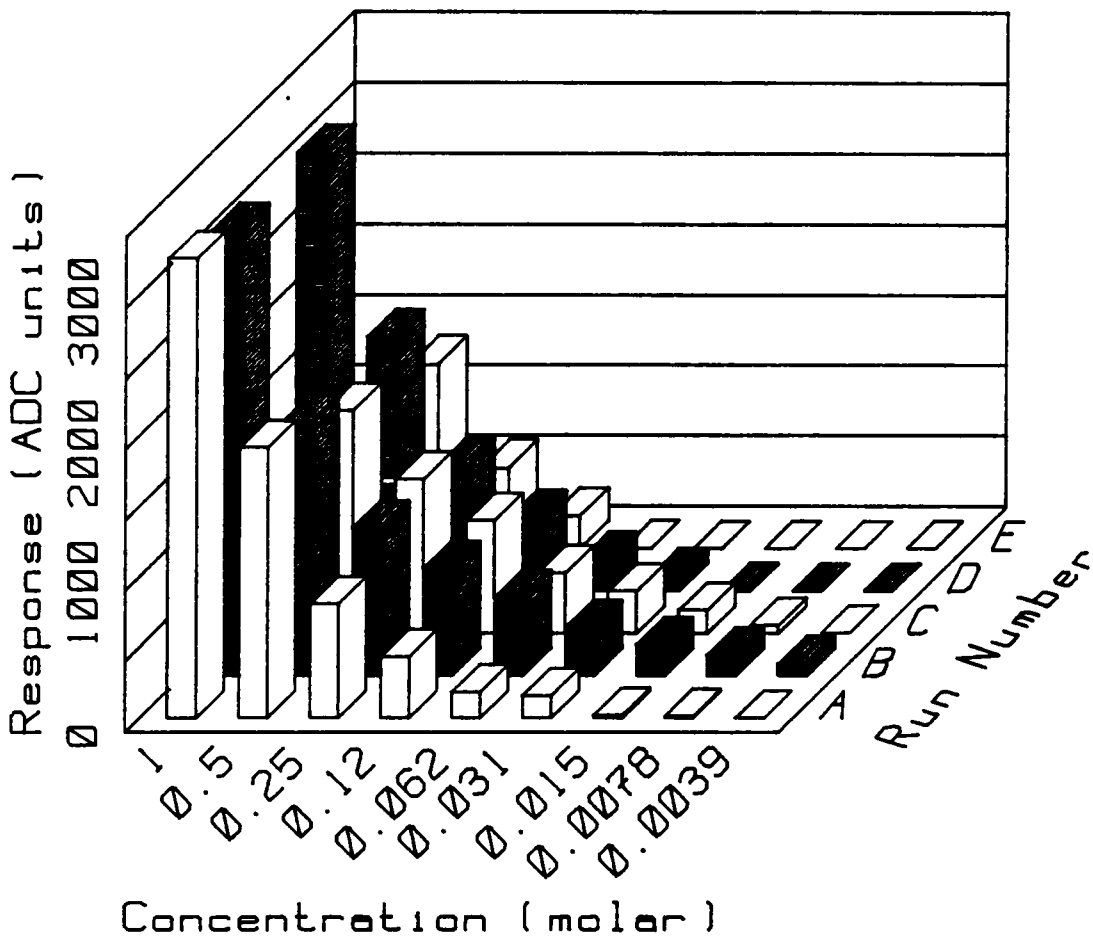

Figure 19. Average response versus concentration with one enzyme preparation over time.

month. The lifetime depends on use and care of the enzyme. If the system is not run for several days, the enzyme may loose activity. This may be from immobilized enzyme drying out and collapse of the hydrated structure.

C. Modelization of Heat Flow through PVDF Bimorph

1. Development of Theory

In an effort to understand how the layers of PVDF film responded to temperature change, the thermal transfer was modeled through a semi-infinite solid. A semi-infinite solid is infinitely thick and has only one surface. This is a reasonable assumption when the PVDF film is backed by Plexiglas because they have similar heat transfer properties. Plexiglas has a higher heat capacity but a lower density and higher thermal conductivity. The overall combination gives Plexiglas a higher thermal diffusivity.

	PVDF[22]	Plexiglas (PMMA)[24]
Density, ρ (g/cm_3)	1.78	1.19
Heat Capacity, C_p (J/g K)	1.3	1.42
Thermal Conductivity, κ (W/cm K)	0.0013	0.00193
Diffusivity, α (cm^2/s)	5.6×10^{-4}	1.1×10^{-3}

The aluminum electrodes are of little consequence to the heat flow. The time scale calculated for temperature flow through 200 Å of aluminum is negligible compared to the flow through 40 μm of PVDF film. It takes about 10^{-7} seconds for 90% of the temperature imposed on one surface to be measured 200 Å into aluminum. The thermal mass of the aluminum is also much less than that of water. For comparison, the

diffusivity, α, for aluminum is 0.93 cm^2/s and for water is 1.4×10^{-3} cm^2/s.[18] Heat flow radially along the aluminum will be absorbed into the PVDF and the Plexiglas very shortly after it leaves the heated area because of their relative diffusivities. Because the heat diffusion is faster along the electrode, the heat loss along the electrode is no longer linear. It will decrease with the square of the distance away from the heat source. The area heated by lateral diffusion through the electrode is negligible compared to the area heated by the flowing stream.

The heat flow through the semi-infinite solid was modeled using numerical integration of the following heat transfer equation. It involves one-dimensional thermal transfer through planes in the solid where the solid before time t = 0 is at one temperature.[55,56]

$$\alpha \frac{\delta^2\theta}{\delta x^2} = \frac{\delta\theta}{\delta t} \quad , \text{ where } \theta = f(x,t) \qquad \text{VI-1}$$

At time t = 0, heat is applied to the surface of the solid. This surface is plane 0 at a distance x = 0 from the surface. At times $t > 0$, a temperature change will have occurred at some plane $x > 0$ into the solid and the temperature difference, θ, (the difference in temperature from the temperature at time 0) at this plane will be a function of x and t. α is the diffusivity of heat for a given substance. As shown in equation VI-2, it is a function of the thermal transfer coefficient, £, density, ρ, and heat capacity, C_p.

$$\alpha = £/(\rho C_p) \qquad \text{VI-2}$$

Equation VI-1 can be approximated by replacing the infinitely small differences δx and δt with finite differences Δx and Δt, thus dividing the system into planes of Δx thickness and observed at Δt intervals of time. Because θ is a function of x and t, a Taylor series is used to substitute for each half of equation VI-1. Neglecting second and higher order terms, the change in temperature with time t, at plane x, is

$$\frac{\delta\theta}{\delta t} = \frac{\theta_{x,t+\Delta t} - \theta_{x,t}}{\Delta t} \qquad \text{VI-3}$$

Likewise, substitution into a Taylor series, again neglecting second order terms and higher, gives

$$\frac{\delta^2\theta}{\delta x^2} = \frac{\theta_{x+\Delta x,t} - 2\,\theta_{x,t} + \theta_{x-\Delta x,t}}{\Delta x^2} \qquad \text{VI-4}$$

A method developed by Schmidt substitutes equations VI-3 and VI-4 into equation VI-1 as follows[87]

$$\theta_{x+\Delta x,t} - 2\,\theta_{x,t} + \theta_{x-\Delta x,t} = \frac{\Delta x^2}{\alpha\Delta t}\left[\theta_{x,t+\Delta t} - \theta_{x,t}\right] \qquad \text{VI-5}$$

Setting

$$M = \Delta x^2/\alpha\Delta t \qquad \text{VI-6}$$

and rearranging the above equation gives

$$\theta_{x,t+\Delta t} = \frac{\theta_{x+\Delta x,t} + (M-2)\,\theta_{x,t} + \theta_{x-\Delta x,t}}{M} \qquad \text{VI-7}$$

Equation VI-7 says that the temperature of plane x at any time $t+\Delta t$ depends on the temperature of plane x and planes to either side $x-\Delta x$ and $x+\Delta x$, at time t.

Equation VI-7 can be derived from a physical explanation as well. To simplify the physical problem of calculating the temperature difference, θ, as a function of x and t, the semi-infinite solid can be divided into planes with thickness Δx numbered 0, 1, 2,..., m - 1, m, m + 1,.... Time is divided into time increments Δt which can be numbered 0, 1, 2,..., n - 1, n, n + 1,... . Thus, θ in planes m - 1 and m + 1 must be determined at time n. For this simplification, the temperature of any plane is only dependent on the adjacent planes at the previous time increment, or mathematically

$$\theta_{m,n+1} = f(\theta_{m-1,n} , \theta_{m+1,n}) \qquad \text{VI-8}$$

The amount of heat Q transferred from layer m - 1 to m at time n is approximately

$$Q = £ S \frac{(\theta_{m-1,n} - \theta_{m,n})}{\Delta x} \Delta t \qquad \text{VI-9}$$

where £ is the thermal conductivity and S is the area of the planar surface. The amount of heat Q transferred from layer m to m + 1 at time n is approximately

$$Q = £ S \frac{(\theta_{m,n} - \theta_{m+1,n})}{\Delta x} \Delta t \qquad \text{VI-10}$$

And the amount of heat transferred from time n to time n + 1 is approximately

$$Q = \int C_p S \Delta x (\theta_{m,n+1} - \theta_{m,n}) \qquad \text{VI-11}$$

where $\int$ is the density and C_p is the heat capacity.

Combining equations VI-9, VI-10 and VI-11 yields equation VI-12.

$$\pounds\, S(\theta_{m-1,n} - 2\theta_{m,n} + \theta_{m-1,n})\Delta t/\Delta x = \rho C_p S\, \Delta x(\theta_{m,n+1} - \theta_{m,n}) \qquad \text{VI-12}$$

By substitution of equations VI-2 and VI-6 into VI-12 and solving for $\theta_{m,n+1}$, equation VI-12 reduces to VI-13,

$$\theta_{m,n+1} = \frac{\theta_{m+1,n} + (M-2)\,\theta_{m,n} + \theta_{m-1,n}}{M} \qquad \text{VI-13}$$

Equation VI-13, derived through physical explanation, is analogous to equation VI-7, which was derived mathematically.

From the derivation of equation VI-6, M must be a number greater than or equal to 2. If M is less than 2, as the wall is heated the body will cool. Schmidt's Rule sets M = 2 in equation VI-13. This is mathematically acceptable because Δx and Δt are not constants and can be chosen to be any number. Smaller Δx and Δt will give better resolution but computational time goes up geometrically. With this substitution, equations VI-7 and VI-13 simplify to the following.

$$\theta_{m,n+1} = \frac{\theta_{m-1,n} + \theta_{m+1,n}}{2} \qquad \text{VI-14}$$

Simply stated, the temperature at plane m at time n + 1 is the average of the temperatures of the adjacent planes m - 1 and m + 1 at time n. At times before n = 0, all θ's are at the same temperature, T_{init}. At time n + 1 = 0, a constant temperature source is applied to plane m = 0, yielding a temperature difference, $\theta_s = T_s - T_{init}$, where T_s is the temperature of the source. The following shows the simple calculations for temperature differences $\theta_{m,n}$ of all planes at times n = 0 to 3, where $T_{init} = 0$.

n+1 = 0 m = 0 $\theta_{0,0} = \theta_S$

$m = 1,2,\ldots \quad \theta_{1,0} = \theta_{2,0} = \ldots = 0$

$n+1 = 1 \quad m = 0 \quad \theta_{0,1} = \theta_S$

$m = 1 \quad \theta_{1,1} = \frac{\theta_{0,0} + \theta_{2,0}}{2} = \frac{\theta_S + 0}{2} = \frac{\theta_S}{2}$

$m = 2,3,\ldots \quad \theta_{2,1} = \theta_{3,1} = \ldots = 0$

$n+1 = 2 \quad m = 0 \quad \theta_{0,2} = \theta_S$

$m = 1 \quad \theta_{1,2} = \frac{\theta_{0,1} + \theta_{2,1}}{2} = \frac{\theta_S + 0}{2} = \frac{\theta_S}{2}$

$m = 2 \quad \theta_{2,2} = \frac{\theta_{1,1} + \theta_{3,1}}{2} = \frac{\theta_{S/2} + 0}{2} = \frac{\theta_S}{4}$

$m = 3,4,\ldots \quad \theta_{3,2} = \theta_{4,2} = \ldots = 0$

$n+1 = 3 \quad m = 0 \quad \theta_{0,3} = \theta_S$

$m = 1 \quad \theta_{1,3} = \frac{\theta_{0,2} + \theta_{2,2}}{2} = \frac{\theta_S + \theta_{S/4}}{2} = \frac{5\,\theta_S}{8}$

$m = 2 \quad \theta_{2,3} = \frac{\theta_{1,2} + \theta_{3,2}}{2} = \frac{\theta_{S/2} + 0}{2} = \frac{\theta_S}{4}$

$m = 3 \quad \theta_{3,3} = \frac{\theta_{2,2} + \theta_{4,2}}{2} = \frac{\theta_{S/4} + 0}{2} = \frac{\theta_S}{8}$

$m = 4,5,\ldots \quad \theta_{4,3} = \theta_{5,3} = \ldots = 0$

Figure 20 graphically shows the above mathematical description, where the x-axis is the plane number, m, and the y-axis is the temperature difference, θ. $\theta_{0,n} = \theta_S$ for all n and $\theta_{m,0} = T_{init}$ for all planes $m > 0$. To represent what happens at time $n + 1 = 1$, a line is drawn between $\theta_{0,0}$ and $\theta_{2,0}$. $\theta_{1,1}$ is determined at the "intersection"

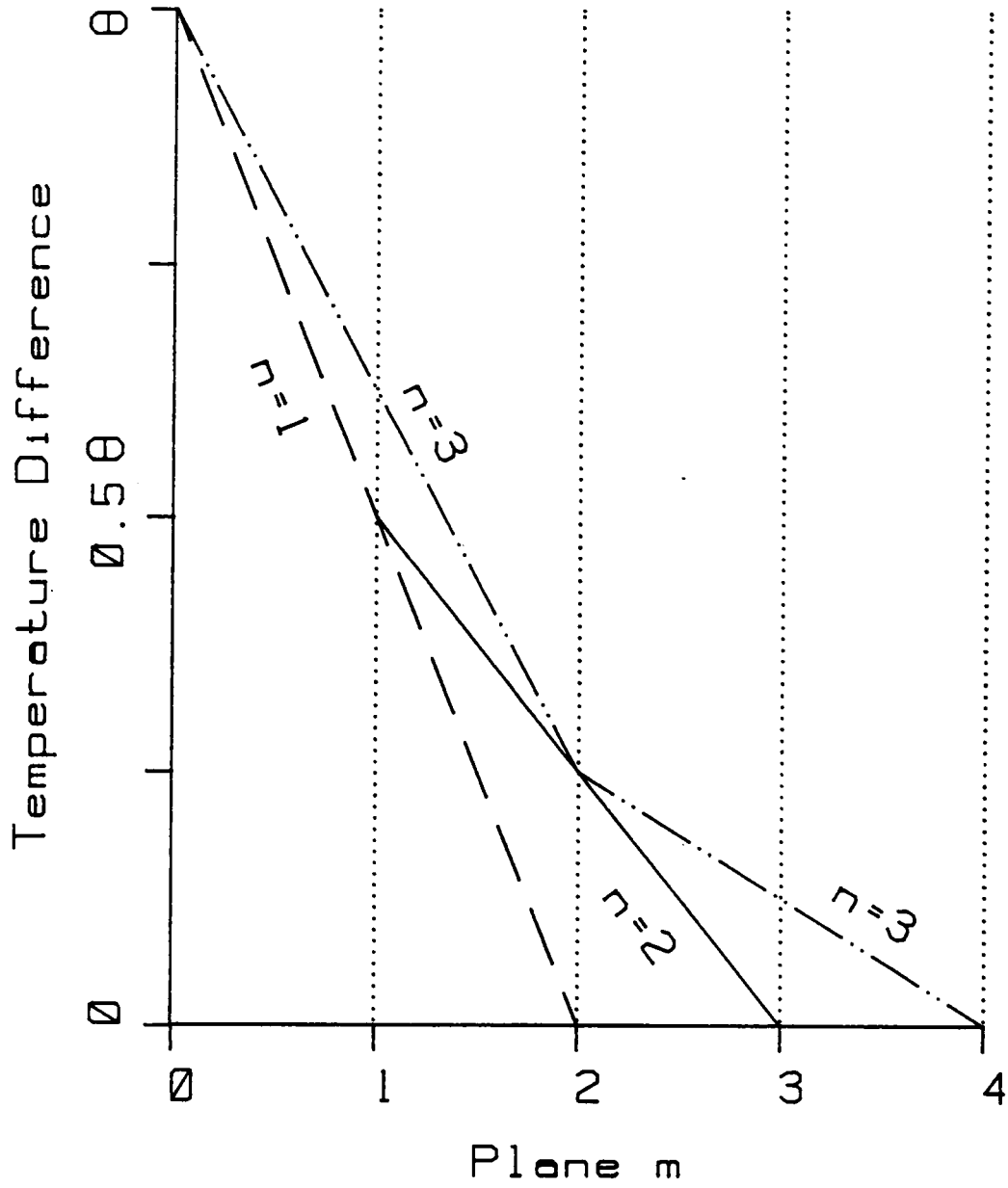

Figure 20. A graphical representation of the finite mathematical diffusion formulas presented in the text.

of plane m and the drawn line. All $\theta_{m,1} = 0$ for $m > 1$. At time n + 1 = 2, a line is drawn from $\theta_{1,1}$ to $\theta_{3,1}$ and the intersection of the line with plane m = 2 is $\theta_{2,2}$. $\theta_{1,2}$ is the same as $\theta_{1,1}$, which happens every other plane every other time period. All $\theta_{m,2} = 0$ for $m > 2$. At time n + 1 = 3, lines are drawn from $\theta_{0,2}$ to $\theta_{2,2}$ and from $\theta_{2,2}$ to $\theta_{4,2}$ the intersection of the line with planes 1 and 3 is $\theta_{1,3}$ and $\theta_{3,3}$. $\theta_{2,2}$ is the same as $\theta_{2,3}$, and all $\theta_{m,3} = 0$ for $m > 3$.

The number of time increments, n, is calculated combining equations VI-2 and VI-6, setting M = 2, and solving for Δt.

$$\Delta t = \int C_p \Delta x^2/2 \pounds \qquad \text{VI-15}$$

Knowing the density, heat capacity and thermal conductivity of the solid, and choosing a suitable plane thickness, Δx, gives the time increments, Δt, for each n.

2. Heat Flow through PVDF with ΔT = Step Function

By choosing the plane thickness, Δx, to be small enough, a smooth curve develops which is a good fit to the ideal function as shown in Figure 21. Figure 21 is a model of a 80 μm of PVDF film with Δx chosen to be 40, 20, 10, and 5 μm. The top lines for each of the time intervals were calculated using the plane thickness increment, Δx = 40 μm, so there are only 2 line segments across the graph. The top line, where Δt = 0.2 sec and Δx = 40 μm, is a straight line because the temperature at plane 1 is the average of plane 0 and 2 for this time increment, as discussed above. This allows rapid calculation of θ at a point, but the accuracy is not very good. The next line down for each of the 3 times were calculated using Δx = 20 μm. They follow more closely the

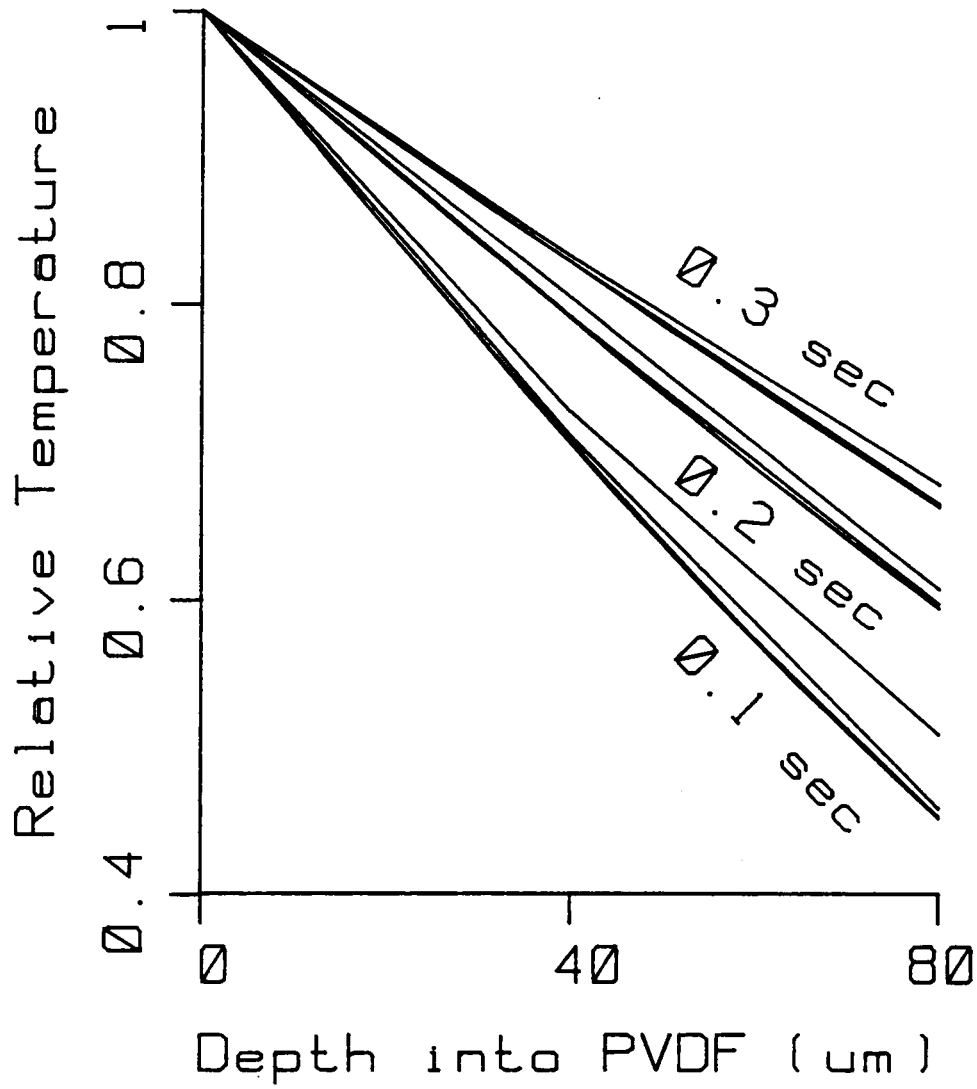

Figure 21. A model of 80 μm of PVDF film with Δx chosen to be 40, 20, 10, and 5 μm. The top lines for each of the time intervals were calculated using the plane thickness increment, Δx = 40 μm, so there are only 2 line segments across the graph. The top line, where Δt = 0.2 sec and Δx = 40 μm, is a straight line because the temperature at plane 1 is the average of plane 0 and 2 for this time increment, as discussed in the text. This allows rapid calculation of θ at a point, but the accuracy is not very good. The next line down for each of the 3 times were calculated using Δx = 20 μm. They follow more closely the curve, but still there is still only 2 or 3 line segments describing the curve. At Δx = 10 and 5 μm, there are more points on the shallow curves and these appear to more or less fall on top of one another.

curve, but still there is still only 2 or 3 line segments describing the curve. At Δx = 10 and 5 μm, there are more points on the shallow curves and these appear to more or less fall on top of one another. The reduction in error can be explained by n, the number of iterations needed to calculate each of these curves. n is proportional to m^2 where m is the number of planes of thickness Δx through the film. The following table shows the number of iterations required to calculate the temperature profile across 80 μm of PVDF film for 0.1 seconds when Δx equals 40, 20, 10, 5 and 2.5 μm.

Table 3. Time required to find response at 0.1 seconds for different thickness increments through 80 μm of PVDF film.

Δx (μm)	m	n for 0.1 sec
40	2	7
20	4	28
10	8	112
5	16	449
2.5	32	1798

Figure 22 shows the temperature profile through 80 μm of PVDF film, two 40 μm pieces of the film, at 0.1 second time slices for a total of two seconds for a temperature step function. When a constant temperature is applied to the surface of the film at time 0, the temperature of the film exponentially approaches the temperature of the surface as can be seen, for example, by following the response curve at 40 μm with time. As one would expect, the deeper portions of the film take longer to approach the applied temperature.

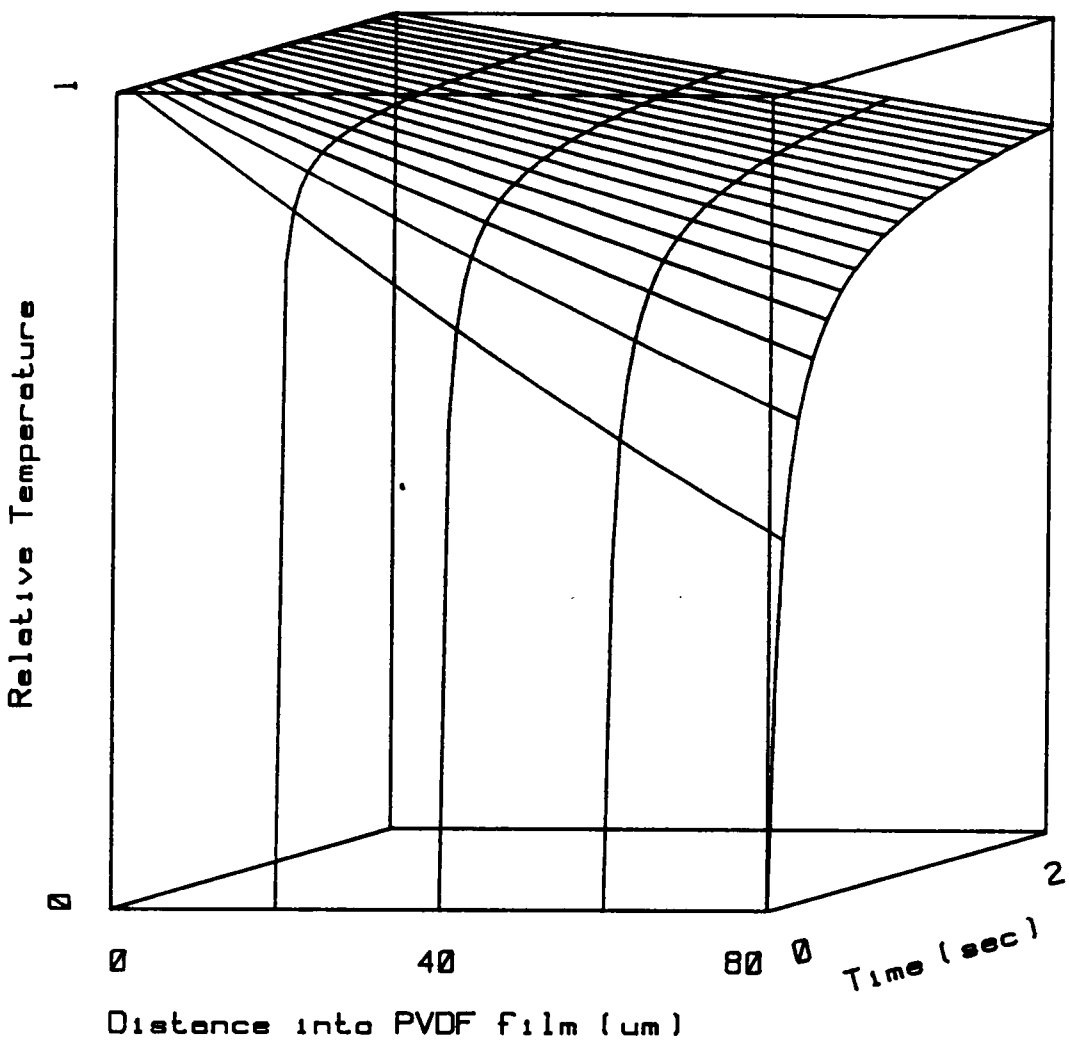

Figure 22. Temperature profile through 80 μm of PVDF film at 0.1 second time slices for a total of two seconds for a temperature step function.

3. Heat Flow through PVDF with ΔT = Gaussian

The above derivation is was made for a temperature step function. But the temperature exposed to the PVDF film surface in the flow channel is not a step function. As discussed in the FIA section of Chapter III, the model for a FIA bolus is a Gaussian distribution. Therefore, the temperature profile caused by the reaction of Gaussian shaped peroxide bolus with the enzyme should also have a Gaussian curve. The equation for a Gaussian curve (normalized so the maximum point is 1) is

$$Y = e^{-[(X - \mu)/\sigma]^2/2} \qquad \text{VI-16}$$

where μ is the mean (maximum) of the curve and σ is the standard deviation around the mean.

The BASIC program, Appendix B, written to calculate temperature profiles using a step function in temperature with time was modified so it would calculate the temperature profile using a Gaussian function in temperature with time. The Gaussian curve starts at 4σ before the maximum, which corresponds to 0.066% of the maximum peak height and continues until 8σ past the peak maximum. Allowing the calculation to continue long past the "return to zero" permits the cooling of the planes away from the film to be observed. The Gaussian peak has a standard deviation of 0.583 seconds which makes the peak width at half height 1.37 seconds. The standard deviation of the Gaussian peak was determined by calculating the approximate bolus shape from the initial size of the bolus and plotting the calculated curve along with several normalized real data sets. The standard deviation in equation VI-16 was then adjusted so that the curves superimposed. The standard

deviation of the calculated curve could not be determined exactly because the volume of the flow channel is only approximately known due to the variability in the thickness of the immobilized enzyme layer. Changes in the volume of the flow channel will change the residence time of the sample in the cell.

Figure 23.A shows the temperature profiles through 80 μm of PVDF film every 0.2 seconds for six seconds with this Gaussian temperature function applied to the surface plane, x = 0, of the film. Figure 23.B shows the temperature versus time at 0, 20, 40, 60 and 80 μm into the film. These profiles better show the decrease in height and delay in time of the maximum temperature experienced at a plane in the film. By taking the temperatures at 20 and 60 μm into the PVDF films, the theoretical output of the pyroelectric can be calculated. As can be seen in Figure 23.A, the temperatures at 20 and 60 μm are approximately the average temperature of the sample and reference film.

The pyroelectric current, i_p, is proportional to the temperature change in the film with time. Therefore, the response of the film next to the heat source is proportional to the temperature curve at thickness 20 μm, and the response of the second film is proportional to the temperature curve at thickness 60 μm. The proportionality constant is the pyroelectric coefficient of the PVDF.

Experimentally, the output of the instrument amplifier is obtained by subtracting the average temperature of the second layer from the average temperature of the first layer. The calculations reported here can be set up to mathematically perform the same function on the calculated data as the amplifier electronics perform on the experimental

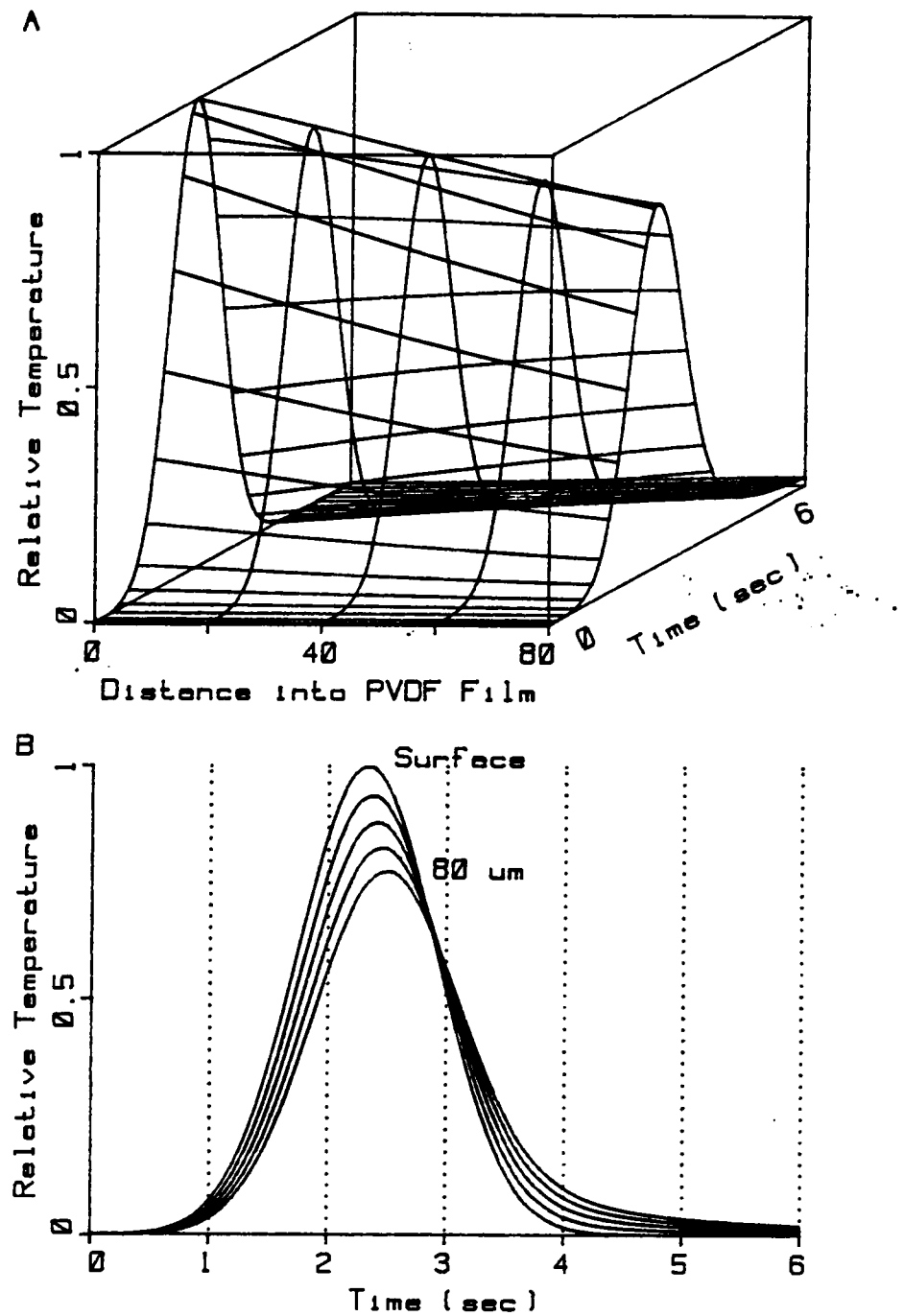

Figure 23.A. Temperature profile through 80 μm of PVDF film at 0.2 second time slices for six seconds with this Gaussian temperature function applied to the surface of the film. B. Temperature versus time at 0, 20, 40, 60 and 80 μm into the film as calculated above.

data. Figure 24 shows the calculated curve and two sets of experimental data from different concentrations, all normalized to one. The theoretical curve agrees very well with the first portion of the curve, the negative peak. The second portion, where the signal is positive, is difficult to model. The flow channel is, in FIA terms, a mixing tank which causes the ideal Gaussian curve to severely tail. The bolus entering the flow channel can be modeled as a Gaussian peak. But processes occurring after the peak maximum complicate the signal. Fortunately, they do not affect the ability to model the quantifying process.

A longer sample loop (see text and Figure 4 in section V.B.7) did not give any improvement in signal. This can be explained by looking at the theoretical response with time, Figures 23.B and 24. At first, the rate of temperature change in the first PVDF film, the sample layer, shown by the 20 μm temperature curve in Figure 23.B, is larger than the rate of temperature change in the second or reference film, the 60 μm curve. As the velocity of the reaction becomes more constant, the temperature difference between the two films starts to decrease. As the change in peroxide concentration with time starts to decrease, the average temperature difference between the films becomes equal. Therefore, the initial change-in-concentration-with-time slope gives the strongest signal. The smallest sample loop still has a large enough volume that it still has a dispersion of one when it reaches the flow channel. The sample volume is approximately the same volume as the flow channel. As long as the sample bolus volume is greater than or equal to the detector dead volume and the dispersion is one, the pyroelectric effect observed will be the maximum possible. Any increase in

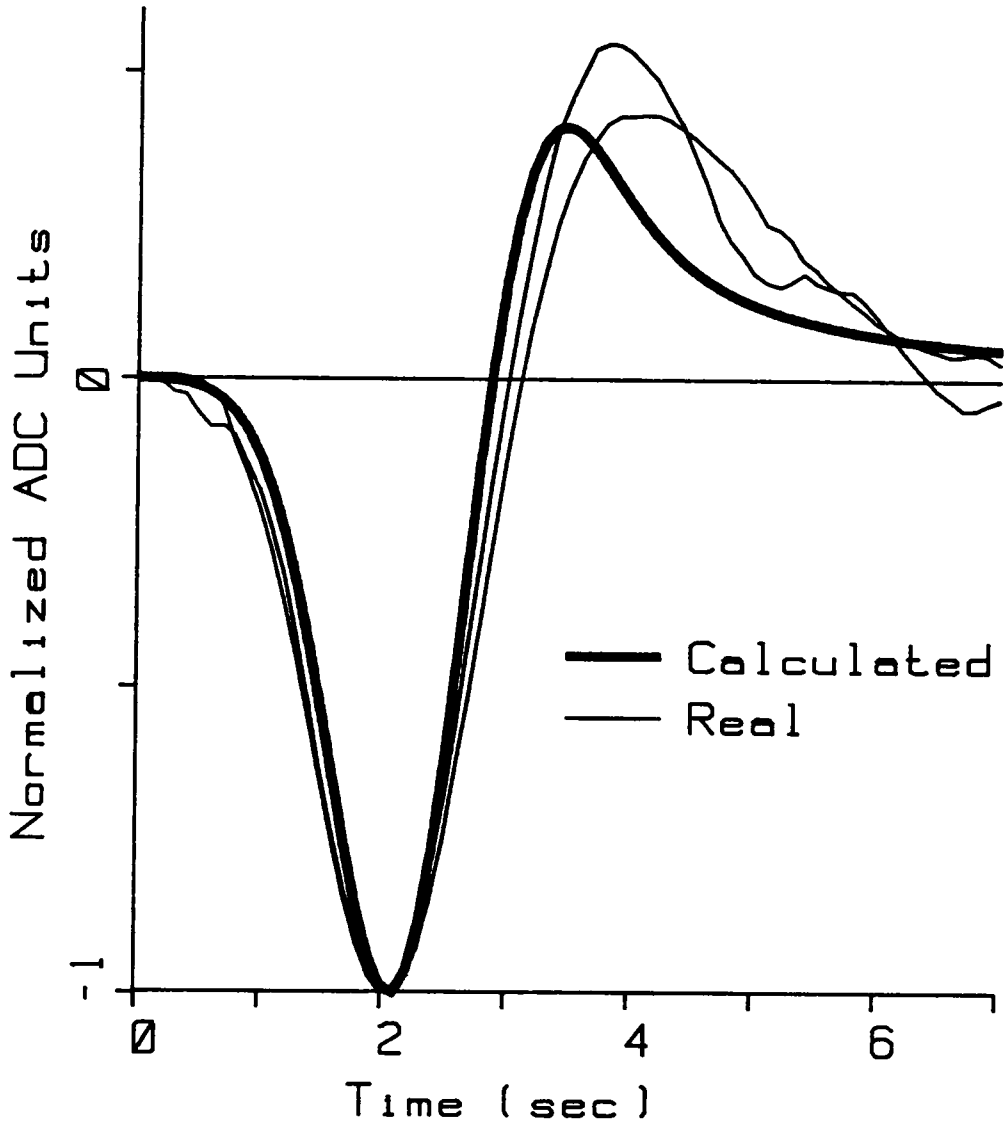

Figure 24. Calculated curve and two sets of experimental data from different concentrations, all normalized to one.

the sample volume beyond this point will not increase the response. This suggests that one of the advantages of the detector is the low total sample volume it requires, 70 µl, in comparison to other detectors such as the calorimeters mentioned in Chapter II. The smallest volume reported there was about 2 ml. This also shows that the minimum detectable number of moles is comparable to other methods, about 7 x 10^{-8} moles. The two thermistor methods for determining peroxide presented in Chapter II had needed 5 x 10^{-8} and 2 x 10^{-7} moles for detection.

The modeling of the system shows that an improvement to the film configuration might be to add a thermal impedance between the sample and reference films. Figure 25.A shows the temperature profile with time through 400 µm of PVDF, 10 layers of 40 µm film, when a Gaussian temperature profile is applied to the surface. Figure 25. B shows, as expected, at larger distances into the film, the maximum temperature moves to a longer time after sample injection. Also at a greater distance into the film, the maximum temperature decreases and the temperature peak is broader. Figure 26.A is a three dimensional representation of the amplifier response to the temperature profile shown in Figure 25. This was done in the same way as discussed earlier in this section for the response of two layers of PVDF (Figure 23.B), but this shows the theoretical response for different thicknesses. Figure 26.B. shows a view looking up the trough in Figure 26.A. Each curve was calculated by taking the temperature difference between the surface and some distance x into the PVDF film. Figure 26.A shows these plotted at this distance x into the film at 0.2 second time slices for 6 seconds.

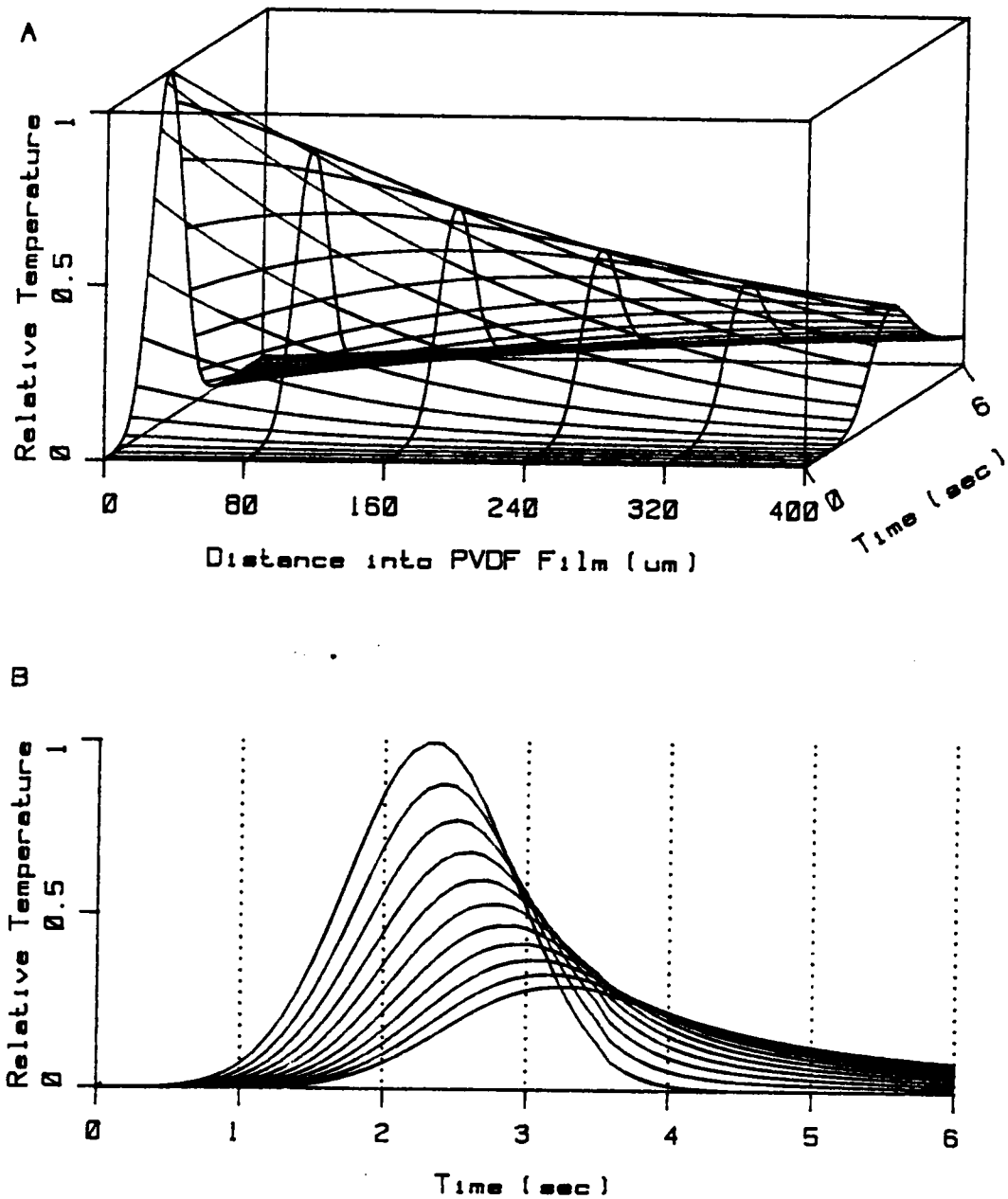

Figure 25.A. Temperature profile with time through 400 μm of PVDF, 10 layers of 40 μm film, when a Gaussian temperature profile is applied to the surface. B. Temperature versus time at every 40 μm through the film (a view up the tunnel from the above graph).

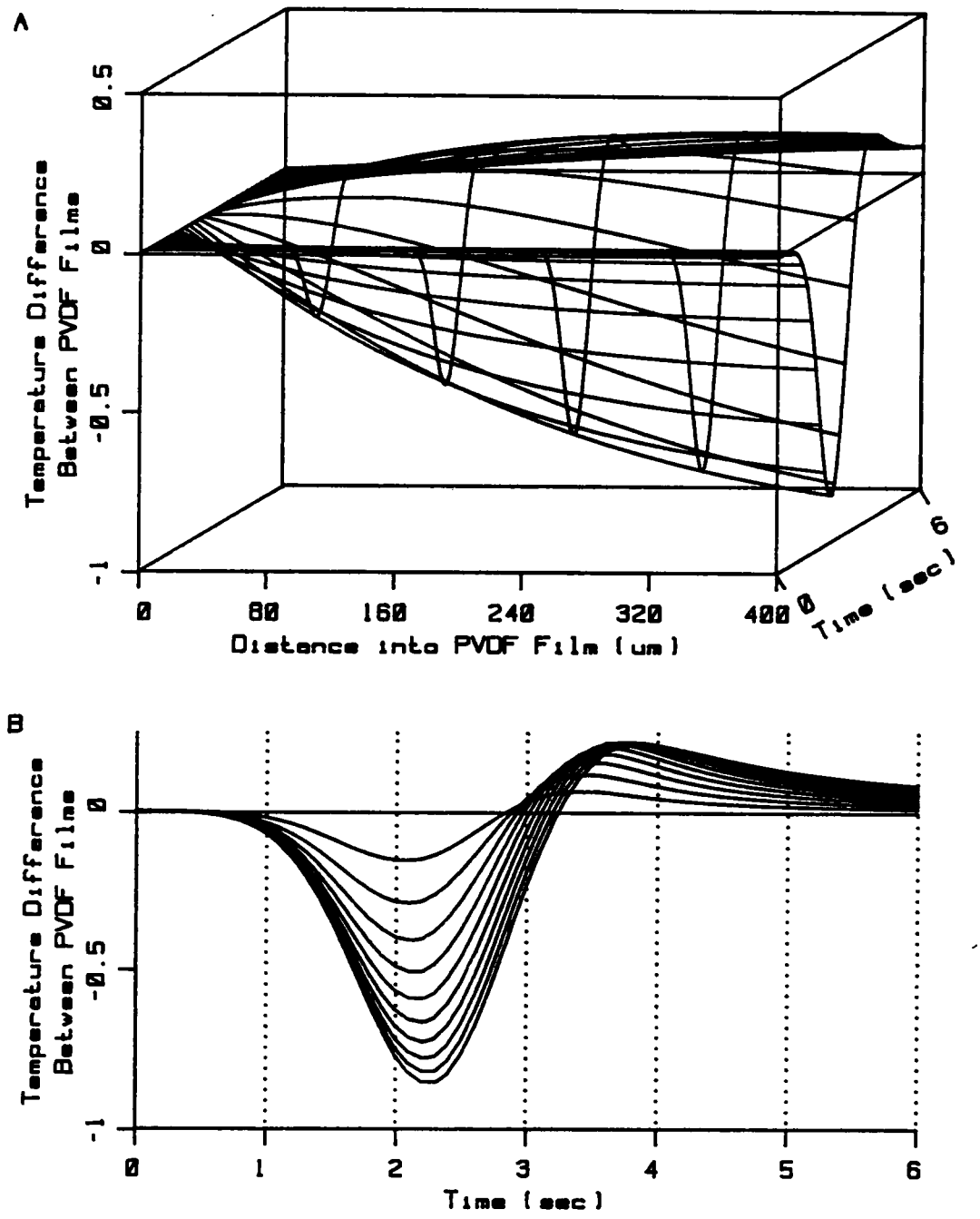

Figure 26.A. A three dimensional representation of the amplifier response to the temperature profile shown in Figure 25. B. Temperature difference versus time at every 40 μm through the film (looking up the trough in the 3D representation above).

Attention Patron:

Page 109 omitted from numbering

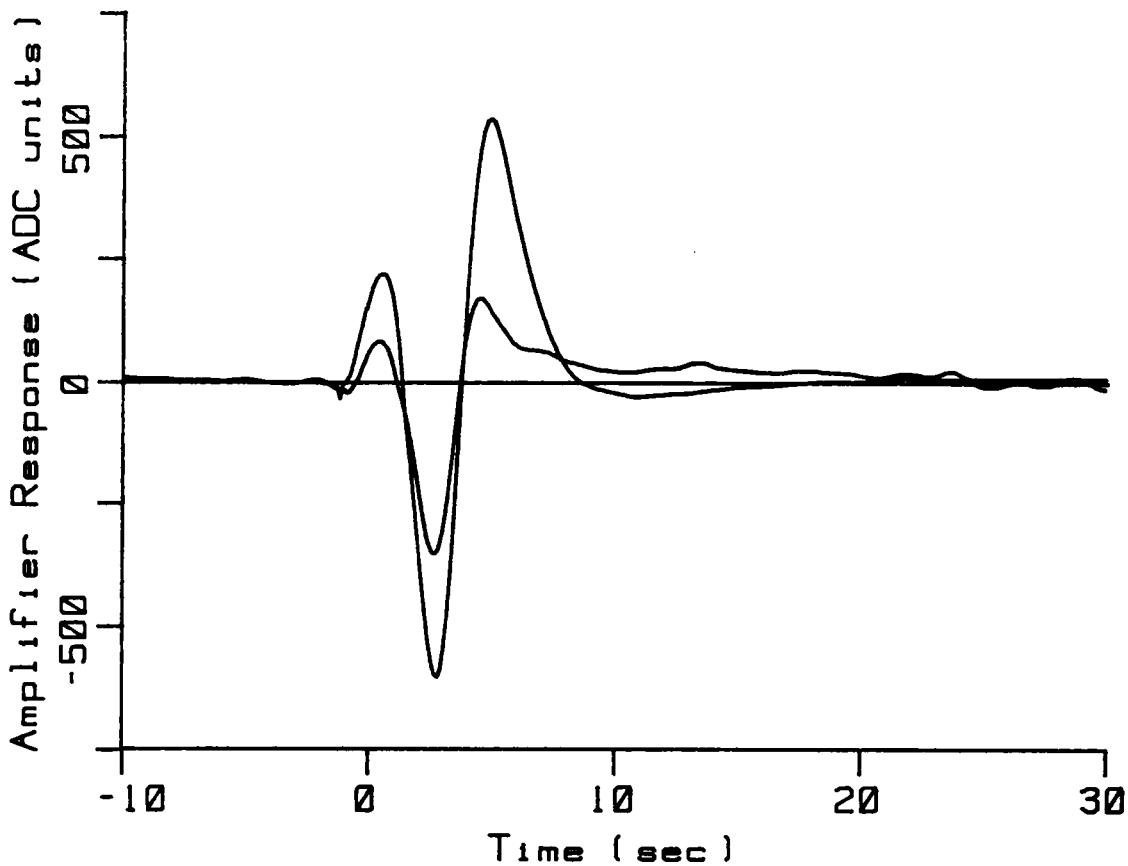

Figure 27. Response of a bimorph and a tetramorph configuration using the outside films as the sample and reference.

the minimum detectible quantity remains about the same. Further increases in the thickness of the thermal impedance layer did not, as expected, improve the situation.

D. Other Enzymes and Possible Detection Limits

The following table presents some other enzymes-substrate reactions that could be applied to this system. Catalase is also presented as a reference. Although they provide less heat as shown by the -d(H), these other enzyme-substrate systems promise better signal-to-noise because they do not have gaseous products.

Table 4. Table of enzyme/substrate pairs with significant ΔH.[18,38]

Enzyme	Substrate	-d(H) kJ/mole	MW	-d(H) kJ/g	d(T) for 1 mM soln
Catalase	Hydrogen peroxide	94.7	34	2.78	0.0226
Cholesterol oxidase	Cholesterol	52.9	387	0.14	0.0126
Glucose oxidase	Glucose	80	180	0.44	0.0191
Hexokinase	Glucose	27.6	180	0.15	0.0066
Lactate dehydrogenase	Sodium pyruvate	62.1	110	0.56	0.0148
Urease	Urea	6.6	60	0.11	0.0016

This sensor could be easily made into a serum analyzer for glucose and urea where concentrations typically run around 25 mM and between 3 and 10 mM, respectively.

VII. CONCLUSIONS

This dissertation has presented results from a novel pyroelectric heat-of-reaction detector accompanied by the development and theory behind the detector. The detector uses inexpensive materials, simple concepts and designs. A simple flow injection analysis system is used for sample delivery. The Plexiglas flowcell housing contains a thin, oval flowcell milled in the Plexiglas. An enzyme, in this study catalase, is immobilized on one side of the cell. Across the flowcell from the enzyme is the sensing element. The energy produced by the reaction of a substrate, in this study hydrogen peroxide, on the enzyme heats a sensing element. The sensing element for this heat of reaction is a pyroelectric polymer, poly(vinylidene fluoride), coated with 200 Å of aluminum electrodes. Two layers of the 40 μm polymer, a bimorph, are used in a sample/reference arrangement. The pyroelectric signals from the two layers are differentiated. The amplifying circuit is a simple, two stage amplification. The first stage does a current-to-voltage conversion; the second stage is an instrument amplifier. Data interpretation is straight forward, maximum peak height is proportional to the concentration. At a flow rate of 4 ml/min the maximum response of a 70 μl sample is attained in less than 5 seconds. The detector has shown a minimum detectable response to 1 mM hydrogen peroxide, and the response is linear over two orders of magnitude in concentration, from less than 10 mM to over 1 M hydrogen peroxide.

There are other thermal sensors that are more sensitive than this poly(vinylidene fluoride) based immobilized enzyme sensor; but, this

sensor has several advantages over other systems. Isoperibol calorimeters have sloping baselines and require extensive correction. The PVDF sensor, being a flow sensor, shows no change in baseline with time. Thermistors are subject to problems with bubbles, and thus their usable range with hydrogen peroxide is limited. The pyroelectric sensor has a larger sensing area than the thermistor and small oxygen bubbles sticking to the film have less effect. Also, fewer bubbles adhere to the film because they are generated across from the film, whereas with a detector where the enzyme is immobilized on the thermistor, the bubbles form between the solution and the sensing mechanism. Very few papers on thermistor biosensors report responses faster than five seconds from the time of injection or the possibility of doing sixty or more thermal analyses an hour. This method is capable of both. Other methods also require much more extensive enzyme preparation, such as column immobilization, or fitting of a thermistor into a column. To change the enzyme or pyroelectric sensor in the PVDF sensor could take less than 10 minutes and less than a minute if the enzyme was prepared in advance or the PVDF was precut. The system presented here can be assembled for a fraction of the cost of other systems. The enzyme and pyroelectric film can be replaced for about a dollar each. An inexpensive plug-in/throw-away detector could be developed combining both enzyme and pyroelectric film. This instrument does not require a reference temperature as required by a thermocouple. A relatively small, 70 µl sample gives a good response; larger samples do not improve the signal. Other flow detectors use over two milliliters. Thus, the minimum detectable number of moles is comparable to

other methods, about 7 x 10^{-8} moles. The carrier stream is inexpensive, distilled water with a very small amount of surfactant, although enzyme/substrate systems requiring buffers or containing high ionic strength solutions would work as well with this system.

The bimorph is used to reduce piezoelectric noise. A simple, one dimensional modeling of the heat flow through the sensor shows that an improvement in signal could be made by placing a layer of thermal impedance between the sample and reference layers. This impedance would cause a greater thermal difference between the sample and reference layers. When a thermal impedance is added to the system, it indeed shows an increase in signal, but it also shows a corresponding increase in noise. This noise comes from cushioning the reference layer from the pressures felt by the sample layer. Therefore, modeling provides a better understanding of the system but does not provide an overall signal improvement.

This system has direct application to the paper industry as the paper industry uses hydrogen peroxide to whiten paper. Calculations show that this sensor has promise for extension to clinical applications for monitoring glucose, urea or cholesterol.

BIBLIOGRAPHY

1. D. Barnaal; Analog and Digital Electronics for Scientific Application, Breton Publishers, North Scituate, Mass., 1982.

2. D. J. Eatough, R. M. Izatt and J. J. Christensen; In Comprehensive Analytical Chemistry, G. Svehla, ed.; Thermal Analysis, Vol XII, Part B, N. D. Jespersen, ed.; Elsevier Scientific Publishing Co., 1982.

3. H. Nilsson, A. C. Akerlund and K. Mosbach; Biochimica Biophysica Acta, 320, 1973, 529.

4. G. Papariello, A. Mukherji and C. Shearer; Analytical Chemistry, 45, 1973, 790.

5. R. Llenado and G. Rechnitz; Analytical Chemistry, 43, 1971, 1457.

6. R. M. Ianniello and N. D. Jespersen; In Comprehensive Analytical Chemistry, G. Svehla, ed.; Thermal Analysis, Vol XII, Part B, N. D. Jespersen, ed.; Elsevier Scientific Publishing Co., 1982.

7. S. Updike and G. Hicks; Nature, 214, 1967, 986.

8. G. G. Guilbault and G. Lubrano; Analytica Chimica Acta, 69, 1974, 189.

9. B. Mattiasson, B. Danielsson, F. Winquist, K. Mosbach and H. Nilsson; Applied Environmental Microbiology, 41, 903-8.

10. H.-L. Schmidt, G. Krisam and G. Grenner, Biochimica Biophysica Acta, 429, 283-90.

11. L. D. Bowers, L. M. Canning, Jr., C. N. Sayers and P. W. Carr; **Clinical Chemistry, 22,** 1314-18.

12. B. Mattiasson; **FEBS Letters, 77,** 107-10.

13. C. Tran-Minh and D. Vallin; **Analytical Chemistry, 50,** 1874-78.

14. S. P. Fulton, C. L. Cooney and J. C. Weaver; **Analytical Chemistry, 52,** 1980, 505.

15. L. W. Burgess; Dissertation, Virginia Polytechnic Institute and State University, Blacksburg, Va., 1984.

16. L. Stryer; **Biochemistry,** 2nd ed, W. H. Freeman and Company, 1981.

17. I. Chibata, ed.; **Immobilized Enzymes,** John Wiley & Sons, New York, 1978.

18. O. Zaborsky; **CRC Immobilized Enzymes,** CRC Press, Cleveland, Ohio, 1973.

19. J. L. Bailey; **Techniques in Protein Chemistry,** Elsevier Publishing Co., Amsterdam, 1967

20. G. R. Schonbaum and B. Chance; in **The Enzymes, Vol XIII, Oxidation-Reduction, Part C,** P. D. Boyer, ed.; Academic Press, New York, 1976, Chapter 7, Catalase.

21. D. D. Pollock; **Physical Properties of Materials for Engineers, Volume III;** CRC Press, Inc., Boca Raton, FL, 1982.

22. Pennwalt Corporation, **KYNAR Piezo Film, Technical Manual.**

23. W. G. Cady; Piezoelectricity, Dover Publications, Inc., New York, 1964.

24. E. H. Putley; In **Semiconductors and Semimetals**, R. K. Willardson, A. C. Beer, Eds.; Academic Press, New York, 1970, Vol. 5, Chapter 6, Infrared Detectors.

25. W. G. Cady; Piezoelectricity, McGraw-Hill Book Co., New York, 1946.

26. H. Kawai; **Japanese Journal of Applied Physics**, 8, 1969, 975.

27. Solvay & Cie, Technical Data Sheet for PVDF, Bruxelles, March 1984.

28. R. A. Anderson, R. G. Kepler, and R. R. Lagasse, **Ferroelectrics**, 33, 1981, 91-94.

29. J. G. Bergman, Jr., J. H McFee, and G. R. Crane; **Applied Physics Letters**, 18, 1971, 203.

30. T. Furukawa; **IEEE Proceedings of the Fifth International Symposium on Electrets**, Heidelberg, 883, 1985.

31. R. G. Kepler and R. A. Anderson; **Journal of Applied Physics**, 49, 1978, 4918.

32. R. G. Kepler and R. A. Anderson; **Journal of Applied Physics**, 49, 1978, 4490.

33. S. Kavesh and J. M. Schultz; **Journal of Polymer Science, A**, 8, 1970, 243.

34. R. G. Kepler, R. A. Anderson and R. R. Lagasse; **Ferroelectrics**, 57, 1984, 151-8.

35. E. L. Nix, J. Nanayakkara, G. R. Davies and I. M. Ward; Journal of Polymer Science: Part B: Polymer Physics, 26, 1988, 127-140.

36. J. Clements, G. R. Davies and I. M. Ward; Polymer, 26, 1985, 208.

37. F. Ishii, T. Sawatari and A. Odajima; Japanese Journal of Applied Physics, 27, 1047-53, 1988

38. H. Sussner and K. Dransfeld, Journal of Polymer Science, 16, 1978, 529.

39. Y. Wada and R. Hayakawa; Ferroelectrics, 32, 1981, 115.

40. J. Ruzicka and E. H. Hansen; Analytica Chemica Acta, 78, 1975, 145.

41. K. K. Stewart, G. R. Beecher and P. E. Hare; Analytical Biochemistry, 70, 1976, 167.

42. A. Savitzky and M. J. E. Golay; Analytical Chemistry, 36, 1964, 1627-39.

43. S. G. Porter; Ferroelectrics, Vol 33, 1981, 193-206.

44. R. C. Weast, ed.; CRC Handbook of Chemistry and Physics, 57th Edition, CRC Press, Cleveland, Ohio, 1976.

45. I. K. Chapple; Ph.D. Dissertation, Virginia Polytechnic Institute and State University, Blacksburg, Va., 1984.

46. Sigma Catalog, 1987.

47. I. M. Kolthoff and E. B. Sandell, Textbook of Quantitative Inorganic Analysis, 3rd Edition, The MacMillan Co, NY, 1952.

48. J. G. Mason, Personal communication, Virginia Tech Department of Chemistry, Blacksburg, Virginia.

49. W. S. Conder, Ph.D. Dissertation, Virginia Polytechnic Institute and State University, Blacksburg, Va., 1985.

50. S. J. Choquette, Ph.D. Dissertation, Virginia Polytechnic Institute and State University, Blacksburg, Va., 1988.

51. Personal communication.

52. R. Bott, Personal communication, Virginia Tech Department of Chemistry, Blacksburg, Virginia.

53. Analog Devices, AD625 Technical Data Sheet.

54. J. Brandrup and E. H. Immergut, eds.; **Polymer Handbook, 2nd Edition**, John Wiley and Sons, New York, 1975.

55. J. Bastick; **Thermocinetique Premiére Partie: La Conduction, Course notes and formulas**, Ecole Nationale Superieure des Industries Chimiques, Mulhouse, France, 1983-84.

56. J. Crank; **The Mathematics of Diffusion**, Oxford University Press, London, 1970, 187.

57. E. Schmidt; **Foppls Festschrift**, Springer, 1924, 179.

58. G. G. Guilbault; **Analytical Uses of Immobilized Enzymes**, Marcel Dekker, Inc., New York, 1984.

Appendix A

Savitzky - Golay Table for Cubic Least-Squares Fit

POINTS	25	23	21	19	17	15	13	11	9	7	5
-12	-253										
-11	-138	-42									
10	-33	-21	-171								
-9	62	-2	-76	-136							
-8	147	15	9	-51	-21						
-7	222	30	84	24	-6	-78					
-6	287	43	149	89	7	-13	-11				
-5	342	54	204	144	18	42	0	-36			
-4	387	63	249	189	27	87	9	9	-21		
-3	422	70	284	224	34	122	16	44	14	-2	
-2	447	75	309	249	39	147	21	69	39	3	-3
-1	462	78	324	264	42	162	24	84	54	6	12
0	467	79	329	269	43	167	25	89	59	7	17
1	462	78	324	264	42	162	24	84	54	6	12
2	447	75	309	249	39	147	21	69	39	3	-3
3	422	70	284	224	34	122	16	44	14	-2	
4	387	63	249	189	27	87	9	9	-21		
5	342	54	204	144	18	42	0	-36			
6	287	43	149	89	7	-13	-11				
7	222	30	84	24	-6	-78					
8	147	15	9	-51	-21						
9	62	-2	-76	-136							
10	-33	-21	-171								
11	-138	-42									
12	-253										
NORM	5175	805	3059	2261	323	1105	143	429	231	21	35

Appendix B

BASIC Program for Calculating Thermal Flow

```
rem  This program calculates the change in temperature, th,
rem  of the planes in a "semi-infinite solid" from the plane
rem  at the surface where a constant temperature is applied,
rem  plane 0, to the plane d thickness away, at plane
rem  thicknesses x at time tf.  To do this, 8 numbers must
rem  be input; thermal conductivity - k, density - r, and
rem  heat capacity - c for the semi-infinite solid; initial
rem  temperature - t0 and temperature placed on plane 0 at
rem  time 0 - t1; thickness of interest into the semi-
rem  infinite solid - d, and a step size through the film
rem  that is a fraction of d - x; and a time at which the
rem  temperature profile will be calculated - tf.  Up to
rem  nmax% thickness elements, d/x, can be calculated.  Also
rem  available is the capability to capture temperature
rem  profiles at time slices by selecting the number of
rem  slices with div%, div% = 1 will give only 1 time slice
rem  at time tf.  The slices are stored so that they can be
rem  read directly into Generic Cadd as a batch file with
rem  each time slice on a different layer.
rem    This program uses the approximations that are used
rem  to derive the thermal equations using Schmidt's Rule
rem  which say the temperature of a plane at a time incre-
rem  ment is equal to the average of the temperatures of the
rem  planes to either side at the time increment before.  The
rem  time increment is calculated from the thickness incre-
rem  ment and the physical constants of the material through
rem  which the temperature is flowing.
rem
rem  Initialize constants and calculate time increments
cls
nmax% = 8190                    : rem  maximum size of data array
dim th(nmax%,1%)
k = .13           : rem  W/m K (thermal conductivity for PVDF)
r = 1780                        : rem  kg/m^3 (density for PVDF)
c = 1300                  : rem  J/kg K (heat capacity for PVDF)
rem k = 226         : rem  W/m K (thermal conductivity for Al)
rem r = 2700                    : rem  kg/m^3 (density for Al)
rem c = 900                : rem  J/kg K (heat capacity for Al)
d = 8e-5        : rem  meters (total thickness, multiple of x)
x = 1e-5       : rem  meters (step size of interest thru film)
tf = 7           : rem  sec (final time increment of interest)
div% = tf*10%                   : rem  divisions for data saves
t0 = 0             : rem  °C (initial temperature of the film)
t1 = 1               : rem  °C (temperature placed at on face)
th(0,0) = t1-t0                   : rem  °C (theta, delta temp)
m = d/x : m% = m                     : rem  (# steps thru film)
xt = 2*k/(r*c)                         : rem  m^2/s (d x^2/d t)
t = x^2/xt                                    : rem  sec (d t)
```

```
n = tf/t      : rem  (# time inc's t to reach final time, tf)
u% = int(n/(3*tf/7))          : rem  center of Gaussian peak
s = u%/4                 : rem  standard deviation of Gaussian
n% = n
pi = 3.1415926
rem
rem  print table of values for current calculation
rem
print "These constants are for PVDF"
print "The thermal conductivity is";
print using "####.###";k; : print " W/m °K"
print "The density is";r;"kg/m^3"
print "The heat capacity is "; : print using "#####";c;
print " J/kg °K"
print : print "The initial temperature is";t0;"°C"
print "The maximum applied temperature is";t1;"°C"
print "Therefore; the maximum temperature change is";
print th(0,0);"°C"
print "The film is "; : print using "#.#^^^^";d+d/1000;
print " m thick"
print "The thickness of the film increments are ";
print using "#.#^^^^";x+x/1000; : print ;" m "
print "Therefore; there are"; : print using "####";m;
print " increments through the film"
print "The time increments of interest, test time, are ";
print using "##.####";tf; : print " s "
print "The length of the time increments are ";
print using "#.#^^^^";t; : print ;" s"
print "Therefore; there are "; : print using "#####";n;
print " time units"
print div%;"time slices are stored"
rem
rem  Check to see if it is within th(nmax%) dimension range
if(n%+m%+1%)/2%>nmax% goto 70
rem
rem  Check to see if its OK to continue
print "Is this OK? (Y or N)
10 a$ = inkey$ : if a$ = "" goto 10
if a$="n" or a$="N" then print,,"No, program stopped" : stop
if a$ <> "y" and a$ <> "Y" goto 10
rem
rem  Print summary of output to appear
40 print : print "At time";
print using " #.#^^^^";tf+tf/1000;
print " sec, these"; : print using "####";m+1;
print " numbers give the temperature profile"
print "These numbers represent each";
print using " #.#^^^^";x+x/1000;
print " m over the range from 0 to";
print using " #.#^^^^";d+d/1000; : print " m"
rem
rem  Initialize all th's to t0
```

```
for j% = 0 to 1
    for i% = 0% to 8100%
        th(i%,j%)=t0
next i%,j%
rem
rem  Get name of output file
print "Input name for Generic Cadd batch file, 8 char ";
input g$
open "c:\generic\" + g$ + ".bat" for output as #1
rem
rem  Title for GenCadd drawing
print#1, "TP,0,0,Heating curves through both 40 um PVDF ";
print#1, "layers at every 0.1 sec for 2 sec#;"
rem
k% = 1          : rem  initialize counter for time slice store
th(0,0) = t1                    :rem  set plane 0 to temp t1
locate 22,1
rem
rem   0 100       Schematic of how program calculates th(m,n)
rem  T  1Y00      At time 0, th(0,0) = 1, the rest are 0
rem  i  1YY00     At time 1, th(1,1) = [th(0,0)+th(2,0)]/2
rem  m  1YYY00    Etc.  At time (n+m)/2, # of calc's decrease
rem  e  1YYYY0    (don't calc x's) because only interested in
rem     1YYYYx    temperature of planes 0 to m at time n
rem   n 1YYYxxx
rem     0  m  Plane #
rem
for j% = 1% to int((n%+m%+1%)/2%) : rem loop to point of Y's
    print n%-j%; : locate 22,1      : rem  print # loops left
    rem  If arg of exp(-arg)^2/2>10 then exp <10^-13, th = 0
if (j%-u%)/s >10 then th(0%,0%)=0% : print"zero "; : goto 30
    th(0%,0%) = exp(-((j%-u%)/s)^2%/2)    : rem gaussian temp
    print using "#.###"; th(0%,0%);
30  if n% = j% goto 60
    for i% = 1% to j%             : rem  calculate next theta
        th(i%,1%) = (th(i%-1%,0%)+th(i%+1%,0%))/2
    next i%
    for i% = 1% to j%                : rem  replace old theta
        th(i%,0%) = th(i%,1%)
    next i%                           : rem  is next division
    if k%/div%*n% >= i% goto 20       : rem    ready to save?
    print#1, "YC,";k%;";"     : rem  increment gencadd layer
    print#1," "
    k% = k%+1%                       : rem  set next division
    for i% = 0% to m%          : rem  write to disk, data for
        print#1, i%;",";
        print#1,using"##.#####";th(i%,0%);
        print#1,";"
    next i%                   : rem  time element of interest
20 next j%
rem
rem  if # time elements < # thickness elements goto end prog
```

```
if n% <= m% goto 60
rem
k% = k% - 2% : rem  reset time slice counter for count down
: rem  start at 1 less than above loop and count down to m
: rem  something funky with roundoff but this works
for j% = int((n%+m%-2%)/2%) to m% step -1%
    print j%-m%; : locate 22,1
if(n%+m%-j%-u%)/s>10 then th(0%,0%)=0%:print"zero ";:goto 80
    th(0%,0%) = exp(-((n%+m%-j%-u%)/s)^2%/2)
    print using "#.###"; th(0%,0%);      : rem  gaussian temp
80  for i% = 1% to j%                      : rem  calc new th
        th(i%,1%) = (th(i%-1%,0%)+th(i%+1%,0%))/2
    next i%
    for i% = 1% to j%                 : rem   replace old theta
        th(i%,0%) = th(i%,1%)
    next i%                           : rem  is next time slice
    if k%/div%*n% <= j% goto 50       : rem      ready to save?
    print#1, "YC,";div%-k%;";"        : rem   inc gencadd layer
    print#1," "
    k% = k%-1%                        : rem   set next division
    for i% = 0% to m%          : rem  write time slice to disk
        print#1, i%;",";
        print#1,using"##.#####";th(i%,0%);
        print#1,";"
    next i%
50 next j%
rem
60 print#1, "YC,";div%;";"              : rem  write last time
locate 22,1                               : rem  slice to disk
print#1," "
for i% = 0% to m%
   print using "##.#####"; th(i%,0%);
   print#1, i%;",";
   print#1, using "##.#####"; th(i%,0%);
   print#1, ";"
next i%
print#1, "PU,ZA;"                   : rem  end of GenCadd file
close #1
stop
rem  Number of time increments too large for dimension
rem  statement, reduce tf or increase x
70 print "which is TOO large for this program" : stop
```

Appendix C

Forth Listing

```
Block  202
 0  ( Directory
 1  BLOCK                  CONTENTS
 2  220     Data Acquisition Using Conder Clock -- INTEGER LOAD BLOCK
 3  221     Data Acquisition -- Variables
 4  222     Data Acquisition -- Assembler Code & Data Acquire
 5  223     Save SINGLE INTEGER ARRAY on DISK as INTEGER
 6  224     Data Acquisition -- SMIN, SMAX, SRANGE & STEP_100
 7  225     Data Store Block -- MAXMIN_STORE, DATA_SAVE
 8  226     Test stuff
 9  227     Plot Block Calc. -- X- Ymin, X- Ymax, X- Ytic
10  228     Plot Block Calculations
11  235     AUTO AQR
12
13
14
15
Block  203
 0  ( Directory
 1  BLOCK                  CONTENTS
 2  260              Auto Plot Load Block
 3  261              Data Plot -- Variables
 4  262              Plot Block Calc. -- @SCALE
 5  263              Plot Block Calc. -- @SCALE & @SPEED
 6  264              Plot Block Calc. -- X- YMIN, X- YMAX, X- YTIC
 7  265              PRE.REAL SPEC COMMAND FILE
 8  266              PRE.REAL SPEC COMMAND FILE (cont)
 9
10
11
12
13
14
15
```

```
Block  204
 0  ( Directory
 1  BLOCK                 CONTENTS
 2
 3  401                   Area Under Peak
 4  405                   Baseline Correction moving both ends to 0
 5  406                   Bline Correction moving the initial avg to 0
 6  410                   Filtering
 7  415                   Integrate Data
 8
 9  420                   Scan Subtraction
10  425                   Stats
11  430                   Peak Height
12  435                   Area Under Peak from Stats Limits
13  440                   Derivative of Data
14  445                   Stats
15  450                   Get Array & Data Save
Block  220
 0  ( Data Acquisition Using Conder Clock -- INTEGER LOAD BLOCK )
 1  EMPTY                      BASE @                    DECIMAL
 2  ( : DELAY   500 0 DO     18 0 DO LOOP    LOOP ;
 3  : SEC   0 DO  I' I - .  1 0 DO  DELAY   LOOP    7 EMIT  LOOP ;
 4
 5  ( 328 LOAD          ( DDUMP, FDUMP, EDUMP)
 6
 7  FLOATING LOAD
 8
 9  221 LOAD 222 LOAD 223 LOAD 224 LOAD 225 LOAD 226 LOAD 227 LOAD
10
11  228 LOAD 235 LOAD
12
13
14                                                    BASE !
15
Block  221
 0  ( Data Acquisition -- Variables )
 1  BASE @                    OCTAL
 2
 3  ( SPEED from 107(71) 0.1hz to 102(66) 10 khz)
 4  ( SCALE: 0=-1 to 1V, 10=-2 to2V, 20=-5 to 5V, 30=-10 to 10V)
 5
 6  167772 CONSTANT OPP              100000 CONSTANT DAT
 7
 8  VARIABLE SCALE  30 SCALE !       VARIABLE BLK
 9  VARIABLE SPEED  105 SPEED !      VARIABLE #PNTS
10  VARIABLE CLOCK  0 CLOCK !        VARIABLE RMAX   VARIABLE RMIN
11
12  : SPEEDS   CR CR 107 .  ." (0.1hz) to "  102 .  ." ('10 khz') "
13             ." SPEED = " SPEED ? CR ;
14
15          BASE !                            SPEEDS
```

```
Block  222
 0  ( Data Acquisition -- Assembler Definition )
 1                          BASE @          OCTAL
 2  ASSEMBLER ( starts, tests & stores data in DAT at SPEED rate )
 3      BEGIN       176770  CTR  MOV        R -) U MOV
 4          U CLOCK MOV
 5          BEGIN   176770  TST B   0< END
 6          PTR  U)  )  176772  MOV
 7          100310 #  PTR U)  CMP   0= IF  167772  12 #  MOV  THEN
 8          PTR  U)  2  # ADD       CNT U) DEC
 9          0=  IF  170000 CLR      U ) WAKE # MOV          THEN
10          U  R  )+  MOV           300  200  INTERRUPT
11
12  BASE !
13
14
15
Block  223
 0  ( Data Acqiusition - Solinoid Control )         BASE @  OCTAL
 1
 2  : SET   ( set parallel output port to 110, bit 3 unchanged)
 3           6  OPP @       OR      OPP !   ;
 4
 5  : FIL   ( set parallel output port to 100 )
 6          14  OPP @       AND     4       OR      OPP !   ;
 7
 8  : INJ   ( set parallel output port to 010 )
 9          12  OPP @       AND     2       OR      OPP !   ;
10
11  : OPPC   BASE @   OPP @   DUP   OCTAL .   BINARY .   BASE !  ;
12
13  BASE !
14
15
Block  224
 0  ( Data Acquisition -- Data Acquire )
 1
 2  BASE @          OCTAL
 3
 4  : AQR#  ( # of pts -- stores ADC data at rate in SPEED )
 5          DUP     #PNTS !         SCALE @ CTR !
 6      CLOCK GET
 7          CNT !   DAT PTR !       SPEED @ 170000 !        STOP
 8      CLOCK RELEASE       ;
 9
10  : AQR   AQR#    14 OPP ! ;
11
12  BASE !
13
14
15
```

```
Block  225
 0  ( I_SAVE -- save SINGLE INTEGER ARRAY on DISK as INTEGER )
 1
 2
 3  : 1I_SAVE  ( blk.buf.addr data.addr cnt -- ) ( save one block)
 4          2*  0 DO         2DUP I + @       SWAP
 5          I + !    2 +LOOP         2DROP    UPDATE  FLUSH ;
 6
 7  : I_SAVE   ( base.blk #data.points -- )
 8          #PNTS !          BLK !            #PNTS @
 9          DUP      500 /MOD         SWAP    0= NOT
10          IF  1+  THEN     0 DO     DUP     500 MIN
11          BLK @ I +        BLOCK 24 +       DAT I   1000 * +
12          ROT      1I_SAVE          500 -   LOOP   DROP ;
13
14
15
Block  226
 0  ( Data Acquisition -- SMIN, SMAX & MAXMIN_STORE )
 1
 2  : SMAX  ( #pnts -- max)          1- 2*   DAT 2+ @
 3          SWAP     2 DO     DAT      I + @   MAX      2 /LOOP ;
 4
 5  : SMIN  ( #pnts -- min)          1- 2*   DAT 2+ @
 6          SWAP     2 DO     DAT      I + @   MIN      2 /LOOP ;
 7
 8  : MAXMIN_STORE   ( #pts -- store 100's range )    DUP
 9          SMAX     DUP       21 < IF
10                   DROP      21      THEN    RMAX !
11          SMIN     DUP      -21 > IF
12                   DROP     -21      THEN    RMIN !  ;
13
14
15
Block  227
 0  ( Data Store Block -- CSPEED, VARI_TO_DISK, DATA_SAVE )
 1  : CSPEED   ( -- pnts/10sec, calculate from SPEED )
 2          71  SPEED @  -  DUP  1 < IF  DROP  1. E 0       ELSE
 3                          DUP  4 > IF  DROP  7. E 4       ELSE
 4          1. E 0  ROT  0  DO   1. E 1  F*    LOOP    THEN THEN ;
 5
 6  : FS   ( vari, n -- ) ( fetch block & store # in position )
 7          BLK @   BLOCK + ! ;
 8
 9  : VARI_TO_DISK   ( -- store variables on disk )
10          RMIN @   0 FS   RMAX @   2 FS   #PNTS @  4 FS
11    SCALE @  6 FS   CSPEED   BLK @  BLOCK 8 +  2!  0 12 FS ;
12
13  : DATA_SAVE  ( beginning-blk -- ) ( write data to disk )
14          616 +          #PNTS @          I_SAVE    #PNTS @
15          MAXMIN_STORE  VARI_TO_DISK    UPDATE FLUSH      SET ;
```

```
Block  228
 0  ( Test stuff )
 1  : CONT   BEGIN 1 AQR DAT @ . ESCAPE  1000 0 DO LOOP   0 END ;
 2  : CONDUMP  BEGIN 8 AQR DAT 16 DUMP ESCAPE 0 END ;
 3  : TSTSC  DAT @ ABS 2040 > IF SCALE @ 24 < IF
 4           8 SCALE +! ELSE ." OVERFLOW ! " THEN   ELSE
 5           DAT @ ABS 800 < IF SCALE @ 0 > IF
 6           -8 SCALE +! THEN       THEN THEN ;
 7  : SCTST  BEGIN 7 AQR DAT 14 DUMP TSTSC SCALE ? ESCAPE 0 END ;
 8  VARIABLE DIV
 9  : PLOT  68 SPEED !
10          DIV !   BEGIN   1 AQR#  DAT @ DUP   DIV @ /  35 +  DUP
11          0 < IF  DROP 0  THEN    23      MOV_CUR
12          ESCAPE  . CR    0 END ;
13
14  : P   64 PLOT ;
15
Block  235
 0  ( AUTO AQR )
 1  VARIABLE NBLK   22 NBLK !       ( next block )
 2
 3  ( VARIABLE BOPP   10 BOPP !      ( beginning OPP setting )
 4  ( VARIABLE EOPP    4 EOPP !      ( end OPP setting short leads )
 5   VARIABLE EOPP   12 EOPP !     ( end OPP setting no short )
 6
 7  : AUTO_AQR  ( n --, calc next block for DATA_SAVE & saves )
 8          ( must set NBLK to current next block ) 69 SPEED !
 9          DUP     AQR#    EOPP @  OPP !           ESCAPE
10          NBLK @  DUP .   DATA_SAVE
11          500 /   NBLK @ +  NBLK !   ;
12
13  : AAQ  ( n--, # AUTO_AQR's)  0 DO  1000 AUTO_AQR  ESCAPE LOOP ;
14
15  : A   NBLK ?   ESCAPE   266 LIST   ESCAPE   1 AAQ   P ;
Block  260
 0  ( Auto Plot Load Block )  ( EMPTY )     107 LOAD      108 LOAD
 1
 2  261 LOAD        ( Data Plot -- Variables )
 3  302 LOAD        ( RETRO-GRAPHICS PLOT PACKAGE -- LOAD BLOCK )
 4
 5  : PLOT  ( blk --, PRE.REAL SPEC COMMAND FILE)
 6                  616 +   265 LOAD   OFF ;
 7  : PPLOT  ( blk --, PRE.REAL SPEC COMMAND FILE & LA50 PRINT)
 8          616 +   265 LOAD   27 EMIT  23 EMIT   OFF ;
 9
10  262 LOAD        ( Calc. -- @SCALE & @SPEED )
11  263 LOAD        ( Calc. -- XMIN XMAX YMIN YMAX X-TIC & Y-TIC )
12  264 LOAD        ( Calc. -- # Decimal Places )
13
14  : PNEXT  ( blk --, add a scan to plot with same scaling )
15          616 +   PNTS    0. E 0  1. E 0  YTPLOT  ;
```

```
Block  261
 0  ( Data Plot -- Variables )
 1
 2  BASE @
 3
 4  VARIABLE BASE.BLK       VARIABLE BASE.ADDR      VARIABLE #PNTS
 5
 6  OCTAL
 7   24366 40634  2CONSTANT  30IF    24366 40434  2CONSTANT  20IF
 8  -22335 40171  2CONSTANT  10IF    60102 37745  2CONSTANT   0IF
 9
10
11
12                                                  BASE !
13
14
15
Block  262
 0  ( Plot Block Calc. -- @SCALE & @SPEED )
 1
 2  : @SC   ( -- get 4th # from disk)  BASE.BLK @  BLOCK 6 + @ ;
 3
 4  : @SCALE   ( -- fetch appropriate constant )    @SC
 5          DUP     24 =    IF      DROP    30IF    ELSE
 6          DUP     16 =    IF      DROP    20IF    ELSE
 7          DUP      8 =    IF      DROP    10IF    ELSE
 8          DROP    0IF     THEN THEN THEN  ;
 9
10  : @SP   ( -- get 5th # from disk)  BASE.BLK @  BLOCK 8 + 2@ ;
11
12  : @SPEED   ( -- fetch appropriate constant )
13          1. E 1  @SP     F/      ;
14
15
Block  263
 0  ( Plot Block Calc. -- XMIN, XMAX, YMIN, YMAX, XTIC, YTIC )
 1  : PNTS  ( -- get 3rd # from disk)  BASE.BLK @   BLOCK 4 + @ ;
 2  : XMIN  0 0 FLOAT ;
 3  : XMAX  ( -- PNTS -1 in E fmt)  PNTS 1-         0 FLOAT ;
 4  : X-TIC  ( -- 5 tics)   PNTS    500 / 100 *     0 FLOAT ;
 5  : YMIN   ( -- get 1st # from disk)   BASE.BLK @     BLOCK @
 6          SDF     @SCALE  F* FIX  DROP    100 / 100 *
 7          DUP     0< IF   100 -   THEN    SDF     @SCALE F/ ;
 8  : YMAX   ( -- get 2nd # from disk)   BASE.BLK @  BLOCK 2+ @
 9          SDF     @SCALE  F* FIX  DROP    100 / 100 *
10          DUP     0> IF   100 +   THEN    SDF     @SCALE F/ ;
11  VARIABLE VA     2 ALLOT         0. E 0  VA 2!
12  : Y-TIC  ( -- tic/100)  1       YMAX    YMIN    F-
13          LOG     FIX DROP        0 DO    10 *    LOOP
14          0 FLOAT         1. E -3 F+      ;
15
```

```
Block  264
 0  ( Plot Block Calc - # Decimal Places )
 1
 2  : DEC_PL    ( -- # decimal places, 0 for times longer than 1 sec)
 3                                  @SP
 4          7. E 4  D= IF 4                     ( 4 places )
 5                             ELSE    @SP
 6          1. E 4  D= IF 2                     ( 2 places )
 7                             ELSE    @SP
 8          1. E 3  D= IF 1                     ( 1 place  )
 9                             ELSE
10                  0                          ( 0 places )
11          THEN THEN THEN ;
12
13  : UFBP     UPDATE   FLUSH   BASE.BLK @  616  -   PLOT ;
14  : UPP      BASE.BLK @   BLOCK 2+ !   UFBP ;
15  : LOW      BASE.BLK @   BLOCK    !   UFBP ;
Block  265
 0  ( PRE.REAL SPEC COMMAND FILE)   ON  WRITE-ACROSS   BASE.BLK !
 1
 2  ( min.X       max.X        min.Y       max.Y     << WINDOW params )
 3    XMIN        XMAX         YMIN       YMAX ( 400. E 0 ) WINDOW
 4
 5  ( 1st.X.tick  X.tick.spacing  1st.Y.tick  Y.tick.spacing       )
 6    0. E 0      X-TIC           YMIN        Y-TIC           TICS
 7
 8    ( X num-scaler)                      ( Y num-scaler)
 9  @SPEED TO XNUMSCALE     (        @SCALE TO YNUMSCALE      )
10                           (        .5 E 0 TO YNUMSCALE      )
11  BASE.BLK @  BLOCK 12 +  @  1+ 1 M* E 0 TO YNUMSCALE
12
13  ( sets scales places)
14  DEC_PL  PLACES !
15                                                          -->
Block  266
 0  ( PRE.REAL SPEC COMMAND FILE - PART II )
 1  TITLE" 5/29/88 A/8, 40 um film, 25 C, 4 ml/min, 200 ohm, BK "
 2  TITLE" 5/29/88 BLINE, 40 um film, 25 C, 4 ml/min, 200 OHM, BK "
 3  ( TITLE" 5/29/88 A, 40 um film, 25 C, Bottom Grd, 510 OHM, BK )
 4  XLABEL" Time (sec) " ( YLABEL" Volts*10 " ) YLABEL" ADC Units "
 5  SPACE-CHECK   CLEAR_SCREEN   AXES   XTICS  XNUM   XLABEL  TITLE
 6  BASE.BLK @ 616 - .       0 PLACES !       YTICS  YNUM   YLABEL
 7  ( <BLK#>  <#POINTS> <STARTING X COORD> <X INCREMENT>)
 8    BASE.BLK @  PNTS         0. E 0          1. E 0        YTPLOT
 9    BASE.BLK @ 2+ PNTS       0. E 0          1. E 0        YTPLOT
10    BASE.BLK @ 4 + PNTS      0. E 0          1. E 0        YTPLOT
11    BASE.BLK @ 6 + PNTS      0. E 0          1. E 0        YTPLOT
12    BASE.BLK @ 8 + PNTS      0. E 0          1. E 0        YTPLOT
13  ( BASE.BLK @ 10 + PNTS     0. E 0          1. E 0        YTPLOT
14    BASE.BLK @ 12 + PNTS     0. E 0          1. E 0        YTPLOT
15                                          ( OFF ) ( QUIT  )
```

```
Block  400
 0  ( Load Block -- Data Manipulation )
 1  450 LOAD          ( Get Array & Data Save )
 2
 3  ( 401 LOAD          ( Area Under Peak )
 4  ( 405 LOAD          ( Baseline Correction moving both ends to 0 )
 5  406 LOAD          ( Bline Correction moving the initial avg to 0 )
 6  410 LOAD          ( Filtering )
 7  ( 415 LOAD          ( Integrate Data )
 8
 9  ( 420 LOAD          ( Scan Subtraction )
10  ( 425 LOAD          ( Stats )
11  430 LOAD          ( Peak Height )
12  ( 435 LOAD          ( Area Under Peak from Stats Limits )
13  ( 440 LOAD          ( Derivative of Data )
14
15  ( 445 LOAD          ( Stats )
Block  401
 0  ( Area Under Peak )
 1
 2  VARIABLE CONST           VARIABLE STEP
 3
 4                                                    -->
 5
 6
 7
 8
 9
10
11
12
13
14
15
Block  402
 0  ( Area Under Peak )
 1
 2  : FIRST_AVG  ( -- n, average 1st 25 points of ARRAY )
 3          ARRAY   100   AVG   ;
 4
 5  : LAST_AVG  ( -- n, average points 276 to 300 of ARRAY )
 6          ARRAY   1800 +  100   AVG   ;
 7
 8  : BASELINE  ( --, calculate the average baseline for peak )
 9          FIRST_AVG    LAST_AVG   2OVER   F-      2E0   F/
10          F+   FIX   DROP   CONST   !  ;
11                                                    -->
12
13
14
15
```

```
Block  403
 0  ( Peak Area )
 1
 2  : AREA  ( --, sums area under peak minus avg baseline )
 3          BASELINE          0. SUM 2!         1800 200 DO
 4                   ARRAY    I + @    CONST @  -
 5                   SUM 2@   ROT      M+       SUM 2!
 6          2 /LOOP           SUM 2@   D.         ;
 7
 8  : AL  ( blk1 blk2 step --, prints peak areas for a range )
 9          CR   ." Block  Area "   CR   STEP !
10          1+ SWAP DO
11                   I   DUP   .   ."     "   ARRAY-GET    AREA    CR
12          STEP @  /LOOP   ;
13
14
15
Block  405
 0  ( Baseline correct )
 1
 2  VARIABLE SLOPE           VARIABLE INTERCEPT
 3
 4  : CORRBL  ( --, averages 1st & last 50 points, calculates line
 5                   and subtracts from scan )
 6      ARRAY 50 + 50 AVG   ARRAY  #PNTS @  2*  +  102 -  50  AVG
 7      2OVER  F-    FIX  DROP   #PNTS @  2*    1000    SWAP    */
 8      SLOPE !      FIX  DROP   INTERCEPT !
 9      #PNTS @  2*  0 DO
10          ARRAY   I + @   SLOPE @   I 1000  */  INTERCEPT @ +  -
11          ARRAY   I + !    ESCAPE
12      2 /LOOP   ;
13
14
15
Block  406
 0  ( Correct baseline by moving the avg baseline to zero )
 1
 2  : CORRBL   ( -- )   ARRAY  50 + 50  AVG   FIX  DROP
 3          #PNTS @  2*  0  DO
 4                   DUP   ARRAY  I  +  DUP  @  ROT  -  SWAP  !
 5          PAUSE   2 /LOOP   DROP ;
 6
 7
 8
 9
10
11
12
13
14
15
```

```
Block  410
 0  ( Filter )
 1
 2  VARIABLE UNF              2040 ALLOT
 3
 4  : GET_UF  ( --, store data in array UNF )  #PNTS @ 2* 0 DO
 5          ARRAY   I +  @  UNF   I  20 +  +  !      2 /LOOP
 6       ARRAY  DUP  @   SWAP   #PNTS @   2* 2 - + @   20 0 DO  2DUP
 7       UNF  I + #PNTS @ 2* 20 + + !  UNF I + !
 8       2 /LOOP      2DROP ;
 9
10                                                        -->
11
12
13
14
15
Block  411
 0  ( Filter )
 1  (
 2  : 7FILT   ( --, filter 1st 500 pts )( GET_UF
 3       #PNTS @ 2* 6 +   6 DO                          ESCAPE
 4           UNF I + 2 - @  6 M*    UNF I + 2 + @  6 M*
 5           UNF I + 4 - @  3 M*    UNF I + 4 + @  3 M*
 6           UNF I + 6 - @ -2 M*    UNF I + 6 + @ -2 M*
 7           UNF I +      @  7 M*
 8           D+ D+ D+ D+ D+ D+  10 0 D+  21 M/
 9           ARRAY  I + 6 -  !
10       2 /LOOP ;
11  )
12                                                        -->
13
14
15
Block  412
 0  ( Filter )
 1  : FILT   ( --, filter 1st 500 pts )  GET_UF
 2       #PNTS @ 2* 20 +  20 DO   ESCAPE   UNF  I +  @  329  M*
 3           UNF I + 2 - @  324 M*   UNF I + 2 + @  324 M*
 4           UNF I + 4 - @  309 M*   UNF I + 4 + @  309 M*
 5           UNF I + 6 - @  284 M*   UNF I + 6 + @  284 M*
 6           UNF I + 8 - @  249 M*   UNF I + 8 + @  249 M*
 7           UNF I + 10 - @ 204 M*   UNF I + 10 + @ 204 M*
 8           UNF I + 12 - @ 149 M*   UNF I + 12 + @ 149 M*
 9           UNF I + 14 - @  84 M*   UNF I + 14 + @  84 M*
10           UNF I + 16 - @   9 M*   UNF I + 16 + @   9 M*
11           UNF I + 18 - @ -76 M*   UNF I + 18 + @ 176 M*
12           UNF I + 20 - @ -171 M*  UNF I + 20 + @ -171 M*
13           PAUSE   21 1 DO  D+  LOOP      1530 0 D+  3059 M/
14           ARRAY  I + 20 -  !
15       2 /LOOP ;
```

```
Block  415
 0  ( Integral of Data )
 1
 2  : SCALE  ( --, divide array by 2 )    #PNTS @  2*  0 DO
 3          ARRAY   I +   DUP   @   2/   SWAP   !
 4          2 /LOOP   1 ISCALE  +!  ;
 5
 6  : INTEG  ( --, integrate ARRAY )
 7      0 ISCALE !   0.  ARRAY @  M+   SUM 2!
 8      #PNTS @  2*  2 DO
 9          SUM 2@   ARRAY   I +   @   M+
10          2DUP   1 M/   ABS   6000
11          >   IF   SCALE   1 2 M*/   I .   THEN
12          2DUP   SUM 2!   1 M/   ARRAY   I +   !  ESCAPE
13      2 /LOOP     ;
14                                                  -->
15
Block  416
 0  ( INTEGRATE )
 1
 2  : BI   ( blk --, integrate block, print area )
 3          ARRAY-GET   CORRBL   FILT    INTEG
 4          ISCALE @ 0 DO   SUM 2@  2DUP D+  SUM 2!   LOOP
 5          SUM 2@ D.  ;
 6
 7  : BL   ( blk1 blk2 --, BI loop )
 8          SWAP DO  CR   I .  I BI    2 /LOOP      ;
 9
10
11
12
13
14
15
Block  420
 0  ( Scan Subtraction )
 1
 2  VARIABLE SCAN                    VARIABLE BLINE
 3
 4  : COMPATIBLE   ( --, check compatibility )
 5          BLINE @          SCAN @          1
 6          12 4 DO          2 PICKUP        2 PICKUP
 7                  BLOCK I + @     SWAP    BLOCK I + @
 8                  =        AND
 9           2 /LOOP         ROT ROT 2DROP ;
10                                                  -->
11
12
13
14
15
```

```
Block  421
 0  ( Scan Subtraction )
 1                                    : 3DUP  DUP 2OVER ROT ;
 2
 3  : SUBLOOP  ( n blk1 blk2 --, n = nth block )
 4          ( subtract BLINE from SCAN & store in ARRAY )
 5          BLOCK   SWAP    BLOCK
 6          500 0 DO
 7                  3DUP   I  12 + 2* + @   SWAP   I  12 + 2* +  @
 8                  -   SWAP  1000 *  ARRAY  I 2*  + +  !
 9          LOOP    2DROP DROP ;
10
11  : DISK>VARI  ( --, read disk, store in vari )
12          SCAN @  BLOCK   DUP 4 + @ #PNTS !
13          DUP 6 + @ #6 !  DUP 8 + @ #8 !  10 + @ #10 ! ;
14
15                                                      -->
Block  422
 0  ( Scan Subtraction )
 1
 2  : SUBT ( blk1 blk2 --, subt BLINE from SCAN store in ARRAY)
 3          ." input SCAN blk, BLINE blk "
 4          616 +  BLINE !       616 +  SCAN !
 5          COMPATIBLE
 6          IF
 7                  DISK>VARI       #PNTS @ 500 /
 8                  0 DO    I       SCAN @  I +
 9                          BLINE @     I +     SUBLOOP
10                  LOOP
11          ELSE
12                  CR      ." scans not equal "    QUIT
13          THEN ;
14
15
Block  425
 0  ( STATS )
 1  : SM   ( addr n-- sum, # to be summed )    0 0  ROT  2*
 2     0 DO  2 PICKUP  I +  @     SDF     F+   2 /LOOP  ROT DROP ;
 3
 4  : SQSUM   ( addr n-- sum^2, # to sqrd & summed )  0 0  ROT 2*
 5     0 DO  2 PICKUP  I +  @  SDF  F**2  F+   2 /LOOP  ROT DROP ;
 6
 7  : VARI  ( addr n -- variance, # of points ) 2/  SWAP 2DUP  OVER
 8          SQSUM   2SWAP   SWAP    OVER    SM      F**2    ROT
 9          SDF     F/      F-      ROT 1-  SDF     F/  ;
10
11  : VAR  ( n1 n2--, output variance as a fn of # pnts )  1+ SWAP
12          DO      I .     ARRAY   I   2DUP  2*  +  ?   AVG   E.
13                  ARRAY   I VARI  E.      CR      LOOP ;
14
15                                                      -->
```

```
Block  426
 0  ( STATS )
 1  : AP   ( n --, DUMP 8 pnts at pt )  DUP ." X= " . ."  Y= "
 2          2*  ARRAY +  DUP  ?  CR
 3          8 -  16  0  DO  DUP  I +  ?  2 /LOOP  DROP  ;
 4
 5
 6
 7
 8
 9
10
11
12
13
14                                                      -->
15
Block  427
 0  ( STATS )
 1  : DA+   ( n1,n2--n1,1 )   OVER  SWAP  ARRAY  +  @   <  ;
 2
 3  : 4SIG   ( --n, X pt of return to -4 sigma )   1ST-MIN
 4      ARRAY   XMIN @   2DUP   AVG   2SWAP   VARI
 5      SQRT    4   SDF   F*   F+
 6      FIX  DROP  1+  #PNTS @ 2*  XMIN @  2*  20 +  DO   ESCAPE
 7          DUP  I  ARRAY  +  @  >  IF   I 2/  LEAVE  ELSE
 8          #PNTS @ 2* I 4 + < IF I 2/  LEAVE  THEN   THEN
 9      2 /LOOP   SWAP   (  #PNTS @ 2*  220  DO   ESCAPE
10          I      DA+  IF   I  2+  DA+  IF  I  4 +  DA+  IF
11          I  6 + DA+  IF   I 8 +  DA+  IF  I 10 +  DA+  IF
12          I 2/  LEAVE  THEN  THEN  THEN  THEN  THEN  THEN
13          #PNTS @ 1- 2* I = IF ." BASELINE " I  LEAVE THEN
14      2 /LOOP   SWAP )  DROP  XMIN @  ;
15                                                      -->
Block  428
 0  ( STATS )
 1
 2  : AREA   ( --, print area from "under curve" )
 3          CORRBL  FILT    4SIG    2DUP  2* ARRAY +  @
 4          SWAP  2*  ARRAY +  @  +  2/  RMIN !  0.  2OVER   DO
 5                  ARRAY  I 2*  +  @  RMIN @ -  M+   LOOP
 6          ." Area "  D.   ."  from "  .  ."  to "  . ;
 7
 8                                                      -->
 9
10
11
12
13
14
15
```

```
Block  429
 0  ( STATS )
 1  : AL   ( blk1 blk2 --, does AREA range )   1+ SWAP   CR   DO
 2          I DUP   ARRAY-GET   .   AREA   CR      2 /LOOP  ;
 3  (
 4  : DL   ( blk1 blk2 --, outputs peak start unfilt & filt )  CR
 5  (       1+ SWAP  DO I . CR I   ARRAY-GET   CORRBL  4SIG   AP
 6                  CR  FILT    4SIG   AP  CR  2 /LOOP  ;
 7  (
 8  : -DL   ( blk1 blk2 --, outputs peak start unfilt & filt )  CR
 9  (       1+ SWAP  DO I . CR I   ARRAY-GET   CORRBL  -4SIG   AP
10                  CR  FILT   -4SIG   AP  CR  2 /LOOP  ;
11  )
12
13
14
15
Block  430
 0  ( Peak Height )
 1
 2  VARIABLE PEAK
 3
 4                                                    -->
 5
 6
 7
 8
 9
10
11
12
13
14
15
Block  431
 0  ( Peak Height )
 1
 2  : PEAK-MAX  ( --, avg 5 points around max )   ( - ) 2048 PEAK !
 3          ARRAY   300  210 DO
 4                  DUP     I +  @  PEAK @    < ( > ) IF
 5                          I RMAX !        DUP  I +  @   PEAK !
 6                  THEN
 7          2 /LOOP          RMAX @  + 5     AVG
 8          FIX  DROP     DUP     PEAK !
 9          ."   Max x "  RMAX @ 2/  .  ." y "   .   ;
10
11                                                   -->
12
13
14
15
```

```
Block  432
 0  ( Peak Height )
 1  (
 2  : 2ND-MIN  ( --, avg 20 pts at 2nd min )(       -2048 2MIN !
 3          ARRAY   2000 400 DO
 4                  DUP     I + @  2MIN @  > ( < )( IF
 5                          I RMIN !        DUP  I + @   2MIN !
 6                  THEN
 7          2 /LOOP
 8          RMIN @ +   20 -   20 AVG   FIX  DROP   DUP   2MIN !
 9          ."   2nd min x "  RMIN @ 2/ 12 - .  ." y "  .  ;
10
11  )
12
13                                                      -->
14
15
Block  433
 0  ( Peak Height )
 1  (
 2  : PKHT  ( --, ARRAY peak height above baseline calc from slope
 3            [y2-y1]/[x2-x1] see page 62 in notebook )     CR
 4  (       1ST-MIN         PEAK-MAX                2ND-MIN
 5          PEAK @          2MIN @ YMIN @ -         RMAX @ 44 -  M*
 6          RMIN @ 44 -     M/      YMIN @ +        -
 7          ."   Peak Height "  .  ;
 8
 9  : HT  ( blk1 blk2 --, limits on loop to calc peak heights )
10  (                       1+ SWAP .S      DO      CR  I .
11                  I ARRAY-GET     ( CORRBL )( FILT   PKHT
12          2       /LOOP  ;
13  )
14                                                      -->
15
Block  434
 0  ( Peak Height )
 1
 2  ( : MIN_INJ   ARRAY  210 +  15  AVG  FIX DROP  ; )
 3
 4  : PKHT2  ( --, avg area around injection then find max & diff )
 5          ARRAY  160 +  10   AVG  FIX  DROP  ." Min "  .S
 6                  PEAK-MAX        PEAK @   -   ABS
 7          ."   Peak Height "  .  ;
 8
 9  : HT2  ( blk1 blk2 --, limits on loop to calc peak heights )
10          1+ SWAP DO      CR
11                  I ARRAY-GET   I .   CORRBL    FILT   PKHT2
12          2       /LOOP  ;
13
14
15
```

```
Block  435
 0  ( Area Under Peak from Stats )
 1  : AREA   ( --, sums area from 1st 3 sigma dev to 3 sig return )
 2          0. SUM 2!  ARRAY  200 +   30  2DUP  AVG   2SWAP  VARI
 3          SQRT   3  SDF   F*    F- ( F+ ) FIX  DROP   1-
 4          ( #PNTS @  2* )  800  260  DO   ESCAPE
 5              DUP  I  ARRAY  +  @   > ( < ) IF  ( I .   )
 6                  SUM 2@   ARRAY  I  +  @  M+  SUM  2!  THEN
 7          2 /LOOP   DROP  SUM  2@  D.  ;
 8
 9  : AL   ( blk blk --, prints area from 1st 3 sigma to last )  CR
10          ." Blk  Area "  1+ SWAP   DO    CR    ESCAPE
11                  I DUP .  ARRAY-GET   CORRBL   FILT   AREA
12          2 /LOOP ;
13
14
15
Block  440
 0  ( Derivative of Data )
 1
 2  : DERIV  ( --, filter 1st 500 pts )
 3      #PNTS @  1 -  2*  0 DO
 4          ARRAY  I +  DUP  2+  @  SWAP  @  -  ARRAY  I +  !
 5      2 /LOOP
 6      ARRAY  #PNTS @  2*  +   DUP   2 - @   SWAP   !   ;
 7
 8
 9
10
11
12
13
14
15
Block  445
 0  ( STATS )
 1  : SM   ( addr n-- sum, # to be summed )    0 0  ROT  2*
 2      0 DO  2 PICKUP  I +  @     SDF     F+   2 /LOOP  ROT DROP ;
 3
 4  : SQSUM   ( addr n-- sum^2, # to sqrd & summed )  0 0  ROT 2*
 5      0 DO  2 PICKUP  I +  @  DUP * SDF  F+   2 /LOOP  ROT DROP ;
 6
 7  : VARI  ( n -- variance, # of points )  DUP ARRAY OVER  SQSUM
 8          ROT ARRAY OVER  SM      F**2    ROT
 9          SDF     F/      F-      ROT 1-  SDF     F/  ;
10
11  : VAR  ( n1 n2--, output variance as a fn of # pnts )  1+ SWAP
12          DO      I .     ARRAY   I   2DUP  2*  +  ?   AVG   E.
13                  I VARI  E.      CR      LOOP ;
14
15                                                      -->
```

```
Block  446
 0  ( STATS )
 1  : AP    ( n --, DUMP 8 pnts at pt )  DUP ." X= " . ."  Y= "
 2          2*  ARRAY +  DUP  ?  CR
 3          8 -  16  0  DO  DUP  I +  ?  2 /LOOP  DROP  ;
 4
 5  : 4SIG   ( --n, X pt of -4 sigma )
 6      ARRAY 105 AVG   105 VARI  SQRT  4 SDF  F* F-  FIX DROP  1-
 7      #PNTS @ 2*  210  DO   ESCAPE
 8          #PNTS @ I 2- = IF ." BASELINE " I LEAVE THEN
 9          DUP  I     ARRAY + @ >  IF   DUP  I  2+  ARRAY + @ > IF
10          DUP  I 4 + ARRAY + @ >  IF   DUP  I  6 + ARRAY + @ > IF
11          DUP  I 8 + ARRAY + @ >  IF   DUP  I 10 + ARRAY + @ > IF
12          I 2/  LEAVE  THEN  THEN  THEN  THEN  THEN  THEN
13      2 /LOOP   SWAP  DROP  ;
14                                                    -->
15
Block  447
 0  ( STATS )
 1
 2  : DL   ( blk1 blk2 --, outputs peak start unfilt & filt )  CR
 3          1+ SWAP  DO I . CR I   ARRAY-GET   CORRBL  4SIG   AP
 4                  CR  FILT    4SIG   AP  CR  2 /LOOP  ;
 5
 6                                                    -->
 7
 8
 9
10
11
12
13
14
15
Block  448
 0  ( STATS )
 1  : -4SIG   ( --n, X pt of return to -4 sigma )
 2      ARRAY 105 AVG   105 VARI  SQRT 10 SDF  F* F-  FIX DROP  1-
 3      #PNTS @ 2*  4SIG 2* 20 +   DO   ESCAPE
 4          #PNTS @ 2* I 4 - < IF I LEAVE THEN
 5          DUP  I  ARRAY + @   <  IF   I 2/  LEAVE  THEN
 6      2 /LOOP   SWAP  DROP  ;
 7
 8  : -DL   ( blk1 blk2 --, outputs peak start unfilt & filt )  CR
 9          1+ SWAP  DO I . CR I   ARRAY-GET   CORRBL  -4SIG   AP
10                  CR  FILT   -4SIG   AP  CR  2 /LOOP  ;
11
12
13
14
15
```

```
Block  450
 0  ( Get Array & Data Save )
 1
 2  VARIABLE BLK            VARIABLE RMAX           VARIABLE RMIN
 3  VARIABLE #6             VARIABLE #8             VARIABLE #10
 4  VARIABLE #PNTS          VARIABLE ARRAY          1998 ALLOT
 5  2VARIABLE SUM           VARIABLE ISCALE         0 ISCALE !
 6  VARIABLE XMIN           VARIABLE YMIN
 7
 8  : DISK>VARI  ( --, read disk, store in vari )
 9          BLK @   BLOCK   DUP 4 + @ #PNTS !
10          DUP 6 + @ #6 !  DUP 8 + @ #8 !  10 + @ #10 ! ;
11
12
13
14                                                      -->
15
Block  451
 0  ( Get Array )
 1  : ARRAY_GET   ( blk --, store data in ARRAY )
 2      616 +     BLK !   DISK>VARI
 3      #PNTS @   500 /   0 DO      BLK @   I +     BLOCK
 4          1000 0 DO
 5              DUP       I +       24 +    @
 6              ARRAY     I +       1000  J *  +    !
 7          2 /LOOP     DROP
 8      LOOP  ;
 9
10  : ARRAY_DUMP   ( pt range --, print range of points in ARRAY )
11      19  +  20  /  SWAP  20  /  SWAP  OVER  +  SWAP  DO
12          CR   I   20   *   .   SPACE
13          20  0  DO   ARRAY  I  2*  +  J  40  *  +  ?   LOOP
14      LOOP CR ;
15                                                      -->
Block  452
 0  ( I_SAVE -- save SINGLE INTEGER ARRAY on DISK as INTEGER )
 1
 2
 3  : 1I_SAVE  ( blk.buf.addr data.addr cnt -- ) ( save one block)
 4          2*  0 DO        2DUP I + @      SWAP
 5          I + !   2 +LOOP        2DROP    UPDATE  FLUSH ;
 6
 7  : I_SAVE   ( base.blk -- )
 8          BLK !           #PNTS @
 9          DUP     500 /MOD        SWAP    0= NOT
10          IF  1+  THEN    0 DO    DUP     500 MIN
11          BLK @ I +       BLOCK 24 +      ARRAY  I   1000 * +
12          ROT     1I_SAVE         500 -   LOOP   DROP ;
13
14                                                      -->
15
```

```
Block  453
 0  ( SMIN, SMAX & MAXMIN_STORE )
 1
 2  : SMAX  ( #pnts -- max)          1- 2*   ARRAY   2+ @
 3          SWAP    2 DO    ARRAY   I + @   MAX     2 /LOOP ;
 4
 5  : SMIN  ( #pnts -- min)          1- 2*   ARRAY   2+ @
 6          SWAP    2 DO    ARRAY   I + @   MIN     2 /LOOP ;
 7
 8  : MAXMIN_STORE   ( #pts -- store 100's range )  DUP
 9          SMAX    DUP      21 < IF
10                  DROP     21     THEN    RMAX !
11          SMIN    DUP     -21 > IF
12                  DROP    -21     THEN    RMIN !  ;
13
14                                                  -->
15
Block  454
 0  ( Data Store Block -- VARI_TO_DISK, DATA_SAVE )
 1
 2  : FS   ( vari, n -- ) ( fetch block & store # in position )
 3          BLK @  BLOCK + ! ;
 4
 5  : VARI_TO_DISK   ( -- store variables on disk )
 6          RMIN @  0 FS    RMAX @  2 FS    #PNTS @  4 FS
 7          #6 @    6 FS    #8 @    8 FS    #10 @   10 FS
 8          ISCALE @  12 FS  ;
 9
10  : DATA_SAVE  ( beginning-blk -- ) ( write data to disk )
11          616 +          I_SAVE          #PNTS @
12          MAXMIN_STORE  VARI_TO_DISK    UPDATE FLUSH      ;
13
14                                                  -->
15
Block  455
 0  ( Average & 1st MIN )
 1  CODE S>D  S ) TST  S -) SXT   NEXT      : SDF  S>D FLOAT ;
 2
 3  : AVG  ( addr n-- avg, average next n pts )
 4          0.   2 PICKUP   2* 0 DO
 5                  3 PICKUP   I +   @   SDF   F+
 6          2 /LOOP
 7          2 PICKUP   2/   SDF   F+   ROT   SDF   F/
 8          ROT    DROP  ;
 9
10  : 1ST-MIN  ( --, avg 5 pts after 1st MIN )   2048 YMIN !
11          150   105  DO    ARRAY I 2* + @  YMIN @  <=  IF
12                ARRAY   I 2* + @  YMIN !   I   XMIN  !  THEN
13          LOOP  ARRAY  XMIN @  2*  +  8  -  5  AVG
14          FIX   DROP   YMIN !  ;
15
```

Appendix D

PVDF and Pyroelectric Terms

AMPLIFIER NOISE[1]

$$i_n = e_n / z_d$$

i_n - equivalent input current noise

e_n - equivalent input voltage noise

z_d - detector input impedance

ANGULAR FREQUENCY OF OPERATION - w (omega) (radians/s) [1,2]

AREA - A

BIMORPH

A two layer piezoelectric. Used with the poled sides of the same sign together to cancel piezoelectric contributions in a pyroelectric setup or oppositely signed poled sides together to increase piezoelectric signal.[2]

CAPACITANCE - C

417 pF/cm^2 for a 28 μm film, $\epsilon/\epsilon_0 = 12$. [2]

CHARGE DUE TO THE PYROELECTRIC EFFECT - Q [1] - q [2]

$$Q = p \, \text{delta}(T) \, A$$

CONDUCTANCE

see thermal, radiative

CRYSTAL STRUCTURE AND PYROELECTRICITY

21 of the 32 crystal structures are noncentrosymmetrical and can exhibit piezoelectric properties. 10 of these can exhibit spontaneous electrical polarization. An external electric field is not usually measurable if the material is conductive. The conductivity allows the charges developed to migrate to neutralize the internal moment. If the material is an insulator, charges will be attracted to and trapped on the surface until the surface charge associated with the polarization is neutralized. This charge distribution on the surface of the insulator is relatively stable and does not respond quickly to changes in the dipole moment. If the temperature is changed, the dipole moment may change and this change will produce an electric field. Although the dipole moment cannot be directly measured, its temperature coefficient can. This temperature coefficient is the pyroelectric coefficient.[3,4,5]

CURRENT RESPONSIVITY - R_i

Gives a measure of current responsivity, charge output per unit energy input, with respect to detector thickness and modulation frequency. Units = amp/Watt or Coul/J [1]

$$R_i = \mathrm{abs}(i/W) = \eta\, p\, A\, w/G_T\, (1 + w^2 \tau_T^2)^{1/2}$$

A plot of R_i vs. angular frequency w for PVDF shows at very low w, <

10^{-5} Coul/J, R_i approaches zero. Between 10^{-5} and 10^{-3} Coul/J, R_i increases to about 10^{-14} and levels off.

if $w \gg 1/\tau_T$, then $R_i = \Pi\ p/s\ d$

As can be seen from the equation above, R_i is inversely proportional to the thickness, d. A film thickness of 6 μm has an R_i of about 10^{-6} Coul/J.

DENSITY - S [5] - rho [1,2]

1.78 g/cm^3

DETECTOR AREA - A

DIELECTRIC

a material, most of the time an insulator, that can have its electrons, ions, or molecules polarized under the influence of an external electric field. Dielectrics are used in capacitors. Ferroelectrics are a subset of this class of materials.[6]

DIELECTRIC CONSTANT - ϵ

(106 - 113) x 10^{-12} F/m. (permittivity of PVDF) [2]

DIELECTRIC LOSS - tanδ

0.015 - 0.02 at 10 - 10^4 Hz for PVDF. [2]

DIELECTRIC NOISE[1]

$$V_D = (4\ k\ T/w\ C\ \tan\delta)^{1/2}$$

$$i_D = (4\ k\ T\ w\ C\ \tan\delta)^{1/2}$$

ELECTRICAL CIRCUIT OF A PYROELECTRIC DETECTOR[3]

With the constants pyroelectric coefficient p and electrode area A, θ_w produces an alternating charge $pA\theta_w$. With capacity C_p in parallel with resistance R_p , the alternating charge on the electrodes is equivalent to a current generator in parallel to the capacity.

$$i_p = wpA\theta_w$$

A plot of $-i_p/A$ vs. w for PVDF at θ_w ranging from 0.0001 to 10°K gives a linear plot. At w = 0.1 and θ_w ranging from 10^{-4} to 10°K, the pyroelectric current i_p ranges from -10^{-13} to -10^{-8}.

If the electrodes are connected to the inputs of an amplifier with a known capacity and parallel resistance, the voltage applied to the amplifier is found by calculating the voltage across the equivalent circuit for the combined impedances.

$$V = i_p\ |Z| = i_p\ R/(1+w^2\ \tau_E^2)^{1/2}$$

$$\tau_E = RC$$

$$V = wpA\theta_w\ R/(1+w^2\ \tau_E^2)^{1/2}\ \ s$$

A plot of voltage per unit area V/A vs. angular frequency w for PVDF film thicknesses of 6 to 100 μm and a theta of 0.1°K shows a linear voltage increase with increasing w until $w = 1/\tau_E$, where the graph levels off showing that the voltage produced per unit area is independent of frequency and thickness. V also increases linearly

with thickness below $1/\tau_E$ and is independent of temperature above $1/\tau_E$. A plot of V vs. w at θ_w's of 0.0001 to 10 with a 28 μm thick film shows a linear increase in V with θ_w.

ELECTRICAL CONDUCTANCE - G_E [1]

$1/G_E$ - resistivity, volume resistivity - $rho_R = 10^{13}$ Ω-m [2] specific resistance

ELECTRICAL TIME CONSTANT - τ_E

This is a relatively long time constant which allows measurements at frequencies below other pyroelectric detectors. τ_E is approximately 10^3 sec. [2] $\tau_E = 10^{-12}$ - 100 sec, depends on detector and shunt resistor for a normal pyroelectric material.[1]

$$\tau_E = C/G_E \quad [1]$$

$$\tau_E = RC \quad [3]$$

A plot of τ_E vs. thickness gives a linear increase in τ_E with increasing thickness from 250 sec at 6 μm to 4000 sec at 100 μm thick PVDF using the second equation above.

EMISSIVITY OF THE SURFACE - η (eta)

η is a relative measure of the amount of the energy absorbed at a surface. This term is used for radiative energy and is not directly applicable to other heat transfer mechanisms. For aluminum, $\eta \approx 0.1$, for carbon black, $\eta \approx 0.95$. [7]

EXCESS TEMPERATURE - θ

See thermal admittance. At the surface, the excess temperature is

$$\theta_o = \theta_w \cos wt$$

The excess temperature at distance x below the surface is[5]

$$\theta_x = \theta_w \exp[(-wc'/2K)^{1/2} x] \cos[wt-(wc'/2K)^{1/2} x]$$

FERROELECTRIC

A ferroelectric a dielectric which has a spontaneous dipole which is usually the result of a non-symmetric crystal lattice; a cation is displaced from the center of a negative charge in the unit cell structure. Ferroelectrics can be pyroelectric and piezoelectric.[6]

HEAT CAPACITY - C_v [2] or - H [1,5]

The amount of heat required to increase the temperature of a system one degree and is an extensive property depending on weight or volume.[7] See thermal capacity.

$$H = c' A d \quad (J/^oK) \quad [5]$$

INCIDENT POWER - I

power of the beam - I_w power of the modulated beam.[5]

INCIDENT RADIANT POWER - W

the amount of power reaching the detector. - W_o is the unmodulated power.[1]

$$W = W_o e^{jwt}$$

NOISE

see amplifier, dielectric, resistor or thermal noise [1]

NORMALIZED DETECTIVITY - D*

This is a pyroelectric figure of merit.[2]

$$D^* = 2\, C_v\, \rho\, (t\, w\, \epsilon\, k_B\, T\, \tan\delta)^{1/2} / (p\, \Omega)$$

PERMITTIVITY OF FREE SPACE - ϵ_0

8.854×10^{-12} F/m [2]

PERMITTIVITY OF PVDF - ϵ_r

$(106 - 113) \times 10^{-12}$ F/m (Dielectric constant)[2]

PIEZOELECTRIC

a dielectric that has a displacement of ions and changes dimensions of the crystal when a dipole is induced by an applied electric field. Conversely, when the piezoelectric is stressed, its dimensions changed, a electric field is induced. The change in dimensions is proportional to the electric field.[2,3,4]

POLING

Poling is the process by which PVDF is made piezo and pyroelectric. There are two methods used to pole PVDF. The first is to stretch a film in one direction. This straightens and aligns the polymer chains. Then the film is placed in a strong electrical field and the temperature is raise to above the t_g, about 120°C, for a couple of

hours. This allows the chains to orient in the electrical field with the electronegative fluorines toward the positive electrode and the relatively electropositive hydrogens toward the negative electrode. This is called a monoaxial film because it is stretched only in one direction. This gives the film different physical and piezoelectric characteristics in the X, Y and Z directions. This type of film is msde by Pennwalt.[2] The second type of PVDF is a biaxial film. This type is made by stretching the film in both the X and Y direction which gives the film uniform physical and piezoelectric constants. This is the type of film made by Solvay. They use a continuous poling method that uses a very high electric field to orient the molecules.[2]

PROPAGATION CONSTANT FOR THE THERMAL WAVE - gamma

See thermal admittance. Units - 1/cm [5]

$$\text{gamma} = (1+j)(wc'/2K)^{1/2}$$

A plot of gamma vs w ignoring the complex component shows, as you can see from the equation, a linear increase of gamma with w. At 0.1 radians/s, gamma is 10 cm^{-1}.

PYROELECTRIC

A pyroelectric is a piezoelectric that changes polarization with changes in temperature. Thermal expansion and contraction change the dipole moment of the crystal. The change in polarization is proportional to the temperature change. All pyroelectrics are piezoelectric.[2,4] Vectoral pyroelectricity, as opposed to tensorial, is

the type usually encountered. Mathmatically, it is a relation between a scalar, temperature, and a vector, polarization. Physically, it is the change with temperature of positive and negative polarization charges on certain portions of crystals belonging to certain classes. See crystal structure and piezoelectricity.[4]

PYROELECTRIC COEFFICIENT - p

A one degree change will produce approximately 10^{-7} Coulombs per square centimeter. $p = -2.5 \times 10^{-5}$ Coul/m^2 °K for PVDF [1,2,3]

PYROELECTRIC CURRENT[5] - i_p

$$i_p = wpA\theta_w$$

A plot of pyroelectric current per unit area i_p/A vs. angular frequency w at θ_w from 0.0001 to 10°K shows, as can be seen from the equation, a linear increase in i_p with increasing w and θ_w. At θ_w = 0.01 and w = 0.1, $i_p = 10^{-12}$ amp/cm^2.

PYROELECTRIC VOLTAGE - V

Voltage rises with the thermal time constant and decays with the electrical time constant. (t - detector thickness) [2]

$$V = p\ t\ \text{delta}(T)/\epsilon$$

QUADRATURE

90 degrees out of phase.

RADIATIVE CONDUCTANCE - G_R

for radiation from one surface. See thermal conductance.[5]

$$G_R = 4 \Pi \sigma A T^3$$

RELATIVE PERMITTIVITY - ϵ_r/ϵ_o

11-13 for PVDF [2,8]

RESISTANCE - R

$$R = \text{rho } 1/A$$

RESISTIVITY - rho - $1/G_E$

see electrical conductance, volume resistivity, specific resistance[7]

RESISTOR NOISE - i_R [1]

$$i_R = (4kT/R)^{1/2}$$

RESPONSIVITY

R_i see current responsivity - R_v see voltage responsivity.

SPECIFIC HEAT - C_v

2.4×10^6 J/m^3 °K [2] (this number is more correctly called thermal capacity) - c units = J/g°K. [5] (Again, this should probably be thermal capacity) the ratio of a substances thermal capacity to that of water at 15°C, no dimensions. The thermal capacity of water at 15°C is 1.000 Cal/g°K or 4.186 J/g°K. [7]

SPECIFIC RESISTANCE - rho

rho is a proportionality constant characteristic of a substance equal to the resistance of a centimeter cube of the substance offers to an electrical potential; the current is perpendicular to two parallel faces. For a given rho, as area increases resistance decreases and as thickness increases so does resistance. For PVDF, $rho_R = 10^{13}$ Ω-m; [2] therefore, for ten square centimeters of a 40 μm film the resistance is approximately $4 \times 10^{11}\Omega$. see electrical conductance, resistivity, volume resistivity.[7]

$$rho = R\ A/l$$

STEFAN'S CONSTANT - σ

5.7×10^{-12} W/cm^2 K^4

TEMPERATURE (absolute) - T

(as opposed to t for time)

TEMPERATURE DIFFERENCE - θ [1] - delta(T) [2] - θ_w [5]

$$\theta = \Omega\ W_o\ e^{jwt}/(G_T + jwH)$$

Logically, from this equation θ will increase with time, t at constant angular modulation frequency, w and constant incident power. This means at longer sampling times there will likely be more change. Ignoring the imaginary part, a plot of θ/W_o (temperature difference per unit unmodulated incident power) vs. angular modulation frequency, w at time, t from 0.001 to 100 sec. shows at $w \ll G_T/H$, θ/W_o decreases with increasing w and is independent of t. At $w \gg$

G_T/H and constant t, θ/W_o increases exponentially with increasing w. When the wt product equals 1, the relationship is at its minimum, i.e., when t = 10 sec and w = 0.1 rad/s, θ/W_o is at a minimum of 10^{-3} °K/Watt. The magnitude of the minimum is directly proportional to the time. At very low w, θ/W_o approaches $1/G_T$.

$$\theta_w = \Pi\ I_w/(G^2 + w^2 H^2)^{1/2} \quad s$$

A plot of $\log(\theta_w/I_w)$ vs. thickness, d, from 6 to 100 μm at angular frequencies, w, from 0.0001 to 10 radians/s for PVDF gives a slowly decreasing θ_w with increasing d and increasing w. A plot of θ_w/I_w vs. temperature at thicknesses from 6 to 100 μm and w at 0.1 radians/s shows, as you would expect, that the response is fairly temperature independent and decreases exponentially with increasing thickness. A plot of θ_w/I_w vs. w at temperatures from 200 to 450°K and 28 μm thick PVDF shows at very low w, $< 10^{-7}$, the temperature related term dominates and θ_w decreases with temperature. At $w > 10^{-6}$, the frequency related term dominates and θ_w decreases with increasing w and is independent of temperature.

THERMAL ADMITTANCE - Y

For a semiinfinite slab on a block, a temperature of frequency w hits the surface of a pyroelectric causing a damped heat wave to propagate into the slab. An element of thickness dx has a thermal capacity c'A dx and a thermal resistance dx/KA. This can be treated similarly to an electrical circuit. The bulk material allows the absorbing layer a thermal admittance Y. See propagation constant and excess temperature.

$$Y = (1 + j)(wKc'/2)^{1/2} A$$

where w is angular frequency, K is thermal conductivity and c' is the volume specific heat. A plot of Y/A vs. w shows a linear increase in thermal admittance Y with w. Y/A is 0.01 W/cm^2°K at 0.1 radians/s. At a depth δ_T below the surface the amplitude drops to 1/e of its surface value.

$$\delta_T = (2K/wc')^{1/2}$$

At a slightly greater depth, δ, the wave is in quadrature.[5]

$$\delta = \pi(K/wc')^{1/2}$$

THERMAL CAPACITY - C_T [2] - s [7]

the quantity of heat necessary to produce unit temperature change in a unit mass. When ratioed to the thermal capacity of water at 15°C, the value is the specific heat. Thermal capacity is heat capacity per unit weight.[7] For PVDF, C_T = 1.3 J/g °K. [2]

$$s = H / m (t_2 - t_1)$$

THERMAL CIRCUIT

Thermal circuit for an enclosure at temperature T and a detector at temperature T + θ, the heat flow from the detector the surroundings is $G_R \theta$, where G_R is the radiative conductance.[5]

THERMAL CONDUCTANCE - G_T, G_R [1]

G_R is the limiting ideal value for radiative energy loss from two surfaces of a detector, units = W/°K. G_T approaches G_R under ideal conditions. See radiative conductance.[5]

$$G_R = 8 \Pi \sigma A T^3$$

THERMAL CONDUCTIVITY - G [2] - K [5]

0.13 watts/m °K

THERMAL DIFFUSION LENGTH[2] - L

$$L = (2G/C_v \text{ rho } w)^{1/2}$$

THERMAL IMPEDANCE - R_T

R_T is dependent on mounting. If the detector is freely mounted, heat losses are radiative making R_T large. This will give a relatively slow but sensitive detector with a time constant of about five seconds. If the detector is mounted on a heat sink - thermally loading the detector - R_T becomes small giving a fast but less sensitive detector.[2]

THERMAL NOISE[1]

$$\text{delta}(W_T) = (4\ k\ T^2\ G_T)^{1/2}$$

$$i_T = R_i(4\ k\ T^2\ G_T)^{1/2}/\Omega$$

THERMAL TIME CONSTANT - τ_T

describes the thermal behavior of a pyroelectric detector.[2]

Generally, τ_T = 0.01 - 10 sec. [1]

$$\tau_T = R_T\ C_T \quad [1]$$

$$\tau_T = H/G \quad [5]$$

A plot of τ_T vs. temperature at thicknesses from 6 to 100 μm shows τ_T increases exponentially with decreasing temperature and increases with increasing thickness. (see thermal conductance)

THERMAL POWER - P_T

P_T governs the temperature rise.[2]

$$\text{delta}(T) = R_T P_T$$

THICKNESS - t [2] - d [1.5] - l [7]

TIME - t [1]

TIME CONSTANT

τ_E see electrical time constant, τ_T see thermal time constant.

UNIFORM HEATING

see thermal diffusion length.[2]

VOLUME RESISTIVITY - rho_R

10^{13} Ω-m [2] See specific resistance

VOLUME SPECIFIC HEAT - s [1] - c' [5]

Specific heat per unit volume. Appears to be used the same as specific heat C_v.

$$c' = c\ S^{-1}$$

VOLTAGE PRODUCED BY PYROELECTRIC - V [1]

$$V = i/(G_E + jwC)$$

VOLTAGE RESPONSIVITY - R_v

R_v is a measure of the voltage response with modulation frequency. Units - 1/amps [1] R_v is the output voltage per unit input (radiant) power.[5]

$$R_v = \text{abs}(V/W)$$

$$= \eta\, p\, A\, w\, /[G_T\, G_E(1+w^2\, \tau_T^2)^{1/2}\, (1+w^2\, \tau_E^2)^{1/2}] \quad [1]$$

A plot of R_v vs. angular frequency w for PVDF gives a linear increase to about 10^{-5} radians/s where R_v levels off at approximately 10^{-7} until about 10^{-3} radians/s where it decays exponentially.

$$R_v = V/I_w$$

$$= \eta w p A R/[G(1+w^2\, \tau_E^2)^{1/2}(1+w^2\, \tau_T^2)^{1/2}] \quad [5]$$

A plot of R_v vs. angular frequency w at different temperatures for a 28 μm film shows R_v increases with decreasing temperature and increasing w for $w < 1/\tau_T$ and $w < 1/\tau_E$. At $w > 1/\tau_T$ and $w > 1/\tau_E$, R_v is independent of temperature and decreases with increasing w. Between $1/\tau_T$ and $1/\tau_E$, R_v is independent of w and increases with decreasing temperature.

A plot of R_v vs. w for film thicknesses of 6 to 100 μm at 300°K shows, at $w < 1/\tau_T$ and $w < 1/\tau_E$, as thickness increases the film shows lower responsivity. For $w > 1/\tau_T$ and $w > 1/\tau_E$, R_v decreases with increasing w. If w is between $1/\tau_T$ and $1/\tau_E$, R_v is independent of w and thickness.

if $w \gg 1/\tau_T$ and $w \gg 1/\tau_E$

$$R_v = \eta\, p/(s\, \epsilon_0\, \epsilon_r\, A\, w) \quad [1]$$

Appendix E

Flow Injection Analysis Terms

AXIAL DIFFUSION COEFFICIENT - D [9]

units - cm^2/s

DIFFUSION

Fick's law of diffusion in the axial direction is

$$\frac{\delta C}{\delta t} = D \frac{\delta^2 C}{\delta x^2}$$

where C is concentration, t is time, x is distance and D is the axial dispersion coefficient with units of area per unit time.[9]

DIFFUSION COEFFICIENT - D [10,11]

$$\Delta t_B = \frac{35.4\ a^2\ f}{D^{0.36}} \left[\frac{L}{q} \right]^{0.64}$$

where Δt_B is the peak width in seconds, a is the flow path radius in centimeters, f is a detector response to concentration factor (which can usually be assumed to be one), D is the diffusion coefficient, L is the length of tubing from the injection port to the detector, and q is the pump speed.

This equation shows that diffusion has more of a contribution with larger diameter and longer length tubing but has less effect with higher pump speeds and a larger sample volume which is proportional to Δt_B.

DISPERSION

Dispersion is the physical process of mixing between a sample bolus and the carrier stream; the more mixing, the larger the dispersion is considered to be.[12] The basic differential equation representing the dispersion plug model is

$$\frac{\delta C}{\delta t/T} = \left[\frac{D}{FL}\right] \frac{\delta^2 C}{\delta z^2} - \frac{\delta C}{\delta z} \quad .$$

where C is concentration in moles/l, D is the axial dispersion coefficient in cm^2/sec, t is time in sec, T is the mean residence time of the bolus in sec, F is the mean linear velocity in cm/sec, L is tube length in cm (1/T = FL) and z is the fraction of the total length, z = x/L, where x is the linear position in cm. Solving this for C at low dispersion numbers (see dispersion number) gives

$$C = \frac{1}{2(\pi\delta)^{1/2}} e^{-(1-t/T)^2/4\delta}$$

The variance is

$$\sigma^2 = 2\delta$$

The maximum concentration is

$$C^{max} = \tfrac{1}{2}(\pi\delta)^{1/2}$$

The peak width at the base is

$$W_b = 4\sigma = 4(2\delta)^{1/2}$$

The peak width at 60% of the peak height is

$$W^{0.6} = 2(2\delta)^{1/2}$$

Taylor describes the concentration curve as[13]

$$C = M \frac{1}{r^2\pi} \left[\frac{1}{2(\pi\delta L^2)^{1/2}} e^{-(L-X)^2/L^2 4\delta}\right]$$

where C is the concentration at distance X in cm, M is the mass of material in grams injected at time t = 0, r is the tube radius and the dispersion number $\delta = D\ t/L^2$.

DISPERSION COEFFICIENT - D

D at any point in time is the ratio of the initial concentration, C^o, of a sample bolus to the concentration of the sample bolus at the detector, C. The maximum dispersion coefficient - D_{max} is the ratio of the initial concentration, C^o, of a sample bolus to the maximum sample bolus concentration at the detector, C_{max}. Dispersion coefficients of less than three, $C_o/C_{max} < 3$, are considered limited dispersions. Dispersion coefficients of greater than ten, $C_o/C_{max} > 10$, are large dispersions.[12,14]

DISPERSION NUMBER - δ *

$$\delta = D / F L = D T / L^2$$

where D is the axial dispersion coefficient in cm^2/sec, F is the mean linear flow velocity in cm/sec, T is the time through the system and L is the tube length in cm which makes δ a dimensionless number.

INTERFERENCES IN FIA

Hansen's paper gives a good discussion of interference and interference handling.[12]

LAMINAR FLOW

This is flow where the Reynolds number, Re, is less than 1000. The stream velocity at the center of the tube is twice the mean velocity of the liquid, and at the tube edges, the velocity is zero. The velocity, F, at distance a from the center of the tube is

$$F_a = F_{max} (1 - a^2/r^2)$$

where F_{max} is the velocity of the axial flow and r is the radius of the tube. Increasing linear velocity will increase the axial concentration gradient until the velocity reaches turbulent flow velocity.[9]

MOLECULAR DIFFUSION COEFFICIENT - D_c [9,13]

Taylor shows that

$$T = r^2/3.8^2 D_c$$

where T is the mean residence time of the sample, and r is the radius if the tubing. As the radius of the tubing decreases, the minimum mean residence time required to to have diffusion significantly affect the dispersion decreases. For a D_c of 7×10^{-6}, the minimum T for a 0.5 mm tube is 6.2 seconds; for a 1 mm tube, it is 25 seconds. Therefore; small tube sizes not only save reagents, they also reduce dispersion.

PEAK VARIANCES - σ^2 [15]

$$m = 1 + k_1\alpha$$

$$\sigma^2 = 1/n + k_2\alpha^2$$

where m is the mean of a peak, σ is the peak variance, n is the number of imaginary tanks, and $\alpha = \Delta L/L$ where ΔL is the slug or sample loop length and L is the tube length from sample to detector. k_1 and k_2 are constants derived for two different types of injection, direct injection into the flowing stream and switching inline of a sample loop. $k_1 = 2/3$ and $k_2 = 2/9$ for direct injection, and $k_1 = 1$ and $k_2 = 1$ for the sample loop. From the equation, variance is minimized by smaller sample volumes.

REYNOLDS NUMBER - Re

$$Re = 21.2\ Q\ /\ 2\ r$$

where Q is pumping speed and r is the tube radius.

TURBULANT FLOW

where Re (Reynolds number) > 1000. Turbulent flow is used in chemical reactors to limit dispersion but is unfeasible in FIA because high flow velocities would consume large volumes of reagents. Smaller tubing, that would reduce reagent consumption, would take very high pressures.

Index for Appendices D and E

References for Appendices D and E

1. S. G. Porter; Ferroelectrics, Vol 33, 1981, 193-206.

2. Pennwalt Corporation, KYNAR Piezo Film, Technical Manual.

3. W. G. Cady; Piezoelectricity, McGraw-Hill Book Co., New York, 1946.

4. W. G. Cady; Piezoelectricity, Dover Publications, Inc., New York, 1964.

5. E. H. Putley; In Semiconductors and Semimetals, R. K. Willardson, A. C. Beer, Eds.; Academic Press, New York, 1970, Vol. 5, Chapter 6, Infrared Detectors.

6. D. D. Pollock; Physical Properties of Materials for Engineers, Volume III; CRC Press, Inc., Boca Raton, FL, 1982.

7. R. C. Weast, ed.; CRC Handbook of Chemistry and Physics, 57th Edition, CRC Press, Cleveland, Ohio, 1976.

8. Solvay & Cie, Technical Data Sheet for PVDF, Bruxelles, March 1984.

9. Ruzicka, J., E. H. Hansen; Analytica Chemica Acta, Vol 99, 1978, 37.

10. Gerhardt, G. and R. N. Adams; Analytical Chemistry, Vol 54, 1982, 2618-20.

11. Gerhardt, G. and R. N. Adams; Analytical Chemistry, Vol 55, 1983, 816. (Correction)

12. Hansen, E. H., J. Ruzicka, F. J. Krug, E. A. G. Zagatto; Analytica Chimica Acta, Vol 148, 1983, 111.

13. Taylor, G., Proceedings of the Royal Society of London, Series A, Vol. 219, 1953, 186.

14. Ruzicka, J., E. H. Hansen; Flow Injection Analysis; John Wiley & Sons, New York, 1981.

15. Reijn, J. M., W. E. Van Der Linden and H. Poppe; Analytica Chemica Acta, Vol 114, 1980, 105-118.

The vita has been removed from the scanned document